GENERATION OF REPORTER CELL LINES BY GENOME EDITING
TO PROBE P53 ACTIVITY

by

NAZİFE TOLAY

Submitted to the Graduate School of Engineering and Natural Sciences
in partial fulfillment of
the requirements for the degree of
Master of Science

Sabanci University
July 2018

GENERATION OF REPORTER CELL LINES BY GENOME EDITING
TO PROBE P53 ACTIVITY

APPROVED BY:

Prof. Dr. Batu Erman
(Thesis Supervisor)

Prof. Dr. Selim Çetiner

Asst. Prof. Dr. Emre Deniz

DATE OF APPROVAL: 24/07/2018

ABSTRACT

GENERATION OF REPORTER CELL LINES BY GENOME EDITING
TO PROBE P53 ACTIVITY

NAZİFE TOLAY

Molecular Biology, Genetics and Bioengineering, MSc Thesis, July 2018

Thesis supervisor: Prof. Batu Erman

Keywords: p53, TALENs, genome editing, cell-based reporter assay, compound
screening

The p53 protein is defined as a sequence-specific transcription factor and functions as a
tumor suppressor protein. The p53 protein is involved in diverse cellular processes which
are important for controlling cell cycle arrest and apoptosis. The regulation of p53 is
governed by an autoregulatory negative feedback loop between p53 and MDM2.
Mutations in the *TP53* gene and defects in the regulation of p53 are mostly associated
with tumor initiation, invasion, and metastasis. Therefore, restoration of p53 functions to
target cancer cell viability has been used for cancer therapy. Genome editing techniques
have been used as an effective method to correct mutations, to integrate a gene of interest,
and to knock out genes. We generated reporter cell lines by using genome editing methods
to probe the transcriptional activation of p53. We showed that TALEN induced genome
editing is an effective method to integrate a reporter gene into a targeted safe harbor site.
We investigated the effects of various compounds on the transcriptional activity of p53
by using these reporter cell lines and found that some of these compounds increased the
transcriptional activity of p53. We also analyzed the effects of the compounds on cell
viability in either the presence or absence of p53 and we showed that these compounds
caused cell death independent of p53. Additionally, we identified that all compounds
stabilized the p53 protein in HCT 116 p53 WT cells. We showed that this stabilization
was because of damage-induced post-translational modification of p53. Lastly, we
showed that these compounds did not block the interaction between MDM2 and p53. In
summary, we developed and tested screening tools to identify modifiers of p53.

ÖZET

P53'ÜN AKTİVİTESİNİ ARAŞTIRMAK İÇİN GENOM DÜZENLEME İLE RAPORTÖR HÜCRE HATLARININ OLUŞTURULMASI

NAZİFE TOLAY

Moleküler Biyoloji, Genetik ve Biyomühendislik, Yüksek Lisans Tezi, Temmuz 2018

Tez danışmanı: Prof. Batu Erman

Anahtar kelimeler: p53, TALEN, genom düzenleme, hücre temelli reporter assay, bileşik tarama

Dizi özgün transkripsiyon faktörü olarak tanımlanan p53 proteini tumor suppressor olarak görev yapar. p53 proteini hücre döngüsünün ve apoptosizin kontrol edilmesinde önemli olan çeşitli hücresel süreçlere katılır. p53'ün düzenlenmesi MDM2 ve p53 arasında olan otodüzenleyici negatif geri bildirimli döngü tarafından yönetilmektedir. *TP53* genindeki mutasyonlar ve p53'ün düzenlenmesindeki bozukluklar çoğunlukla tümör başlangıcı, invazyon ve metastaz ile ilişkilidir. Bu nedenle p53 fonksiyonlarının restorasyonu kanser hücrelerinin canlılığını hedeflemede kullanılmaktadır. Genom düzenleme teknikleri mutasyonları düzeltmek, ilgili genleri genoma sokmak ve genleri silmek için etkin bir yöntem olarak kullanılmaktadır. p53 proteinin aktivitesindeki değişimleri araştırmak için genom düzenleme metodlarını kullanarak raportör hücre hatları geliştirdik. TALEN ile uyarılan genom düzenlemenin reportör genin hedeflenen güvenli bölgeye entegre etmek için etkin bir yöntem olduğunu gösterdik. Bu raportör hücre hatlarını kullanılarak çeşitli bileşiklerin p53'ün transkripsiyonel aktivitesi üzerindeki etkilerini araştırdık ve bazı bileşiklerin p53'ün transkripsiyonal aktivitesini arttırdıklarını bulduk. Ayrıca bu bileşiklerin p53 varlığında veya p53 yokluğunda hücre canlılığı üzerindeki etkilerini analiz ettik ve bileşiklerin p53'ten bağımsız olarak hücre ölümüne neden olduğunu gösterdik. Ayrıca, tüm bileşiklerin hücre içindeki p53 proteinini stabilize ettiğini belirledik. p53'ün DNA hasarına bağlı translasyon sonrası modifikasyonunun bu stabilzayona neden olduğunu gösterdik. Son olarak, bu bileşiklerin MDM2 ve p53 arasındaki etkileşimi engellemediğini gösterdik. Özet olarak p53 düzenleyen molekülleri tanımlamak için tarama araçları geliştirdik ve test ettik.

To my beloved family…

Sevgili aileme…

#ŞANS

ACKNOWLEDGEMENTS

I would like to express my appreciation to my thesis advisor Prof. Batu Erman for his immense support. Prof. Erman always answers my questions with great enthusiasm and helps me whenever I encounter a problem during my research. Prof. Erman is a great teacher and group leader. I am grateful to him for giving me a chance to study in his lab.

I am thankful to my jury members Prof. Selim Çetiner and Asst.Prof. Emre Deniz for their supports and feedbacks about my thesis project. I am thankful to Prof. Burak Erman from Koc University and Prof. Nilgün Karali from Istanbul University for their collaboration. I am very appreciative to Dr. Tolga Sütlü for his all support and scientific comments. I would like to thank Asst. Prof. Nazlı Keskin for her help.

I would like to thank all the past and present members of our lab: Dr. Bahar Shamloo, Dr. Canan Sayitoğlu, Asma Al Murtadha, Hülya Yılmaz, Melike Gezen, Sofia Piepoli, Sarah Mohammed Barakat, Ronay Çetin, Liyne Noğay, Sanem Sarıyar, Hakan Taşkıran, and Sinem Usluer. I'm thankful to Bahar for her help. I am very thankful to Ronay for his help, scientific comments, and friendship. I am thankful to Melike, Sarah, and Sofia for being a nice friend. I am appreciative to Liyne and Sanem for their friendship. I am very grateful to Hakan for his unique friendship. To work with Hakan was very enjoyable and informative. I am very thankful to Sinem for her friendship and endless supports in every situation.

I would like to thank all members of Sütlü lab: Cevriye Pamukçu, Ayhan Parlar, Didem Özkazanç, Mertkaya Aras, Alp Ertunga Eyüpoğlu, Pegah Zahedimaram, Lolai Ikromzoda, Elif Çelik for their help and friendship.

I am very grateful to my family for their endless support and faith in me. I could not have fulfilled my studies without having their supports and helps. They make the world meaningful for me.

TABLE OF CONTENTS

LIST OF FIGURES

LIST OF TABLES

LIST OF ABBREVIATIONS

α	Alpha
β	Beta
β-gal	Beta-galactosidase
γ	Gamma
μ	Micro
AAVS1	Adeno-associated virus site 1
APS	Ammonium persulfate
ATM	Ataxia-telangiectasia mutated
ATP	Adenosine triphosphate
ATR	Ataxia-telangiectasia and Rad3-related protein
Bax	Bcl-2 associated X
BHK	Baby hamster kidney
Cas9	CRISPR associated protein 9
CAT	Chloramphenicol transferase
CBP	CREB binding protein
CCR5	Chemokine receptor 5
CDC2	Cell division control 2
CDK	Cyclin-dependent kinase
Chk	Serine/threonine protein kinase
CIAP	Calf intestinal alkaline phosphatase
CRISPR	Clustered regularly interspaced short palindromic repeats
DBD	DNA binding domain
DMEM	Dulbecco's modified eagle medium
DMSO	Dimethyl sulfoxide
DNA	Deoxyribonucleic acid
dNTPs	Deoxynucleotide triphosphates
DP	Dimerization partner
DR5	Death receptor 5
DSB	Double strand break
E. coli	*Escherichia coli*
ECL	Enhanced Chemiluminescence
F2H	Fluorescent two-hybrid
Fas	First apoptosis signal
FBS	Fetal bovine serum

Gadd45	Growth arrest and DNA damage-inducible 45
GFP	Green fluorescent protein
gRNA	Guide ribonucleic acid
GSHs	Genomic safe-harbors
HCT	Human colon carcinoma
HDR	Homology directed repair
HIV-1	Human immunodeficiency virus 1
INDELs	Insertions and deletions
kDa	Kilo Dalton
LB	Luria broth
MDM	Mouse double minute
mRNA	Messenger RNA
MTT	3-(4,5-Dimethylthiazol-2-Yl)-2,5-Diphenyltetrazolium Bromide
NES	Nuclear export sequences
NHEJ	Non-homologous end-joining
NLS	Nuclear localization sequence
NOXA	Phorbol-12-Myristate-13-Acetate-Induced Protein 1
PAM	Protospacer adjacent motif
PBS	Phosphate-buffered saline
PBS-T	PBS-Tween20 Solution
PCR	Polymerase chain reaction
PEI	Polyethyleneimine
PPP1R12C	Protein protease 1-regulatory subunit 12C
PRR	Proline-rich region
PUMA	p53 upregulated modulator of apoptosis
PVDF	Polyvinylidene difluoride
Rb	Retinoblastoma protein
Rcf	Relative centrifuge force
RFP	Red fluorescence protein
RING	Really interesting new gene
RITA	Reactivation of p53 and induction of tumor cell apoptosis
RNA	Ribonucleic acid
Rpm	Revolution per minute
RVD	Repeat variable di-residue
SDS	Sodium dodecyl sulfate
SV40	Simian virus 40
TAD	Transactivation domain

TALEN	Transcription activator-like effector nucleases
Taq	*Thermus aquaticus*
TBE	Tris-Borate-EDTA
TD	Tetramerization domain
TEMED	Tetramethyl ethylenediamine
TF	Transcription factor
UT	Untreated
VMD	Visual Molecular Dynamic
WT	Wild-type
X-gal	5-bromo-4-chloro-3-indolyl galactoside
ZFNs	Zinc-finger nucleases

1. INTRODUCTION

1.1. The p53 Protein

1.1.1. The p53 Protein; Cellular Gatekeeper[1]

The p53 protein was first identified as a complex with the SV40 large T antigen in 1979[2]. In 1983 p53 was cloned from an SV40 virus transformed-mice cell line to demonstrate its function and subsequently, it was defined as an oncogene[3,4]. However; in 1989 an observation which showed the inactivation of p53 by retroviral insertion made a striking impact on the definition of p53 function. Thereafter, p53 was finally defined as a tumor suppressor protein[5] and functionalized as a sequence-specific transcription factor[6].

In normal cells, p53 protein cannot be detected because of its short half-life; however, activation by several factors such as DNA damage, hypoxia, reactive oxygen species, and oncogene activation enables its detection[7,8]. Upon activation, the p53 protein binds to response elements on DNA and regulates the expression of several genes which control apoptosis, cell cycle arrest, senescence, and cell metabolism[8]. The first clearly described function of p53 is to induce apoptosis in tumor-derived cell lines[9]. p53 activates apoptosis by using transcription-dependent and -independent mechanism. In the transcription-dependent activation of apoptosis, p53 induces the expression of proapoptotic genes encoding proteins such as BAX, DR5, FAS, PUMA, and NOXA. These proteins can either induce the extrinsic apoptotic pathway or the intrinsic apoptotic pathway. Translocation of BAX, PUMA, and NOXA to mitochondria induces the loss of mitochondrial membrane potential causing the release of Cytochrome c. PUMA can initiate a rapid apoptosis response after its expression and is involved in both transcription-dependent and -independent apoptosis. In the extrinsic apoptotic pathway, p53 activates death receptors on the plasma membrane, such as FAS followed by induction of apoptosis[10,11]. p53 is directly involved in transcription-independent apoptosis under certain circumstances: p53 facilitates BAX-dependent mitochondrial changes by going to mitochondria and promotes BAK oligomerization which helps to release Cytochrome c[10].

Another pivotal role of p53 as tumor suppressor protein is the induction of cell cycle arrest to regulate cellular growth and to provide additional time for cells to repair DNA damage before DNA synthesis[12]. One of the targets of p53 is p21$^{Waf1/Cip1}$ which is a cyclin-dependent kinase (CDK) inhibitor. In the presence of DNA damage, p53 stimulates the expression of *p21$^{Waf1/Cip1}$* to induce cell cycle arrest in G1 phase. Overexpression of p21$^{Waf1/Cip1}$ arrests the cell cycle at G1 phase through blocking cyclin E/CDK2-mediated phosphorylation of Rb and dissociates of E2F-DP proteins from the Rb complex. Thus, this dissociation results in the repression of the expression of required genes for S phase entry[10]. p53 can also induce cell cycle arrest at G2 phase by increasing expression of *GADD45*. GADD45 binds to CDC2 and block cyclin B/CDC2 complex formation followed by the inhibition of kinase activity resulting in cell cycle arrest in the G2 phase[1,10].

In some circumstances, p53 can induce senescence, which is an irreversible cell cycle arrest program acting as a barrier against tumorigenesis[13]. Cellular senescence can be initiated in response to telomere dysfunction, oncogene activation, and DNA damage. Upon oncogene activation, p53 is upregulated and modulates cellular senescence by activating several genes which are involved in senescence. For example, E2F7 is upregulated by p53 and functions in the arrest of the cell cycle at mitosis by repressing essential mitotic genes, such as *CDC2/CDK1*[14,15].

p53 is also involved in the regulation of autophagy which is defined as self-eating, where damaged organelles, misfolded proteins, and other components are degraded by specialized lysosomes called autophagosomes. This process allows cells to recycle and resynthesize essential structure. As a non-canonical function, p53 can either inhibit or activate autophagy depending on its status in cells. For instance, in the presence of stress p53 activates autophagosome formation; however, in basal condition p53 has been shown to inhibit autophagy[16,17].

1.1.2.   The Structure of p53

p53 contains an acidic amino-terminal transactivation domain (TAD), which is required for the transactivation of target genes, followed by a proline-rich region (PRR). The central part of p53 includes a sequence-specific DNA binding domain (DBD), which provides specificity for the regulation of target genes. To provide sequence-specific binding the DBD needs consensus sequences which contain two copies of the 5'-PuPuPuC(A/T)-(T/A)GPyPyPy-3' motif, separated a by 0-13 base pair spacer[10,18]. The carboxyl-terminal region of p53 contains a tetramerization domain (TD), a nuclear localization sequence (NLS) and a nuclear export sequences (NES). The NSL and NES are prominent in the shuttling of p53 between nucleus and cytoplasm. Tetramerization of p53 ensured by the TD is required for high-affinity DNA binding and for transcriptional activation[19]. The C-terminal region is important for the regulation of p53 and undergoes posttranslational modifications such as phosphorylation and acetylation, among others[20,21,22]. These modifications enhance the sequence-specific binding activity of p53[23]. In addition to sequence specificity, the C-terminal region enables stable p53-DNA complex formation by inducing conformational changes in the DBD (Figure 1.1)[24].
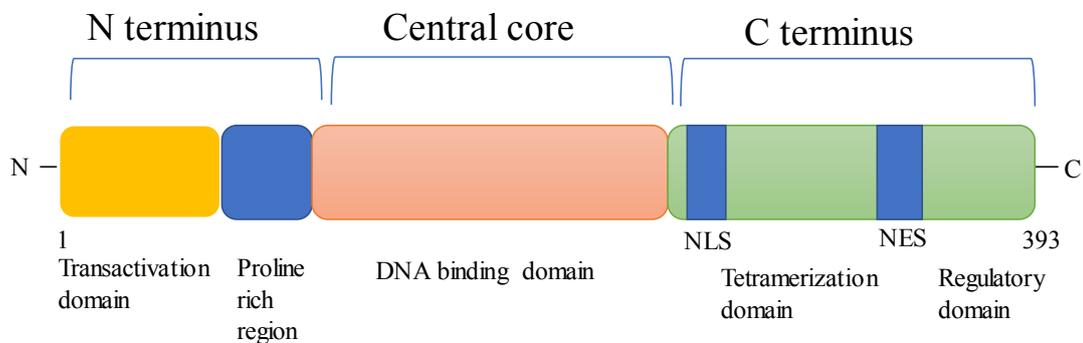
Figure 1.1. The structure of the p53 protein. p53 consist of transactivation domain, a proline-rich region, DNA binding domain, tetramerization domain, and regulatory domain.

1.1.3.   The Regulation of the p53 Protein

p53 can be regulated through a variety of mechanisms, the most prominent is carried out by MDM2 which is an interacting partner of p53[25]. The *Mdm2* gene was first identified on double-minute chromosomes of spontaneously transformed mouse 3T3 fibroblasts and then described as an oncogene[26]. *Mdm2* gene expression is controlled by p53 binding to

the P2 promoter region on the *Mdm2* gene[27]. On the other hand, MDM2 regulates the activity of p53 at the protein level[27]. Therefore, p53 and MDM2 create an autoregulatory negative feedback loop.

Structure of the MDM2 protein is essential to understand its role in the regulation of the p53 protein through the autoregulatory negative feedback loop. The 491 amino acid MDM2 protein consists of an amino-terminal domain, central acidic domain, and a carboxy-terminal RING finger domain[28]. It also includes a nuclear export sequence, a nuclear localization sequence, and a nucleolar localization sequence[28]. The autoregulatory feedback loop between MDM2 and p53 controls the stability and activity of the p53 protein in cells[29,30,31]. In normal cells, the p53 protein is degraded through a ubiquitin-dependent mechanism by nuclear and cytoplasmic 26S proteasomes[32]. The ubiquitination of the p53 protein is achieved by MDM2 which has an E3 ubiquitin ligase activity[28,33]. Furthermore, MDM2 can inhibit the transcriptional activity of p53 by interacting with the TAD of the p53 protein through its N-terminal region[25]. MDM2 can also promote the nuclear export of p53 by monoubiquitination[33]. The action of MDM2 on p53 depends on its protein level: the low levels of MDM2 promotes mono-ubiquitination and nuclear export of p53, whereas the high levels of MDM2 induces its polyubiquitination and nuclear degradation (Figure 1.2)[7,34]. This regulation mechanism keeps the p53 protein at low level in normal cells. In the case of genotoxic stress, p53 and MDM2 undergo posttranslational modifications through ATM, ATR, Chk1, and Chk2 signaling. Subsequently, the MDM2-p53 interaction is blocked and p53 translocates the nucleus to activate its target genes[33,35].

MDMX (also known as MDM4) is another important protein which is involved in the regulation of p53. MDMX was first identified to be an interacting partner of p53. Later, it was found that MDMX is structurally related with MDM2[36,37]. They have a similar acidic core domain and RING domain, although MDMX does not have any E3 ligase activity[38]. MDMX interacts with the transactivation domain of p53 and blocks its transcriptional activity. Additionally, MDMX promotes the E3 ligase activity of MDM2 and prevents MDM2 from autoubiquitination by interacting with the RING domain of MDM2 (Figure 1.2)[39]. As a consequence, MDMX can increase the stability of MDM2.

Additionally, p53 can be indirectly regulated by ARF, which is a tumor suppressor protein. ARF is induced via oncogenic activation such as *Ras* and *c-myc*. The presence of oncogene activity results in the elevation of AFR levels, then ARF binds to the RING domain of MDM2 to inhibit its E3 ligase activity. In the nucleus, ARF can also sequester MDM2 into the nucleolus and then block the MDM2-p53 interaction. Thereby, ARF can increase the stability of p53 (Figure 1.2)[33,40].
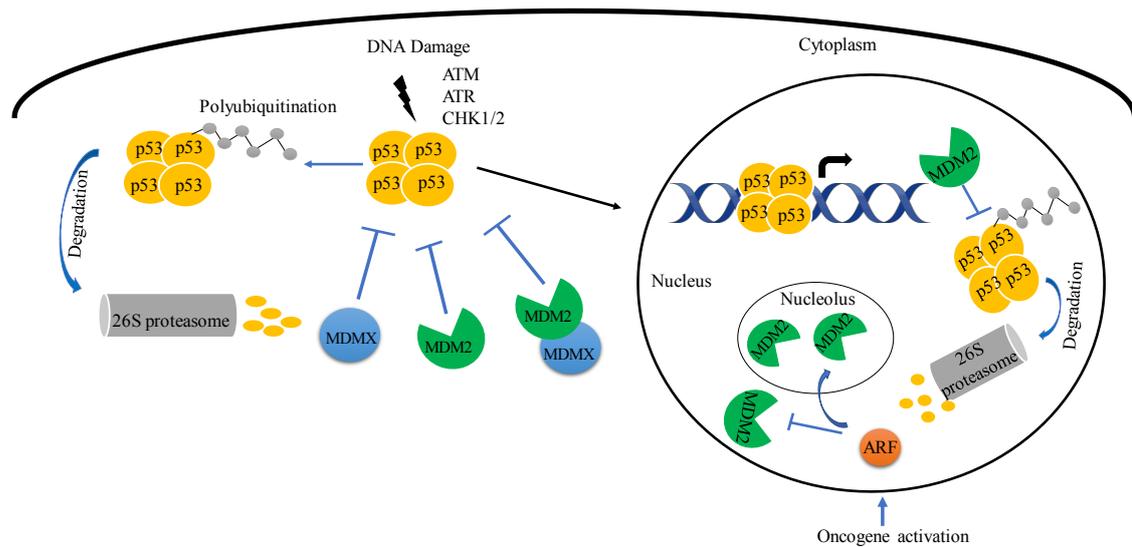
Figure 1.2. The regulation of p53. There is an autoregulatory negative feedback loop between p53 and MDM2. p53 stimulates the expression of MDM2; MDM2, in order, inhibits the activity of p53 by stimulating its ubiquitin-dependent degradation by the 26S proteasome in the cytoplasm or in the nucleus. MDMX can inhibit the activity of p53 by binding to its TAD and it also promotes the stability of MDM2. In the presence of DNA damage or deregulated oncogenes, p53 is activated by inhibiting the interaction between MDM2/X and p53.

Post-translational modification of the p53 protein is a prominent mechanism to generate transcriptionally active p53. The presence of stress is critical to launch an early p53 response to keep the balance in cells. Post-translational modifications have a crucial role to produce p53-dependent early responses[35,41]. One of the most important post-translational modifications for the stabilization and activation of p53 is phosphorylation. In response to genotoxic stress, p53 is phosphorylated at several residues[35]. Phosphorylation of p53 is mostly associated with its stabilization. However, certain phosphorylation in specific residues can increase the transcriptional activity of p53, such as Serine33, Theroine55, and Serine315[42].

Acetylation is another important post-translational modification which occurs at lysine residues and can change protein conformation and/or interaction with its partners. This modification was first identified on histone proteins and was shown to cause chromatin condensation which is a sign for the activation of gene expression. Therefore, acetylation is mostly associated with transcriptional activation[43]. Later, it was shown that non-histone proteins are also subjected to this modification. The p53 protein is the first protein that was shown to undergo acetylation[44]. Acetylation of the p53 protein is induced by cellular stress and genotoxic insults. The carboxy-terminal domain of p53 is acetylated at several specific lysine residues (Lys370, Lys371, Lys372, Lys381, and Lys382) by CBP/p300 which has histone acetyltransferase activity[41,42]. Thus, the acetylation of p53 at these specific residues results in its stabilization and an increase in its sequence-specific DNA binding ability[42]. In addition to activating p53, acetylation provides efficient recruitment of cofactors to stimulate p53 target genes *in vivo*[35]. A study showed that the acetylation of certain lysine residues is required for p53 to activate certain target genes. For instance, Tip60-dependent Lys120 acetylation is necessary for the expression of proapoptotic target genes, such as *PUMA* and *BAX*, whereas the expression of *p21^{Waf1/Cip1}* and *Mdm2* are not changed[45,46]. Different acetylation patterns of p53 might be related with the determination of cell fate depending on the stimulus. Therefore, a variety of post-translational modifications might produce a barcode that can define the function of p53 in certain circumstances.

1.1.4.   The Interaction Between p53 and MDM2

Understanding the interaction between p53 and MDM2 is important to demonstrate the regulation mechanism of p53 and is also crucial to clarify p53-dependent cancer development. The regions which are involved in the interaction between p53 and MDM2 protein were revealed by yeast two-hybrid screening and by immunoprecipitation experiments[47]. The N-terminus of the transactivation domain of p53 between 1-41 residues and the N-terminus of MDM2 between 1-118 residues were determined to be essential parts for this interaction[47,48]. The atomic properties of the interaction were determined by X-ray crystallography in 1996 and the residues between 18-26 of p53 were mapped as essential residues for the interaction[47,49]. The high-resolution crystal structure of human and *Xenopus laevis* MDM2 complexed with short p53 peptides indicated that MDM2 has a well-defined hydrophobic cleft, which provides a convenient structure for

6

the interaction. This study also showed that three key hydrophobic residues in p53 (Phe 19, Trp 23, Leu 26), which construct an amphipathic alpha-helix structure, were buried into this MDM2 cleft (Figure 1.3)[47,50]. The interaction is mostly provided by Van der Waals contacts that occurred in the hydrophobic cleft. Additionally, two hydrogen bonds augment this interaction: one is between Phe19 and Gln72 of MDM2, and another is between Trp23 and Leu54 of MDM2[49]. Later, site-directed mutagenesis demonstrated the importance of these three key residues for the interaction. Similarly, it was shown that the mutations at Gly58, Glu68, Val75, and Cys77 residues in MDM2 protein cause the loss of binding ability of MDM2 to p53[33].
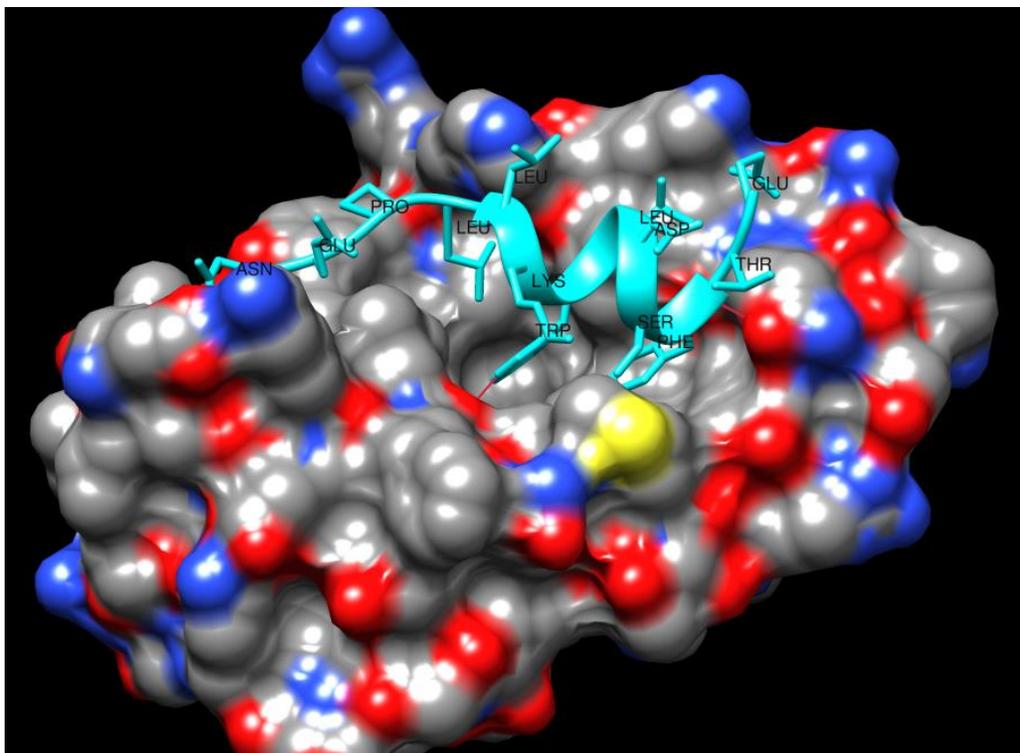
Figure 1.3. The crystal structure of MDM2-p53 complex. MDM2 possesses a hydrophobic cleft, which is occupied by p53 peptide (cyan). p53 can build two hydrogen bonds (shown as a red line) with MDM2: Phe19 residue of p53 makes a hydrogen bond with Gln72 residue and Trp23 residue of p53 makes a hydrogen bond with Leu54 (PDB ID: 1YCR).

1.1.5.   Mutations in the *TP53* Tumor Suppressor Gene

 Mutations in the *TP53* gene can induce development of various cancers due to its diverse function in the regulation of cell cycle and apoptosis. Mutations in the *TP53* gene can lead to deregulated cell cycle, failure in apoptosis and stress signaling. These mutations

thus increase genomic instability which is prominent cancer-driving factor[51,52]. Mutant p53-deriving tumor developments have apparently been observed in Li-Fraumeni syndrome patients since these patients have germline mutation on *TP53* gene. p53 knockout mouse models also affirmed that the loss of p53 function is often related to tumor initiation and progression[53,54,55]. 50% of human cancers harbor various mutations on *TP53* gene[56]. Although p53 mutations can be found almost everywhere in the protein, cancer-derived mutations are mostly localized in the DNA binding domain of p53. Six amino acid residues (R175, G245, R248, R249, R273, and R282) located at the DBD of the p53 protein have been identified as hotspots for cancer development. Mutations at these hotspots affect the binding ability of p53 to target sequences, therefore impair the transcriptional activity of p53[55,57]. Besides, some of the p53 mutations are defined as conformational mutations which disrupt the tertiary structure of p53. Hence, the conformational mutations might affect the interaction of p53 with other proteins[58]. Additionally, mutant p53 proteins can display a dominant negative effect on the wild-type p53 by tetramerizing with wild-type p53 and might inhibit the function of wild-type p53. Because of the mutations, p53 can also gain new functions which might be oncogenic[52,56]. For instance, a specific mutation that can affect the DNA binding domain of p53 without suppressing its transcriptional activation might allow mutant p53 to recognize unique response elements to which wild-type p53 does not bind. Hence, mutant p53 might show oncogenic function[55]. Additionally, it was shown that some of the mutant p53 protein promoted cell proliferation, survival, migration, and invasion in tumors[56].

p53 can also lose its activity without having any mutations due to defects in other regulator proteins. For example, MDM2 has been found at overexpressed state in some cancer cases that prominently keep p53 at the inactive state. Consequently, the overexpression of MDM2 provides to cancer cells a growth advantage and promotes tumorigenesis[58,59]. Additionally, the overexpression of MDMX has been detected in some tumor cell lines which carry wild-type p53. The knockdown of overexpressed MDMX rescued the function of wild-type p53 in breast carcinoma and retinoblastoma cell lines[58,60].

1.1.6. Reactivation of p53 for Cancer Therapy

The regulation of p53 is pivotal for cells to maintain their healthy state. The mutations on the *TP53* gene have crucial effects on cancer development. While almost 50% of cancers carries mutated *TP53* gene, the rest contains wild-type p53 whose regulation is disrupted by MDM2/X overexpression or amplification and the loss of ARF[60,61]. Restoration of wild-type p53 functions leads to regression of in situ tumors[62]. This study has offered a possibility to stimulate tumor suppressor activity of p53. Therefore, several different therapeutic strategies have been suggested to reactivate wild-type p53 function for cancer treatment[63].

Due to fact that the regulation of p53 mostly depends on MDM2, targeting the MDM2 can be an effective strategy for restoration of p53 functions. A strategy suggested to reactivate p53 is to inhibit the E3 ligase activity of MDM2, thus the stability of p53 can be increased by preventing its ubiquitination. For this purpose, a compound (HLI98) was developed and was shown that it could activate p53. However, its effect on inhibition of E3 ligase activity was very low due to its low solubility. This study might be seen as a starting point for the development of potent inhibitory compounds[64].

Another promising strategy is that blocking the interaction between MDM2 and p53 by small molecules or peptides[63]. The development of small molecules for inhibiting non-enzymatic protein-protein interactions is traditionally seen as problemmatic[65]. However, the X-ray co-crystal structure of p53 and MDM2 enables the design of a small molecule inhibitor to block the interaction. Because, the hydrophobic pocket of MDM2, which is occupied by p53, provides highly suitable structure for the development of small molecule inhibitors[49,65]. Therefore, various studies have been performed to develop small molecule inhibitors, and some of these studies have successfully developed small-molecule inhibitors binding specifically to MDM2[10].

In 2004 first potential inhibitor Nutlin, that belongs to the class of cis-imidazoline compounds, was discovered by screening synthetic chemical library via surface plasmon resonance method. After the discovery of Nutlin, Nutlin-3a which is an enantiomer of Nutlin has been developed with higher activity. Nutlin can mimic the interaction between MDM2 and p53 properly. A crystal structure of the MDM2-Nutlin-2 complex shows that

one bromophenyl moiety perfectly fills the Trp pocket, the other bromophenyl group holds the Leu pocket, and an ethyl ether side chain occupies the Phe pocket (Figure 1.4)[65]. Thus, the cis-imidazoline scaffold represents the alpha-helical structure of the p53 peptide with high specificity.

a)

b)
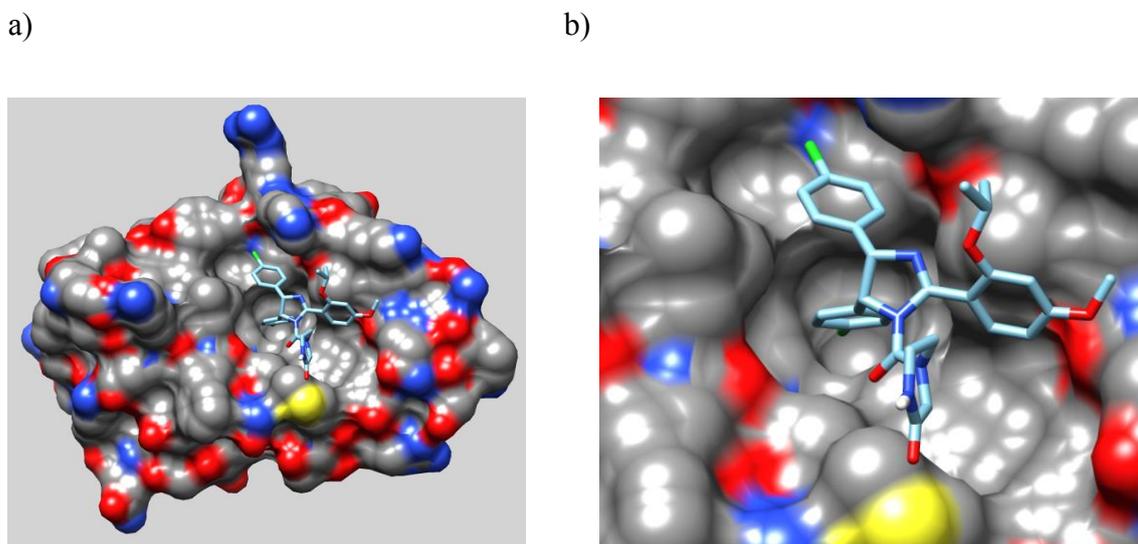
Figure 1.4. Docking of MDM2-Nutlin-3a. (a) Docking was performed by using AutoDock, coordinates of MDM2 and Nutlin-3a were obtained through VMD, and the result was analyzed by using Chimera. Nutlin-3a perfectly occupies the hydrophobic cleft on the MDM2 protein. (b) Nutlin-3a can perfectly represent Phe, Thr, and Leu residues which are important for MDM2-p53 interaction. MDM2 protein structure and Nutlin-3a was obtained from PDB (MDM2 PDB ID: 1YCR Nutlin-3a PDB ID: 5C5A).

In 2005, following the development of Nutlin, benzodiazepinedione-based compounds were developed by designing compound libraries by Direct Diversity software and these compounds were analyzed by affinity-based screening assay and fluorescent peptide displacement assays. The activity of benzodiazepinedione was validated by *in vitro* analysis of p53 target genes[66]. In 2006, spirooxindoles were reported as new small molecule inhibitors. They were developed via structure-based *de novo* design and their binding ability to MDM2 was confirmed by fluorescence polarization-based binding assay. After production of the highly active spirooxindole-based compound, its MDM2 binding mode was analyzed. The spirooxindole-based compound can mimic Phe19, Trp23, Leu26 as well as Leu22, which might provide better affinity towards MDM2 than Nutlin[67]. Spirooxindole-based compound MI-219 was shown to selectively kill tumor

cells and to increase the expression of p21$^{\text{Wafl/Cip1}}$ and MDM2. MI-219 specifically induced apoptosis in wild-type p53 carrying cells rather than mutant p53 carrying cells[8].

An alternative strategy to reactive p53 might be the development of small molecules that can bind to p53 and prevent its interaction with MDM2. A compound which is called reactivation of p53 and induction of tumor cell apoptosis (RITA) was developed using a cell-based assay. RITA stimulated the expression of p53 target genes by blocking the interaction between p53 and MDM2[68].

The inhibition of the interaction between p53 and MDMX might be another approach to increase the efficiency of cancer treatment besides inhibiting p53-MDM2 interaction. For this purpose, a few molecules were developed. For example, SJ-172550 was first identified compound through biochemical and cell-based assay, which can inhibit MDMX. It was indicated that this compound can effectively kill the MDMX overexpressing retinoblastoma cells by binding reversibly to MDMX[69].

Moreover, there is another approach that can be applied when tumor cells have mutant p53 protein. In the case of tumor cells carrying mutant p53, the main strategy is to refold mutant p53 into wild-type conformation to restore its function[58]. To reactivate wild-type function of the mutant p53 protein, several small molecules were developed. One of them is carbazole derivative PhiKan083 which can bind to mutant p53 and then reactivate its function by raising its melting temperature. Another small molecule is CP-31398 that changed protein folding of the mutant p53 protein into wild-type form that gained its original function[70].

1.2. Cell-Based Reporter Assays

Cell-based assays are effective tools to study signal transduction, gene expression, cell proliferation, protein-protein interaction, signal transduction, toxicity and to evaluate the activity of novel compounds[71]. Most widely used application of cell-based reporter assays is the investigation of the function of cis-acting elements, such as promoters and enhancers (Figure 1.5)[72]. For instance, after creating mutations on promoter sequences, the effects of the mutations can be monitored through reporter genes[72]. Many cell-based

assays are utilized from reporter genes whose products facilitate the development of cell-based reporter assays. In addition to studying cellular processes, cell-based assays are extensively employed for high throughput screening, due to the sensitivity, low labor cost, and miniaturization[73]. On the other hand, cell-based reporter assays have some drawbacks. For example, they might need long response time depending on the signal cascade or gene expression pathway and they might interfere with other cellular pathways[71]. Thus, discoveries made with cellular reporter assays must be complemented with other *in vivo* or *in vitro* tests.
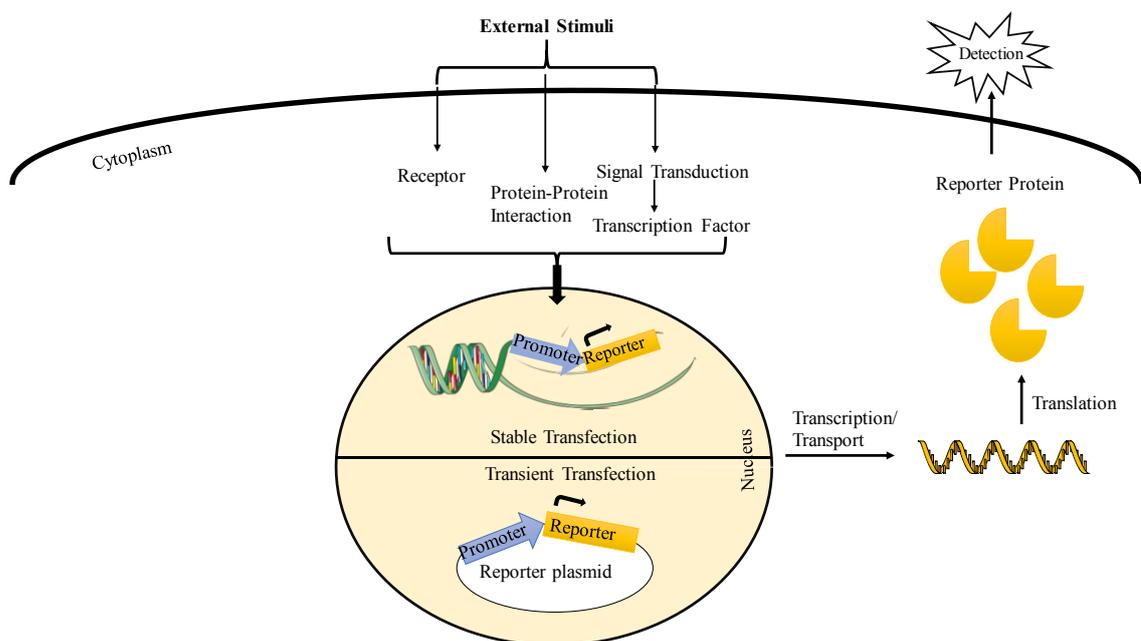
Figure 1.5. Schematic representation of cell-based reporter systems. Cell-based reporter system can be created by stable transfection or transient transfection of a reporter gene. The external stimulus is translated to the cell by receptors, protein-protein interaction, and transcription factors. Translated signal causes a change in reporter gene expression which is easily detected.

There are several considerations to create a cell-based reporter assay. First, cell type should be selected carefully. There are two cell type options for the construction of cell-based assays which are immortalized cell lines and primary cell lines[71]. Secondly, cell-based reporter assays need a highly detectable expression of the reporter gene which can be provided either transient or stable transfection. Because of the variation of transient transfection efficiency, stable transfection is the more reliable way to create reporter cell lines. Stable expression can provide long-term, consistent expression for reporter genes. Finally, when a reporter system is designed, properties of the promoter and upstream

control elements of the reporter gene should also be considered. Because constitutive cryptic promoter activity can affect the sensitivity of assays, potentially a transcription stop element should be inserted upstream of the promoter of choice. The half-life of the reporter protein is also important to design a reliable assay, because a long half-life might increase background, decrease response sensitivity and cause false-positive results[74].

There are several reporter genes that have been used for the construction of cell-based reporter assays for over a decade. Reporter genes can be grouped as intracellular and extracellular. While intracellular reporter gene products retained in the cell, extracellular gene products are transported into the cell culture medium[73]. Chloramphenicol acetyl transferase (CAT), which is a bacterial enzyme, has been utilized to study transcriptional regulation in mammalian cells. CAT is basically trimeric protein which is composed of three identical subunits of 25 kDa and catalyzes the switch of an acetyl group from acetyl-coenzyme A to chloramphenicol. It is a very good candidate as a reporter gene and widely used to study the regulation of gene expression in mammalian cells because there is no counterpart of this enzyme in mammalian cells. Thus, it does not cause any conflict between endogenous and ectopic expression. However, this method requires the use of C14 radioisotope-labeled acetyl CoA, which limits its use in living cells[75]. Beta-galactosidase (β-gal) is also bacterial enzyme which is encoded by the *lacZ* gene. Its activity in cells can be detected easily with a colorimetric assay. This enzyme can hydrolyze various β-galactoside molecules. For example, 5-bromo-4-chloro-3-indolyl galactoside (X-Gal) is cleaved and indolyl group is released from the substrate. This hydrolysis enables the easy detection of the reporter protein, because free indolyl produces an indigo blue insoluble derivative by oxidation. Therefore, β-galactosidase is extensively used as an internal control for normalization of variability in reporter protein activity, due to differences in transfection efficiency[75,76]. Beta-lactamases are crucially important for bacteria to gain resistance against penicillin and cephalosporin-based antibiotics. The genes that encode these enzymes have also been used as reporter genes for studying gene expression *in vitro* and *in vivo*. For instance, TEM-1 β-lactamase has been used to detect protein-protein interactions and other biological processes[75]. Alkaline phosphatase is yet another reporter gene and its secreted form is widely used to observe inflammatory events, for high throughput compound screening, and to study promoter activity. The secreted alkaline phosphatase enables easy detection from cell culture

medium without the need to lyse the producing cells [75,76]. Green fluorescent protein (GFP) is a very convenient reporter gene which does not have any enzymatic activity in contrast to other reporter genes. GFP has originated from jellyfish *Aequorea victoria*. GFP is particularly used to visualize protein localization, spatial gene expression, and protein-protein interaction. Despite its wide usage, it cannot be counted as quantitative reporter gene[77]. Luciferase enzymes are widely used as reporters, thanks to the bioluminescence features of their products, which can cover wide dynamic range of gene activity. Luciferases which generate very bright bioluminescence have been utilized to create cell-based reporter assays[78]. Luciferase genes which are originated from firefly *Photinus pyralis,* jellyfish *Aequorea Victoria,* and sea pansy *Renilla reniformis* are mostly used to construct bioluminescence reporter assay. In the presence of oxygen, magnesium ion, and ATP, firefly luciferase catalyzes the oxidation of luciferin and produces light with broad-band emission spectra and this light can be detected easily by luminometers[71,75]. Due to its sensitivity and easy detection, firefly luciferase has been employed for the examination of the activity of transcription factors and screening of inhibitor or activator molecules[79]. Additionally, luciferases are excellent reporter genes to study cellular processes and to establish high throughput screening methods, because they do not require post-translational modifications and also they do not have any counterpart in mammalian cells[75].

1.3. Genome Editing

Genome editing is a current and effective method broadly applied in biomedical research, medicine and biotechnology. It is a powerful tool to study the regulation of gene expression, to investigate the function of the genes, and to change genome architectures. In detail, genome editing can be used to knock out specific genes by non-homologous end joining (NHEJ) which causes insertions and deletions resulted in frameshifts in the coding region followed by gene disruption[80]. Most attractive use of genome editing is its ability to insert a gene of interest into targeted site by homology directed repair (HDR). Engineered nucleases can increase the specificity of homology-directed repair by creating site-specific double strand breaks[81]. Particularly, gene insertion through genome editing requires a specific donor DNA which should contain the gene of interest flanked by

homology arms that are homologous to the targeted site[80]. In addition to gene insertion and deletion, genome editing tools can be used to correct or to introduce the point mutations in the genome through the delivery of engineered nucleases with specific vectors[82] or with single-strand oligodeoxynucleotides[83].

1.3.1. Programmable Nucleases

Historically, the genome editing approach has utilized programmable nucleases, which can be classified as zinc-finger nucleases (ZFNs), transcription activator-like effector nucleases (TALENs), and clustered regularly interspaced short palindromic repeats (CRISPR) and CRISPR-associated system 9 (Cas9) enzyme[84]. ZFNs have been used to modify the genome *in vitro* or *in vivo*. ZFNs consist of the DNA restriction domain of the Fok I restriction endonuclease fused to a Cys2-His2 zinc-finger DNA binding domain which can be designed to bind target sequences[85]. The Cys-2-His2 zinc-finger domain is the most common DNA-binding motif found in eukaryotic transcription factors[86]. Every zinc-finger motif contains approximately 30 amino acids in a conserved ββα configuration and the α-helix usually makes a contact with three base pairs located in the major groove of DNA with different selectivity[86,87]. ZFNs have been designed to work as a dimer: each monomer of the ZFN binds to a half of the target site through its DNA binding domain which guides the dimerization of the Fok I domain, which creates specific double strand breaks[85]. ZFNs have two main disadvantages which are the difficulties of assembling multiple zinc finger motifs that generate a sequence-specific DNA binding domain and the off-target issue. Nevertheless, ZFNs have a prominent potential for efficient genome editing[84].

Another nuclease generated from genome engineering, TALENs also use the Fok I cleavage domain[88]. To recognize DNA specifically, these human-made nucleases use transcription activator like-effector (TALE) domains copied from natural bacterial effector TALE from bacterial *Xanthomonas sp.* to regulate gene transcription in host plants for providing an advantage for bacterial colonization[89]. Natural TALE proteins contain a central DNA binding domain, a type II secretion signal, a nuclear localization signal, and a transactivation domain. The DNA binding domain is composed of monomers, which are tandem repeats of conserved 34 amino acid residues. In these repeats, only two amino acid residues located at positions 12 and 13 are highly variable and they provide specificity for the recognition of DNA and are called repeat variable di-

residues (RVD)[86]. In contrast to zinc-fingers, where one finger contacts 3 nucleotides, each TALE motif can only recognize a single nucleotide which is determined by the identity of the RVD.

A natural code determining the recognition specificity was recently discovered, where the identity of the amino acid residues of the RVD is used recognize the four DNA bases: TALE repeats that contain RVD amino acids NI recognize A, HD recognize C, NG or HG recognize T, NN recognize G or A. Unlike zinc-fingers, each TALE motif provides mostly individual recognition as independent from neighboring motifs[90]. Because TALEs bind to DNA with high specificity, they have been used for genome editing[90]. For that purpose, multiple repeats forming the DNA binding domain of the TALE were fused to Fok I nuclease coding sequences in a plasmid. The protein product is referred as transcription activator like-effector nuclease (TALEN)[88]. To function properly, TALENs require two pairs which bind to the target sequence in a head to head opposite orientation and thus leaving a spacer sequence between the DNA recognition sequences. Once a TALE pairs binds to the target sequence, the Fok I domains homodimerize and induce a double-strand break in the spacer sequence[91]. Additionally, target site selection is important to design efficient TALENs. For target site selection, there is a structural limitation which requires the presence of a T before the 5' end of the target sequence[91]. Unfortunately, TALENs have some drawbacks, especially in their construction. The construction of TALENs is cumbersome because of the large number of repeated motifs. To deal with this issue, several methods have been developed, such as Golden Gate cloning[92] and ligation-independent cloning[93]. As a result, the enhanced efficiency and simpler construction protocols compared to ZFNs, make TALENs an attractive tool for genome editing[90].

The latest version of programmable nuclease is the CRISPR/Cas9 system. CRISPR/Cas9 system was discovered in bacteria which uses this system as an adaptive defense mechanism[90]. CRISPR/Cas9 system is composed of a guide RNA and the Cas9 enzyme. While guide RNA directs sequence-specific recognition, Cas9 enzyme mediates DNA cleavage[91]. Cas9-mediated cleavage of DNA is linked to guide RNA (gRNA) which is customizable and provides sequence specificity for DNA cleavage[90]. To cleave DNA, Cas9 enzyme also requires a specific three base pairs-sequence which must contain 5'-NGG-3' or 5'-NAG-3' before the gRNA binding site in the target sequence. These

sequences are called the protospacer adjacent motif (PAM)[80]. CRISPR/Cas9 system has simpler construction procedure compared to other programmable nucleases and it also has better or equal efficiency[80,81]. For this reason, it has been the most popular choice in genome editing systems. Because of pre-existing reagents, we chose the TALEN method to target the human genome in this thesis. However, the CRISPR/Cas9 enzymes targeting the same site in the human genome have also been developed.

Overall, these programmable nucleases recognize specific sites and generate a double strand break on the DNA. This double strand break can be repaired by the cells with two different mechanisms: non-homologous end-joining (NHEJ) and homology-directed repair (HDR) (Figure 1.6)[94,95].
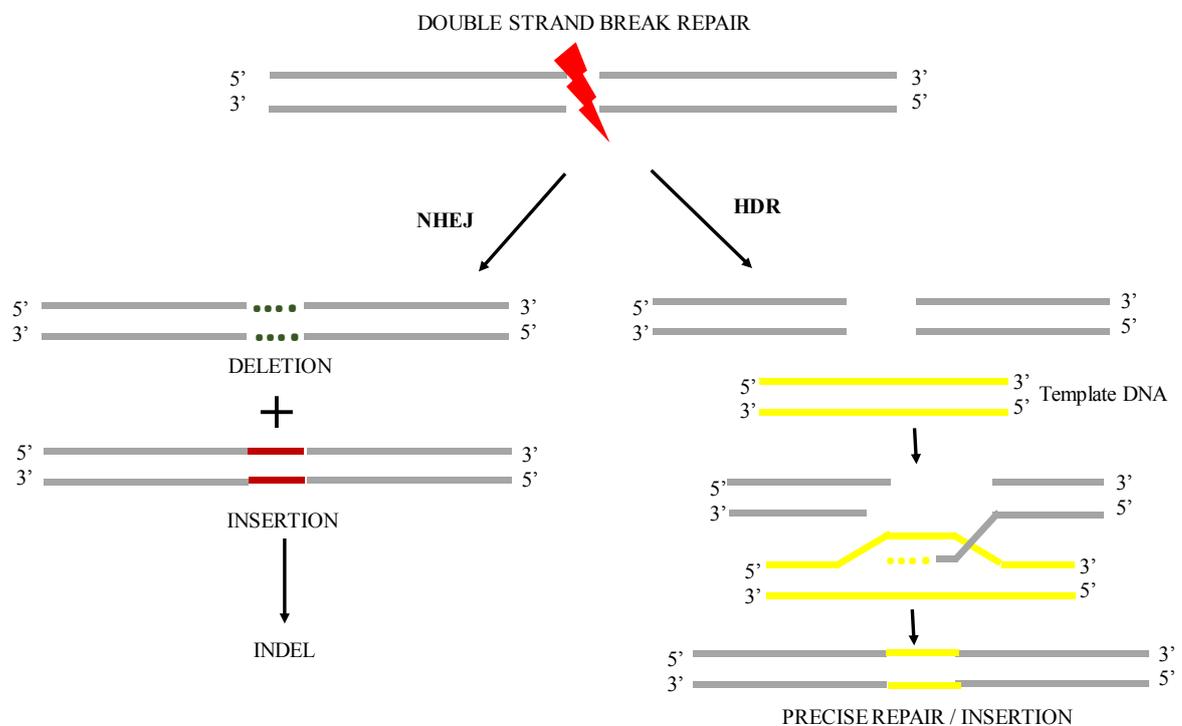
Figure 1.6. DNA double strand break repair. DSBs are repaired through non-homologous end joining (NHEJ) or homology-directed repair (HDR).

In NHEJ repair, Ku70/80 binds to the end of the broken DNA to recruit other proteins which form a stable repair complex on DSB. Then, broken ends are processed by specific DNA end-processing enzymes to create compatible ends for ligation. In the final step of NHEJ, the broken ends get ligated to each other by DNA Ligase IV[96]. The NHEJ pathway performs an error-prone repair, thus resulting in insertions and deletions (INDELs)[95]. In

HDR, the broken ends are processed by the Mre11/Rad50/Xrs2 complex and Sae2 protein to generate free 3' single-strand ends which produce D-loop by attacking to undamaged DNA duplex with the help of Rad51 filaments. This mechanism is called stand invasion. After D-loop creation, DNA polymerase synthesizes new DNA by using undamaged DNA as template. Subsequently, new synthesized DNA is dissociated form heteroduplex[97]. In contrast to NHEJ, HDR provides accurate repair for cells, however, its frequency is lower than NHEJ[95]. These two repair mechanisms can be used for different applications genome editing technology. While NHEJ is used for mutation generation, HDR is employed for targeted gene integration and gene correction. The outcome of HDR depends on the design of donor DNA carrying the gene of interest flanked with suitable homologous sequences[94,98].

1.3.2.   Genomic Safe-Harbors (GSHs)

GSHs are found in the genome located in intragenic or extragenic regions and provide reliable and stable transgene expression[99,100]. GSHs are valuable sites for targeted gene integration. In contrast to random integration, the fate of targeted gene insertion is more predictable in terms of position effects and silencing[100]. Determination of genomic sites as safe harbors depend on several criteria. For example, its proximity to tumor suppressor genes and oncogenes is important to define the risk of malignant transformation. Several studies about integration-dependent activation of cancer genes have identified unsafe sites for integration[99]. Additionally, transformation promoting sites and promising safe-harbor sites have been investigating by retroviral gene trap screening[101]. According to these criteria, the human genome has three genomic safe harbor sites which have been employed for transgene insertion. These are the adeno-associated virus integration site 1 (AAVS1), a human orthologue of the mouse ROSA26 locus, and the chemokine receptor 5 (CCR5) gene locus. The murine ROSA26 locus was found by retroviral gene trapping screen[102]. This region has been widely used to insert transgenes into the mouse genome[103]. The CCR5 gene encodes a major co-receptor for HIV-1 and its null mutation provides resistance for HIV-1 infection[104]. However, recently it was observed that CCR5 knock-out mice display susceptibility to West Nile virus infection[100]. Although there is a safety issue, the CCR5 locus has been used for transgene integration.

18

The intron 1 of the protein protease 1-regulatory subunit 12C (*PPP1R12C*) gene on human chromosome 19 is mostly employed for the gene integration by adeno-associated viruses (AAVs). The intron 1 is referred to as the AAVS1 locus[105,106]. The AAVS1 locus has been utilized for a long term, stable transgene expression. The disruption of *PPP1R12C* by transgene integration has not been reported as being related to any known abnormalities[81].

As a conclusion, transgene integration into genomic safe-harbors has many advantages. For instance, it provides predictable gene expression and reduces the risk of unwanted integration. The gene integration can be achieved by using ZFN, TALEN or CRISPR/Cas9 system through a creation of DSB on DNA and by applying homology-directed repair to integrate the gene of interest into the genome[107]. This thesis uses this approach to generate human cell lines used as reporters of transcription.

2.   AIM OF THE STUDY

In the first part of the study, we aimed to generate reporter cell lines by using genome editing tools to investigate the activity of p53. For this purpose, we generated a donor DNA which includes homology arms targeting the human AAVS-1 genomic safe harbors, puromycin gene for selection and a luciferase cassette, which contains thirteen p53 binding sites (p53 response elements), a heterologous promoter, and the firefly luciferase gene. In this reporter system, luciferase expression is activated by the binding of p53 to its response elements located upstream of the promoter of the luciferase gene. To integrate the luciferase cassette and puromycin gene into the genomic safe-harbor AAVS-1 site, HCT 116 WT cell line was cotransfected with customized TALENs and donor DNA.

Besides, TALEN-dependent genome editing, we conducted another experiment to create reporter cell line by using another approach, which is random integration. For random integration, we used two different plasmids. One of these includes a luciferase cassette for the construction of reporter system and the other plasmid contains the neomycin gene for selection. HCT 116 WT cell lines were cotransfected with these two plasmids.

In the second part of the study, we aimed to screen a variety of small molecule compounds to reveal their effects on cell viability, DNA damage, and the accumulation, posttranslational modification, and activation of the p53 protein. Principally, p53 can be activated by several factors, such as DNA damage, oxidative stress, and small-molecule inhibitors that separate it from its inhibitor MDM2. Upon activation, p53 translocate to the nucleus to activate the expression of its target genes[35]. In detail, the aim of the cell viability assay was to check the impact of the compounds on cell viability and to study whether the compounds cause cell death in a p53-dependent manner. To evaluate the impact of the compounds on the accumulation of the p53 protein, we decided to check total p53 protein levels by western blotting. To determine if the accumulation of p53 results from its specific phosphorylation, we selected the serine 15 residue of the p53 protein whose phosphorylation is induced by DNA damage signaling and performed western blotting to determine Ser15 phosphorylation levels.

We also aimed to study the effect of the compounds on DNA in terms of the induction of double-strand breaks. For this purpose, we determined changes in phospho-H2A.X levels which is an indicator of the presence of double-strand breaks by western blotting. Another goal was to investigate the effect of compounds on p53 activity. To carry out this goal, we generated a cell-based reporter system. By using this system, we identified the changes in the transcriptional activity of p53 depending on treatment with a variety of compounds.

The last goal of the study was to identify whether the chemical compounds being tested have any potential to block the interaction between MDM2 and p53 by using the fluorescent two-hybrid assay and live cell imaging.

3. MATERIALS & METHODS

3.1. Materials

3.1.1. Chemicals

Chemicals used in this thesis are presented in Appendix A.

3.1.2. Equipment

Equipment used in this thesis are presented in Appendix B.

3.1.3. Solutions and Buffers

<u>Calcium Chloride ($CaCl_2$) Solution:</u> 60 mM $CaCl_2$ solution, 15% Glycerol, 10 mM PIPES (pH 7.0) solution were mixed and total volume completed to 500 ml with distilled H_2O (dd H_2O). The solution was filter sterilized and stored at 4°C.

<u>Agarose Gel:</u> For 100 ml 1% w/v agarose gel, 1 g of agarose powder was dissolved in 100 ml 0.5X TBE buffer by heating and 0.002% (v/v) ethidium bromide was added to the solution.

<u>Tris-Borate-EDTA (TBE) Buffer:</u> For 1 L 5X stock solution, 54 g Tris-base, 27.5 g boric acid, and 20 ml 0.5M EDTA (pH 8.0) were dissolved in ddH_2O. The solution is stored at room temperature.

<u>Phosphate-Buffered Saline (PBS):</u> For 1 L 1X solution, 100 ml 10X PBS was mixed with 900 ml ddH_2O to make 1 L solution. The solution was filter-sterilized.

<u>PBS-Tween20 Solution (PBS-T):</u> For 1 L 1X solution, 0.5 ml Tween20 was added into 1L 1X PBS.

<u>Blocking Buffer</u>: For 10 ml blocking buffer, 0.5 g skim milk powder was dissolved in 10 ml PBS-T.

Protein Loading Buffer: For 10 ml 4X protein loading buffer, 2.4 ml Tris-base (1M pH 6.8), 0,8 g SDS, 4 ml glycerol (100%), 0.01% bromophenol blue, and 2 ml β-mercaptoethanol were mixed in ddH$_2$O.

SDS Separation Gel: For 10 ml 10% gel, 2,5 ml Tris (1.5M pH 8.8), 4 ml ddH$_2$O, 3.34 ml Acrylamide/Bis-acrylamide (29:1), 100 μl 10%SDS, 100 μl 10% APS, and 10 μl TEMED were mixed.

SDS Stacking Gel: For 5 ml 4% gel, 1.25 ml Tris (0.5M pH 6.8), 2.70 ml ddH$_2$O, 1 ml Acrylamide/ Bis-acrylamide (29:1), 50 μl 10%SDS, 15 μl %10 APS, and 7.5 μl TEMED were mixed.

Tris-Glycine Solution: For 1L 10X stock solution, 40 g Tris base, 144 g Glycine were dissolved in dH$_2$O and its pH was adjusted to 8.3. For 1X SDS running buffer, 100 ml tris-glycine solution was mixed with 895 ml dH$_2$O and 5 ml 20% SDS solution. For 1X transfer buffer, 100 ml Tris-glycine solution was mixed with 200 ml methanol, and 700 ml dH$_2$O.

Antibody Dilution Solution: 1% BSA, and 0.5% sodium-azide in PBS-T.

Enhanced Chemiluminescence (ECL) Solution: For 5 ml ECL, 234 ml Tris (1.5M pH 8.8), 25 µl luminol, 12,5 µl coumaric acid, 4.728 ml ddH2O, and 1.5 µl H$_2$O$_2$ were mixed.

Polyethyleneimine (PEI) Solution: For 1mg/ml solution, 20 mg polyethyleneimine powder was dissolved in 20 ml ddH$_2$O by heating at 80°C and the pH was adjusted to 7.0 with hydrochloric acid (HCl). The solution was filter-sterilized, aliquoted as 1 ml in each 1.5 ml tube and kept at -20°C.

3.1.4. Growth Media

Luria Broth (LB): To prepare 1 L LB media, 20 g LB powder was dissolved in 1 L ddH$_2$O and then autoclaved at 121°C for 15 minutes. For selection, ampicillin at a final concentration of 100 μg/ml, kanamycin at final concentration 50 μg/ml was added to the liquid medium just before use.

LB-Agar: To prepare 1 L LB-agar medium, 35 g LB-Agar powder were dissolved in 1 L ddH$_2$O and then autoclaved at 121°C for 15 minutes. After cooling down to 50°C the LB-Agar solution was poured into sterile petri dishes. Before pouring onto sterile petri dishes, ampicillin at a final concentration of 100 μg/ml or kanamycin at a final concentration of 50 μg/ml was added to the medium for selection. Sterile agar plates were kept at 4°C.

DMEM: DMEM is supplemented with 10% heat-inactivated fetal bovine serum (FBS) and 1% Pen-Strep (100 U/mL Penicillium and 100 μg/mL Streptomycin).

Freezing Medium: Heat-inactivated FBS containing 10% DMSO (v/v) was filtered-sterilized.

3.1.5. Molecular Biology Kits

Commercially available molecular biology kits used in this thesis given in Appendix C.

3.1.6. Enzymes

Restriction enzymes, DNA modifying enzymes, polymerase enzymes, and their corresponding buffers were obtained from either New England Biolabs (NEB) or Fermentas.

3.1.7. Antibodies

Antibodies used in this thesis are given in Appendix D.

3.1.8. Bacterial Strains

E. coli DH-5α strain is used for general transformation and cloning applications.

3.1.9. Mammalian Cell Lines

Human colorectal carcinoma cell line, its p53-null derivative (ATCC CCL-24[TM]) and Baby hamster kidney cell line (ChromoTek) are used in this thesis.

3.1.10.   Plasmids and Primers

Oligonucleotides which were used in this thesis are shown in Table 3.1.

OLIGONUCLEOTIDE NAME	SEQUENCE	PURPOSE OF USE
AAVS forward	CTGTCTCTGACCTGCATTC	PCR
AAVS reverse	GGTCCAGGCCAAGTAGGTG	PCR
Luciferase forward	ATCTTCCAGCGGATAGAATGGC	PCR
Luciferase reverse	GGAGGAGTTGTGTTTGTGGACGAAG	PCR
HA-R reverse	CTCAGGTTCTGGGAGAGGGTAG	PCR

Table 3.1. List of oligonucleotides.

Plasmids which were used in this thesis are shown in Table 3.2.

PLASMID NAME	PURPOSE OF USE	SOURCE
pSV2-Neo	Selection plasmid containing neomycin gene for selection	ATCC
pG13-luc	Donor plasmid for luciferase cassette	Addgene (#16442)
pGL3-Basic	Intermediate plasmid for construction of luciferase cassette	Promega
AAVS1 SA-2A-puro-pA-donor plasmid	Plasmid for donor DNA construction	Addgene (#22075)
hAAVS1 1L TALEN	Mammalian expression plasmid for TALEN system	Addgene (#35431)
hAAVS1 1R TALEN	Mammalian expression plasmid for TALEN system	Addgene (#35432)
pcDNA3-GFP	To check transfection efficiency	Lab construct

Table 3.2. List of plasmids.

3.1.11. DNA and Protein Molecular Weight Markers

DNA ladders and protein ladders used in this thesis are given Appendix E.

3.1.12. Software, Computer-based Programs, and Websites

Software, computer-based programs, and websites used in this thesis are given in Table 3.3.

SOFTWARE, PROGRAM, WEBSITE NAME	COMPANY/WEBSITE	PURPOSE OF USE
CLC Main Workbench v7.9.4	QIAGEN Bioinformatics	Molecular cloning
NCBI PRIMER-BLAST	https://www.ncbi.nlm.nih.gov/tools/primer-blast/	Basic local alignment tool, primer design
Ensembl Genome Browser	http://www.ensembl.org	Human genome information
Addgene	https://www.addgene.org	Plasmid map information
Chimera	https://www.cgl.ucsf.edu/chimera/	Visualization of PDB files
Visual Molecular Dynamic (VMD)	http://www.ks.uiuc.edu/Research/vmd/	Analysis PDB files
AutoDock	http://autodock.scripps.edu/	Docking
IN Cell Developer	GE Healthcare	Analysis of colocalization

Table 3.3. List of software, computer-based programs and websites.

3.2. Methods

3.2.1. Bacterial Cell Culture

3.2.1.1. Bacterial culture growth

E. coli DH5α strain was cultured in LB supplemented with appropriate antibiotic for overnight (16 hours) at 37°C with shaking at 221 rpm. In order to obtain single bacterial colonies, bacterial culture was spread onto petri dishes containing LB-agar with suitable antibiotic by using glass beads and they were incubated overnight (16 hours) at 37°C without any shaking. For long term storage, bacterial culture was mixed with the sterile glycerol at 10% (v/v) final concentration in a cryo-vial. Bacterial glycerol stocks were stored at -80°C.

3.2.1.2. Preparation of competent bacteria

Previously prepared competent *E. coli* DH5α strain was inoculated in 50 ml LB without any antibiotic in a 200 ml flask and incubated overnight at 37°C by shaking at 221 rpm. Next day, 4 ml from overnight grown bacterial culture were inoculated in 2 L flask containing 400 ml LB without antibiotic and incubated at 37°C with shaking at 221 rpm until the optical density of the culture reached to 0.375 at 590 nm. 400 ml culture was divided into 8 sterile 50 ml polypropylene tubes and incubated on ice for 10 minutes, followed by a centrifugation at 1600 rcf for 10 minutes at 4°C. Then supernatant was removed, and each bacterial pellet was resuspended in 10 ml ice-cold $CaCl_2$ solution and centrifuged at 1100 rcf for 5 minutes at 4°C. Each bacterial pellet was resuspended again in 10 ml ice-cold $CaCl_2$ solution and incubated on ice for 30 minutes. Following the final centrifugation at 1100 rcf for 5 minutes at 4°C, the pellets were resuspended in 2 ml ice-cold $CaCl_2$ solution and all bacterial suspensions were pooled in one polypropylene tube. The suspension of competent bacteria was dispensed into 200 μl aliquots into pre-chilled microcentrifuge tubes. Competent cells were frozen immediately in liquid nitrogen and were stored in -80°C freezer.

Transformation efficiency of the competent bacteria (typically10^7-10^8 cfu/μg) was calculated by transforming of pUC19 plasmid at different concentrations (1000-100-10 pg) by using heat-shock transformation method.

3.2.1.3. Transformation of competent bacteria

Heat-shock transformation method was applied through all transformation experiments. Chemically competent *E. coli* DH5α cells were taken from -80 C and thawed on ice. While 1 pg-1 ng DNA was mixed with competent bacteria for pure plasmid transformation, 5 μl- 20 μl ligation mix was added into competent bacteria for ligated product transformation. The cells were then incubated on ice for 30 minutes. After the incubation period, the cells were heat-shocked at 42°C for 90 seconds and placed again on ice for 2 minutes. 800 μl LB (without any antibiotic) was added on the heat-shocked cells and this culture was incubated at 37°C for 45 minutes. After the incubation cells were spread with glass beads on LB-agar plate containing appropriate antibiotic for selection. The plates were incubated at 37°C overnight (16 hours) without any shaking.

3.2.1.4. Plasmid DNA isolation

Plasmid DNA isolation from bacteria was performed by using alkaline lysis protocol as described in Molecular Cloning: A Laboratory Manual (Sambrook *et al*). In addition to alkaline lysis protocol, PureLink HiPure Plasmid Midiprep and ZymoPure Plasmid Maxiprep commercial kits were employed for plasmid DNA isolation according to manufacturer protocols.

3.2.2. Mammalian Cell Culture

3.2.2.1. Maintenance of cell lines

HCT 116 WT cells, HCT 116 p53-/- cells, and BHK cells were maintained in DMEM medium in sterile tissue culture plates and incubated in an incubator set to 37°C with 5% CO_2. When the confluency of the cells reached to 80%, the cells were split into sterile tissue culture plate containing pre-warmed, fresh medium with a 1:10 ratio.

3.2.2.2. Cell cryopreservation

Cells were frozen in the freezing medium for later use and storing at early passage. The cells at the exponential growth phase were counted and centrifuged at 300 rcf for 5 minutes. 1-5x10^6 cells were resuspended in 1 ml freezing medium and transferred into cryovials. Cryovials were placed into a freezing container and stored at -80°C freezer for at least 24 hours and then transferred to liquid nitrogen tank for long term storage.

3.2.2.3. Thawing frozen mammalian cells

Cryovial was removed from liquid nitrogen storage and thawed. After thawing the cells, they were immediately mixed with 9 ml growth medium in 15 ml centrifuge tube to dilute DMSO in the freezing medium. The cells were centrifuged at 300 rcf for 5 minutes to remove any residual DMSO. Cell pellet was resuspended in DMEM medium. The cells were placed into sterile tissue culture plate and incubated at 37°C with 5% CO_2.

3.2.2.4. Transient transfection of mammalian cells by polyethyleneimine (PEI)

One day before the transfection, the required number of cells were split onto 6-well tissue culture plate. On the day of the transfection, 3 µg of total plasmid DNA was mixed in 200 µl serum-free phenol-free DMEM in a sterile microcentrifuge tube. PEI (1µg/µl) was added to the DNA-DMEM mix at a 3:1 ratio of PEI (µg) to total plasmid DNA (µg) and mixed immediately by vortex. After 15 minutes of incubation at room temperature, the mixture was added dropwise onto the cells.

3.2.2.5. Genomic DNA isolation

Genomic DNA isolation was performed by PureLink Genomic DNA Mini Kit and Multisource Genomic DNA Miniprep Kit according to manufacturer's protocol.

3.2.3. Vector Construction

3.2.3.1. Vector construction protocol

Restriction enzyme digestion: Digestion reactions were performed by mixing desired amount of DNA and required enzymes with their compatible buffers in PCR tube, followed by incubation in Thermal Cycler for 1-3 hours at the optimum temperature regarding to the enzyme.

De-phosphorylation of 5' phosphate groups: If the plasmid DNA was digested with a single enzyme or compatible enzymes and was planned to be used in a ligation reaction, then 5' phosphate groups of linearized plasmids were removed by alkaline phosphatase enzyme (calf intestinal alkaline phosphatase, (CIAP) to block self-ligation.

Agarose gel electrophoresis and DNA purification from the gel: PCR products, digestion reaction and other DNA samples were separated and visualized by agarose gel. Gel were prepared by dissolving the required amount of agarose depending on the size of the DNA fragment (in 0.7-2 g range) in 100 ml 0.5X TBE. This mixture was heated in a microwave in order to completely dissolve the agarose. The solution was then cooled down and 2 µl ethidium bromide (0.002% v/v) was added. DNA samples were mixed with DNA loading dye and loaded into solidified agarose gel and electrophoresis was performed at 100V for 45-90 minutes in 0.5X TBE. For the gel extraction DNA band of interest was cut from the gel under the UV light with minimum UV exposure. DNA was purified by commercially available gel purification kits. For the visualization of the bands Bio-Rad Image Analyzer was used.

Ligation: Ligation reactions were performed by utilizing T4 DNA Ligase (NEB) with appropriate buffer. For all ligation experiments, 1:3 vector versus insert ratio was considered. Ligation was performed either at 16°C for 16 hours or at room temperature for 4 hours. In each cloning, vector only ligation was performed to control if self-assembly is occurred. The ligation reaction was transformed into chemically competent *E. coli* DH5α bacteria and plated onto LB-agar petri dishes containing appropriate antibiotic for selection and incubated at 37°C for 16 hours without any shaking.

3.2.3.2.   Donor DNA construction

Intermediate vector construction: To construct a cassette which includes p53 binding sites, a promoter, and a luciferase gene, pGL-3 basic vector was used as backbone, since it has own luciferase gene. p53 binding sequences and promoter sequences were obtained from pG13-luc (wild-type p53 binding sites) plasmid by restriction digestion. The digestion reaction was incubated at 37°C for 2 hours to obtain linearized-vector and insert. After digestion reaction 1,5 µl CIAP (20,000U/ml-Fermentas) was directly added into reaction mix and incubated at 37°C for 30 minutes. Digested products were run on 1% agarose gel and linearized-vector and insert were extracted from the gel.

	pGL3-Basic (vector)	pG13-luc (insert)
Plasmid DNA	1 µg	3 µg
Cutsmart-Buffer (NEB)	5 µl	5 µl
Hind III-HF (20,000U/ml) (NEB) (NEB)	2 µl	2 µl
ddH$_2$O	To 50 µl	To 50 µl

Before ligation reaction, control gel was performed to calculate required amount of vector and insert for ligation. Afterward, ligation reaction was performed as considered to 3:1 insert to vector molar ratio. The ligation reaction was performed either at 25 °C for 4 hours or 16 °C for overnight. Following the incubation, transformation was performed.

	1.condition	2.condition	Control
Vector	3 µl	6 µl	3 µl
Insert	1 µl	2 µl	-
T4 ligase (4000,000 U/ml) (NEB)	1 µl	1 µl	1 µl
T4 ligase buffer (NEB)	2 µl	2 µl	2 µl
ddH$_2$O	To 20 µl	To 20 µl	To 20 µl

Diagnostic digestion reaction was performed with Xho I and Eco RI-HF enzymes to select the correct intermediate vector.

Plasmid DNA	1 µg
Cutsmart Buffer (NEB)	2 µl
Xho I (20,000U/ml) (NEB)	0,3 µl
Eco RI-HF (20,000U/ml) (NEB)	0,3 µl
ddH$_2$O	To 20 µl

The digestion reaction was incubated at 37°C for 2 hours and digestion reaction was run on 2% agarose gel to select positive colony having insert.

Donor vector construction: To obtain final construct, which has right and left homology arms, a puromycin gene, and luciferase cassette (p53 binding sites, promoter and luciferase gene), second cloning experiment was performed. The AAVS1 SA-2A-puro-pA donor plasmid was used to create final donor vector. The luciferase cassette was obtained from the intermediate vector. While the AAVS1 SA-2A-puro-pA donor plasmid cut with Sal I, insert was obtained from intermediate vector by cutting with Sal I and Xho I. Due to compatibility between Sal I and Xho I, vector and insert ligated each other successfully.

	AAVS1 SA-2A-puro-pA donor (vector)	Intermediate vector (insert)
DNA	1 µg	1 µg
NEB 3.1 Buffer	5 µl	5 µl
Sal I (20,000U/ml) (NEB)	1 µl	1 µl
Xho I (20,000U/ml) (NEB)	-	1 µl
ddH$_2$O	To 50 µl	To 50 µl

Before the ligation reaction, control gel was performed to calculate required amount of vector and insert for ligation. Then, ligation reaction was performed as considered to 4:1 insert to vector molar ratio. The ligation reaction was performed either at 25 °C for 4 hours or 16 °C for overnight. Following the incubation, transformation was done.

	1.condition	2.condition	Control
Vector	2 µl	3 µl	2 µl
Insert	4,4 µl	6,6 µl	-
T4 ligase (4000,000 U/ml) (NEB)	1 µl	1 µl	1 µl
T4 ligase buffer (NEB)	2 µl	2 µl	2 µl
ddH$_2$O	To 20 µl	To 20 µl	To 20 µl

Diagnostic digestion reaction was performed with Hind III-HF restriction enzyme and incubated at 37°C for 2 hours and digestion reaction was run on 1% agarose gel to select correct donor vector.

Plasmid DNA	1 µg
Cutsmart Buffer (NEB)	2 µl
Hind III-HF (20,000 U/ml) (NEB)	0,3 µl
ddH$_2$O	To 20 µl

3.2.4. Cell-Based Reporter Assay Generation

3.2.4.1. Random gene integration

To integrate luciferase cassette into HCT 116 WT cells randomly, we used two plasmids which are pG13-luc and pSV2-Neo. First, these plasmids were linearized with Pdm I, which cut these plasmids inside ampicillin gene, by incubating at 37°C for 2 hours. Linearization was controlled in agarose gel and linearized-plasmids were purified by PCR clean-up according to manufacturer's protocol and their concentrations were then checked by NanoDrop. Later, linearized-purified plasmids were used for transfection.

Given restriction reaction was performed to linearize these plasmids.

	pG13-luc	pSV2-Neo
DNA	12 µg	6 µg
Tango Buffer	3 µl	3 µl
Pdm I (10 U/µl) (Fermentase)	2 µl	1 µl
ddH$_2$O	To 30 µl	To 30 µl

For transfection, $2,5x10^5$ cells were seeded in 6-well plate. On the transfection day, 2 µg linearized-pG13-luc plasmid and 1 µg linearized-pSV2-Neo plasmid were mixed in 200 µl phenol-free serum-free DMEM and then 15 µl PEI (1 µg/µl) was added as considering to the molar ratio of 5:1 PEI/DNA and mixture was vortexed immediately. After 15 minutes incubation at room temperature, the mixture was added dropwise onto the cells. In the meantime, to control whether transfection protocol works, another transfection was performed with pCDNA3-GFP plasmid. After 48 hours from transfection, transfected cells were treated with G418 at 800 ng/µl final concentration for 10-14 days. G418 resistance colonies were picked up under inverted light microscope and then they were analysed to check the integration.

3.2.4.2. Genome editing with TALENs and donor DNA

One day before the transfection, $8x10^5$ HCT 116 WT cells were split onto sterile tissue culture plate. On the day of the transfection, 5 µg of total plasmid (1 µg TALEN-L, 1 µg TALEN-R, and 3 µg AAVS1 SA-2A-puro-pA donor luciferase cassette plasmid) was mixed with 1 ml serum-free phenol-free DMEM in a sterile microcentrifuge tube. 25 µl PEI (1 µg/µl) was added into DNA-DMEM mix as considering to the molar ratio of 5:1 PEI/DNA and mixed immediately by vortex. After 15 minutes incubation at room temperature, the mixture was added dropwise onto the cells. After 48 hours from transfection, puromycin selection was started. Transfected cells were treated with puromycin at 1µg/ml concentration for 10-14 days. Subsequently, puromycin resistant colonies were picked up under inverted light microscope and then they were analysed to determine the integration.

3.2.4.3.   Analysis of the random and targeted integration

To examine if the random integration and targeted integration were successful, two different approaches were conducted which were polymerase chain reaction (PCR) and luciferase assay. While PCR was only performed for targeted integration, luciferase assay was applied for both integration methods.

Polymerase Chain Reaction: To determine the integration of donor DNA into targeted locus, three different polymerase chain reactions were performed. PCR with *Taq* DNA Polymerase (NEB) was performed with two different sets of primer to show the integration of luciferase cassette into targeted genomic site. Additionally, Phusion High Fidelity DNA Polymerase (NEB) reaction was performed with another primer set, which includes AAVS-forward and HA-R reverse primer, to show whether integration is homozygous or hemizygous.

We performed the following reaction with either the couple of AAVS-forward and Luciferase reverse primers or Luciferase forward and AAVS-reverse primers

Standard *Taq* Buffer	2,5 µl
MgCl$_2$	1,5 µl
10 mM dNTPs	0,5 µl
10 µM Forward Primer	0,5 µl
10 µM Reverse Primer	0,5 µl
5 M Betaine	5 µl
Taq DNA Polymerase (5,000 U/ml) (NEB)	0,125 µl
Genomic DNA	50 ng
ddH$_2$O	To 25 µl

Following PCR was performed with the pair of AAVS-forward and HA-R reverse primer.

5X Phusion GC Rich Buffer	4 µl
10 mM dNTPs	0,4 µl
10 µM Forward Primer	1 µl
10 µM Reverse Primer	1 µl
Phusion HF DNA Polymerase (2,000 U/ml) NEB	0,2 µl
Genomic DNA	50 ng
ddH$_2$O	To 20 µl

Luciferase Assay: To detect the p53-dependent luciferase expression of the colonies which were derived from random integration or targeted integration luciferase assay was performed. One day before, all colonies were seeded onto 6-well plate as $2,5 \times 10^5$ cells per well. All colonies were treated with doxorubicin at 1 µM concentration for 24 hours. Following 24 hours treatment, doxorubicin was removed, and equal number of cells were harvested from each colony to perform luciferase assay. To measure the luciferase activity of the colonies, 20 µl cell lysate was loaded into Lumitrac 600 96-well plate and then 40 µl luciferase assay buffer was added onto them. Immediately, luciferase activities of the colonies were measured by spectrophotometry.

3.2.5. The Screening of Compound Library

3.2.5.1. Compound preparation

All compounds were dissolved in dimethyl sulfoxide (DMSO) at 100 mM stock concentration and stored at – 20°C. Then, 10 mM working stock was prepared by diluting 100mM stock in DMSO. All treatment experiments were conducted by using 10 mM stock.

3.2.5.2.   Cell viability assay

To check the effects of the compounds on cells, MTT assay was used. HCT 116 WT and HCT 116 p53-/- cells were treated with compounds at increasing doses (1-5-10 μM) and incubated for 48-96 hours, then cell viability was measured with MTT assay according to manufacturer's protocol. DMSO-treated cells were used to normalize the cell viability.

3.2.5.3.   Treatment, cell lysis, and western blotting

One day before the treatment, cells were seeded as $2,5x10^5$ cells/ well onto 6-well plate and then cells were treated with a variety of compounds at certain concentrations and incubated for different time intervals. After the treatment, cells were trypsinized and counted to prepare cell lysate with equal number of cells for each compound. $5x10^5-1x10^6$ cells for each compound were centrifuged at 300 rfc for 5 minutes and then supernatant was discarded. The cells were washed with 1 ml 1X PBS and centrifuged at 300 rcf for 5 minutes to remove 1X PBS. The cell pellets were mixed with appropriate volume of 1X PBS and 4X protein loading buffer depending on cell number. The mixture was boiled at 95°C for 10 minutes. Cell lysates were either used immediately or stored at -80°C for later use.

SDS polyacrylamide gels were prepared depending on the molecular weight of the protein of interest. Depending on the interested proteins, either 12,5% separating gel or 10% separating gel, and 4% stacking gel were prepared during all western blotting experiments. After the preparation of gel and loading of the samples as 20 μl in each well, SDS polyacrylamide gels were run with 1X running buffer at 80 V (constant voltage) for 1.5-2 hours using a BIORAD Mini Protean Tetra Cell. After separation of proteins, SDS polyacrylamide gels were transferred to 0.45 μm PVDF transfer membrane (Thermo Scientific) in 1X transfer buffer at 250 mA (constant current) for 1-1.5 hours depending on the molecular weight of protein at 4°C using BIORAD Mini Trans-blot. After the transfer of protein to membrane, membrane was blocked in 10 ml PBST-milk (5% w/v) at room temperature for 1 hour by shaking at 25 rpm and then membrane was washed 3-times with 10 ml PBS-T for 10 minutes each by shaking at 31 rpm. Primary antibody

incubations were performed overnight (16 hours) at 4°C with constant shaking and then membrane was incubated with secondary antibody which is in PBST-milk (5% w/v) for 1 hour at room temperature with constant shaking. After incubation with antibodies, same washing steps were repeated and then membrane was treated with an enhanced chemiluminescent substrate and analysed by using ImageQuant™ LAS4000 Biomolecular imager.

3.2.5.4.   Screening of the compounds with cell-based reporter assay

One day before treatment with the compounds, colony 6 was seeded in 24-well plate as $4x10^4$ cells/ well. The reporter cells were treated with different compounds at a final concentration of 1 μM for 72 hours. After the incubation, compounds were removed, and cells were washed with 1 ml 1X PBS. Then, 150 μl 1X Passive Lysis Buffer was added onto cells in 24-well plate and 24-well plate was shaken at 900 rpm for 20 minutes at 25 °C for lysis. Cell lysate from each compound was collected into microcentrifuge tubes and centrifuged at 1300 rpm for 30 seconds. BCA protein assay was performed according to manufacturer's protocol to measure total protein amount. To measure luciferase activity, 20 μl lysate was loaded into Lumitrac 600 96-well plate for each compound and 40 μl luciferase assay buffer was added onto the cell lysate and immediately luciferase activity was measured by spectrophotometry.

3.2.5.5.   Fluorescent two-hybrid assay

Fluorescent two-hybrid (F2H) assay is microscope-based technique which is used to evaluate inhibitors for protein-protein interaction. Principally, in F2H assay tethering strategy is applied by using lac operator sequence whose repeats are specifically integrated into the genome of modified mammalian cells. Green fluorescence tagged bait protein can be localized in lac operator site by using lac I sequence which can specifically bind lac operator sequence[108]. Lac I sequences can either linked to green fluorescence protein or can be used as separated system. In separated system green fluorescence binding protein (GBP) which is a nanobody is linked to Lac I sequences. Thus, Lac I bring GBP to lac operator site, followed by the recruitment of GFP and its tagged bait

protein resulted in the formation of green spot. Red fluorescence tagged prey protein binds to bait protein and cause red spot formation[109]. Finally, co-localization occurs in the lac operator site. F2H system enables to visualize the interaction between two partner proteins and to screen specific inhibitors which can block this interaction.

To visualize compound-dependent blocking of the interaction between p53 and MDM2, we used F2H assay system according to manufacturer's protocol and performed live cell imaging. In our case p53 protein is tagged with GFP and MDM2 protein is tagged with RFP, also another vector produces Lac I linked to GBP. Baby hamster kidney cell line (BHK) which has lac operator sequences in its genome is used for F2H assay and live cell imaging. To perform F2H assay and live cell imaging, BHK cells were transfected with TagGFP-p53, TagRFP-MDM2, and GBP-Lac I plasmids by using PEI as considering to 3:1 or 4:1 DNA/PEI molar ratio. After 24 hours from transfection, BHK cells were treated with various compounds at different concentrations and compound-dependent disappearance of the interaction was scanned by In Cell Analyzer (General Electric).

Given ingredients and required amounts was used for the transfection.

Ingredients	6-well plate	24-well plate	96-well plate
TagGFP-p53	1 μg	0,3 μg	0,1 μg
TagRFP-MDM2	1 μg	0,3 μg	0,1 μg
GBP-Lac I	1 μg	0,3 μg	0,1 μg
PEI (1ng/ μl)	9 μg	1,8 μg	1,2 μg
Serum-free phenol-free DMEM	200 μl	50 μl	20 μl
BHK cell number	$2,5x10^5$ cells/well	$5x10^4$ cells/ well	$1x10^4$ cells/well

4.   RESULTS

4.1. Cell – Based Reporter Assay Generation

The sequence-specific transcription factor p53 binds to its response element and then activates the expression of target genes[6]. To detect the activity of p53 directly, we generated reporter cell lines which can express the luciferase enzyme under the control of p53 in a sequence-specific manner. We used two different approaches to integrate a luciferase gene into the HCT 116 WT genome: TALEN aided homology-directed repair and random integration. For targeted integration, we selected the safe-harbor AAVS1 site which is located in intron 1 of the *PPP1R12C* gene[105,106]. In the second approach, non-homologous insertion/transformation ability of these cells was used to integrate the luciferase gene randomly into the human cellular genome. Non-homologous insertion needs little or no dependence on sequence homology, hence it mostly results in random and high copy number integration.

4.1.1.   Donor DNA Construction

To generate a donor DNA that targets the AAVS1 site, we used a donor vector which includes suitable homology arms for the site (Addgene plasmid #22075)[110]. Because there were no suitable restriction sites in the donor vector, we created an intermediate vector by integrating p53 binding sequences and a promoter upstream of the luciferase gene. First, the pG13-luc plasmid[111] was cut with Hind III to obtain a fragment containing the p53 binding sequences and the polyoma promoter. The p53 binding sequences and polyoma promoter were ligated into the pGL-3-Basic plasmid to create an intermediate vector. Insertion was confirmed with diagnostic digestion performed with XhoI cutting from the vector and Eco RI cutting from the insert. Colonies with correct oriented inserts were selected, because forward-oriented inserts gave a 282 bp digestion product, while reverse-oriented inserts gave a 225 bp digestion product. Later, this luciferase cassette was removed from the intermediate vector by Xho I and Sal I digestion and cloned into Sal I digested AAVS1 SA-2A-puro-pA-donor plasmid. The cloning strategy is shown in Figure 4.1.
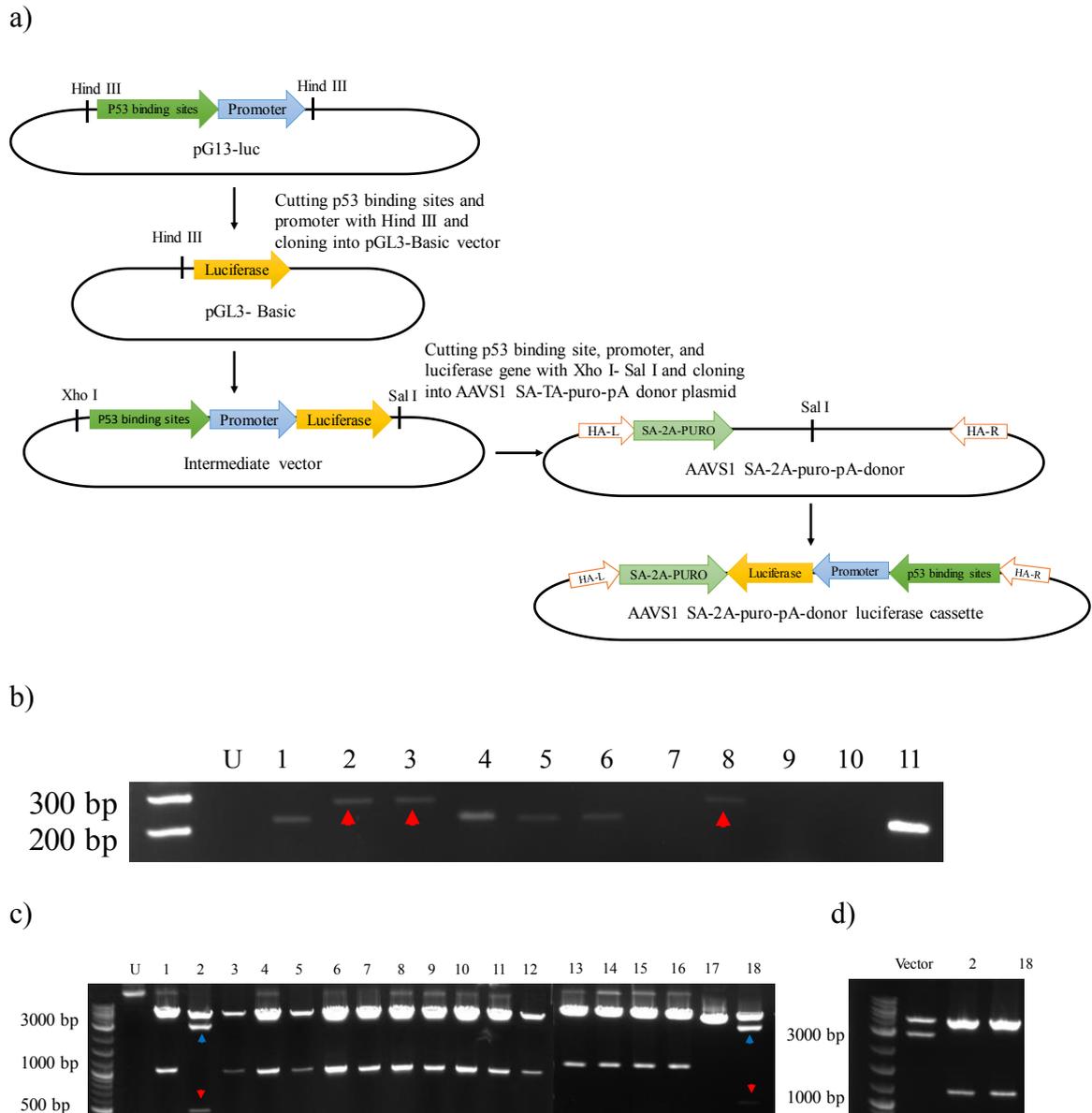
Figure 4.1. The donor vector construction. a) Schematic representation of cloning: pG13-luc, pGL-3-Basic, and AAVS1 SA-2A-puro-pA-donor plasmid were used to create donor DNA. b) Restriction digestion with Xho I and EcoRI to select correct intermediate vector. Red arrows show the inserts in the forward orientation. c) Cloning of the luciferase cassette into the donor plasmid: Restriction digestion with Hind III displayed that colony 2 and 18 have the insert (red arrows) in reverse orientation (blue arrows) d) EcoRI restriction digestion reconfirmed that colony 2 and 18 have the insert in the reverse orientation. V: vector, U: uncut.

To confirm the identity of this final plasmid, the diagnostic digestion was carried out with Hind III, which has two restriction sites in the vector and two restriction sites inside the luciferase cassette. We observed 3 different situations for Hind III digestion: (1) empty vector gave 992 bp product- (2) the vector which has forward oriented luciferase cassette gave 465 bp, 1001 bp, 1969 bp, and 5610 bp products and- (3) the vector which has reverse-oriented luciferase cassette gave 33 bp, 465 bp, 2937 bp, and 5610 bp products. We obtained two colonies which contain the luciferase cassette in the desired, reverse orientation. Additionally, these two colonies were re-confirmed with Eco RI digestion. These digestions showed that both have the correct insert the in reverse orientation. Therefore, colony 2 was selected as a template DNA for the generation of reporter cell lines (Figure 4.1c-d). We wanted to insert the luciferase expression cassette in the reverse orientation into the AAVS site because we did not want to interfere with the *PPP1R12C* gene expression.

4.1.2.   Luciferase Cassette Integration by TALENs and HDR

The AAVS1 site which is mostly used for the integration by adeno-associated viruses was chosen to integrate the luciferase cassette. This site provides long-term expression for integrated genes[106]. We used two plasmid that were previously developed that encode a pair of TALEN proteins targeting AAVS1 site (Addgene numbers #35431 and #35432)[92]. To integrate the luciferase cassette into this site, HCT 116 WT cells were transfected with three plasmids encoding the Left-TALEN, the Right-TALEN, and the AAVS1 SA-2A-puro-pA-donor luciferase cassette. First, double-strand break was formed specifically in this site by TALENS. Subsequently, the created double-strand break was repaired by the cells with either HDR or NHEJ. The AAVS1 SA-2A-puro-pA-donor luciferase cassette plasmid was used by the cells as a template to repair the break by HDR. This plasmid contained homology arms for the integration into the AAVS1 by HDR. The sequences between two the homology arms were integrated into this site via HDR (Figure 4.2). Transfected cells were treated with 1 μg/ml puromycin to select the cells having integration. Because the puromycin gene is located between these two homology arms. In the case of puromycin integration into this site, the cells start to express puromycin under the control of an endogenous promoter and become puromycin resistant.

In addition to using puromycin for selection, it might be used an indicator of specific integration because the puromycin gene does not contain any promoter. Thus, its expression is regulated by the promoter of *PPP1R12C* gene only after homologous integration. After puromycin treatment for 10-14 days, puromycin positive cells formed individual colonies. These colonies were picked up and grown individually. Later, these colonies were analyzed with the polymerase chain reaction method to show specific luciferase cassette integration and luciferase assay was performed to confirm the functionality of the cell-based reporter assay.
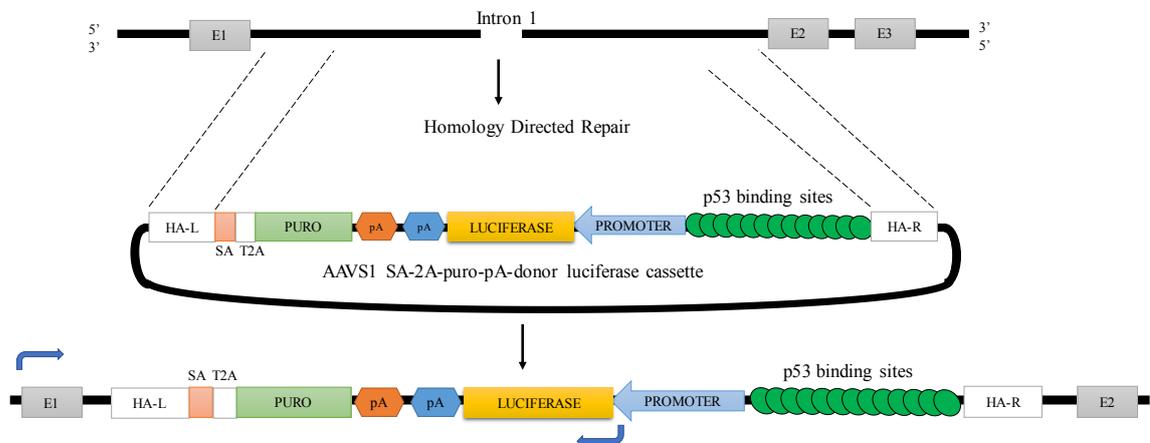
a)
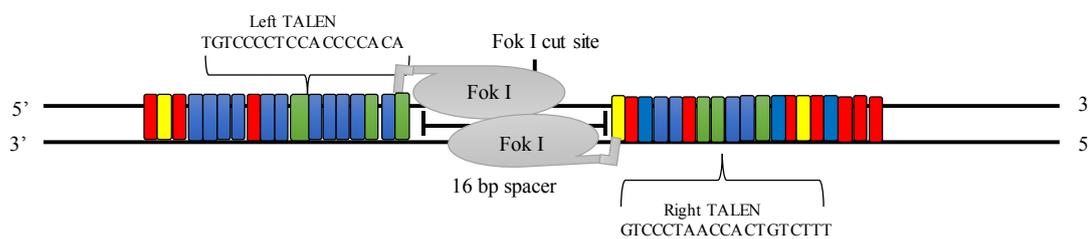
b)

Figure 4.2. Schematic representation of luciferase cassette integration by TALENs and HDR. a) TALENs work as a pair. When right TALEN and left TALEN bind to the target sequence in intron 1 of *PPP1R12C* gene specifically Fok I can cleave DNA from both strands and create the double-strand break. b) Luciferase cassette integration into the AAVS1 site through HDR.

4.1.2.1. Analysis of the integration with polymerase chain reaction

We conducted three different polymerase chain reaction experiments to determine whether the integration of the donor construct was homozygous or hemizygous. We designed five primers: while two of them bind to intron 1 of the *PPP1R12C* gene without binding to donor DNA, other two primers only bind to the luciferase gene (Figure 4.3a). The last primer can bind to both intron 1 and the luciferase cassette. The pair of AAVs-forward primer and luciferase-reverse primer and the pair of luciferase forward primer and AAVs-reverse primer were used to conclusively demonstrate the presence of targeted integration (Figure 4.3b-c). Additionally, we carried out another PCR with a pair of AAVs-forward and HA-R reverse primers to determine whether the integration was hemizygous. Because the pair of AAVs-forward and HA-R reverse primer gives a specific product for wild-type genome. PCR results showed that most of the colonies have luciferase cassette integration in just one allele. However, some colonies did not give any products for both wild-type genome and luciferase cassette in the PCR with AAVs-forward and HA-R reverse primer. These colonies were determined to contain the insertion in both alleles (Figure 4.3d).
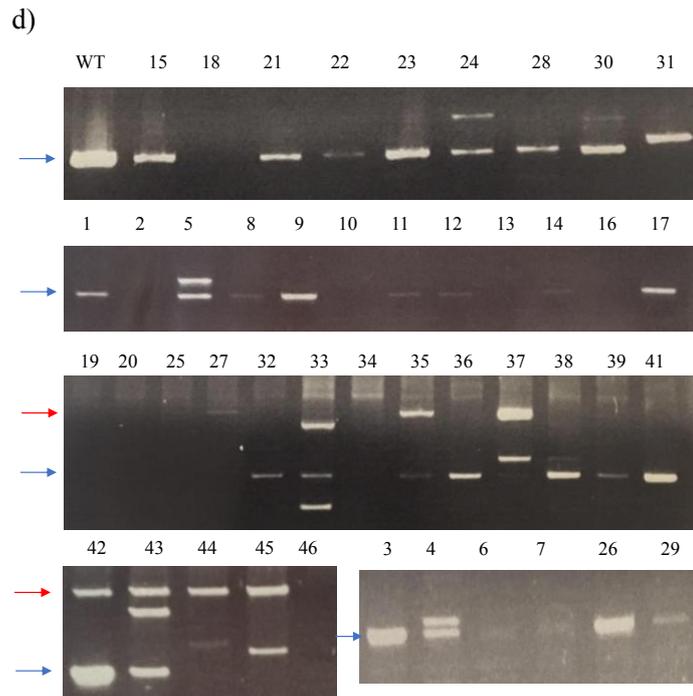
d)
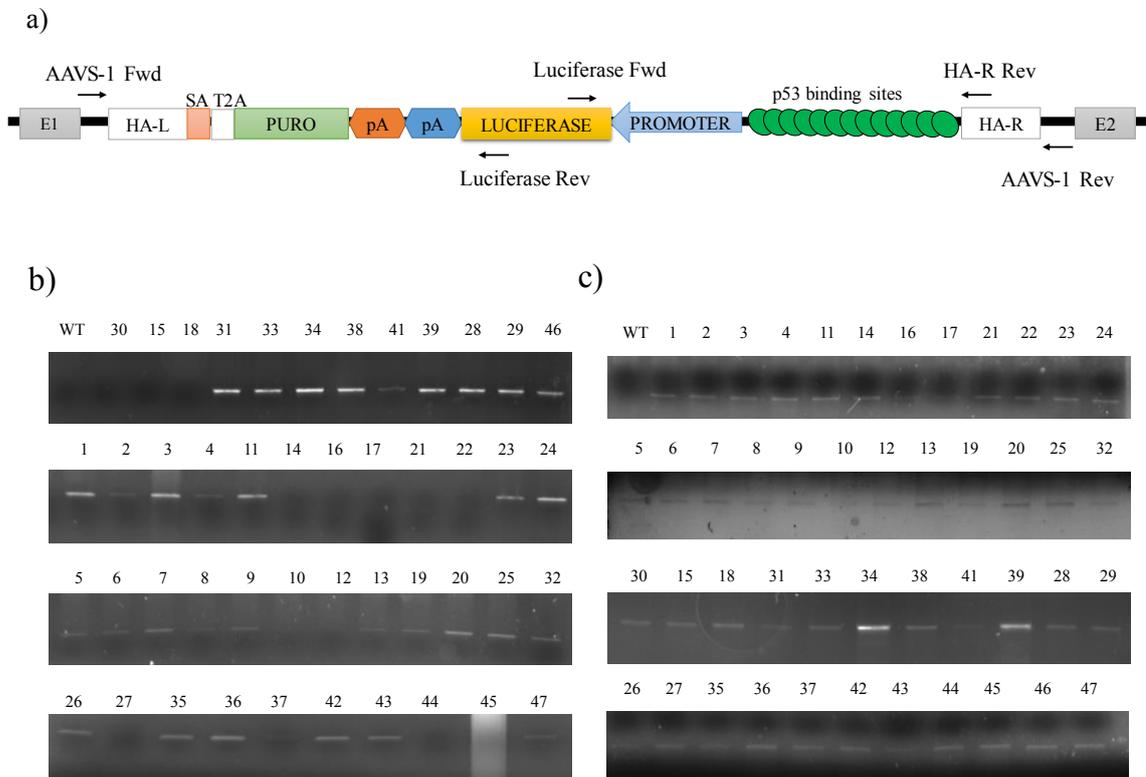
Figure 4.3. Analysis of the integration by polymerase chain reaction. a) Binding sites of the primers were shown. b) PCR was carried with the pair of AAVS-forward and luciferase reverse primer. Most of the colonies gave 2.4 kb PCR product because of insertion. c) PCR was conducted with the pair of luciferase-forward and AAVS-reverse primer. PCR product in 1.5 kb length showed successful integration. d) PCR was conducted with a couple of AAVS-forward and HA-R reverse primers. While 1.7 kb (red arrow) PCR product indicated wild-type allele, 4.7 kb (red arrow) band showed that luciferase cassette integration.

4.1.2.2.   Detection of the functionality of the reporter cell lines

After the determination of luciferase cassette integration into the genome, the next step was the evaluation of the functionality of the reporter cell lines. In this reporter system, luciferase expression is controlled by p53. In detail, 13 consecutively repeated p53 binding sites act as an enhancer to activate the polyoma promoter driving luciferase expression. Therefore, we checked if the system works when p53 is activated by DNA damage in these cells. For this purpose, the p53-dependent luciferase activities of colonies were evaluated by a luciferase reporter assay after doxorubicin treatment. Doxorubicin increases p53 level in cells by causing DNA damage[112]. In the presence of DNA damage, p53 is activated by several kinases and then p53 translocate into the nucleus. The translocation of p53 into the nucleus initiates the expression of p53 target genes[7].

Puromycin resistant 47 colonies were treated with 1 μM doxorubicin for 24 hours and their luciferase activity were measured by luciferase assay (Figure 4.4). We observed three different patterns in luciferase activity of the colonies: (1) 22 colonies showed very low luciferase activity, (2) 18 colonies showed moderate luciferase activity, (3) 7 colonies showed high luciferase activity. In accordance with luciferase assay results, these 7 colonies (colony 3-4-6-7-26-29-46) were selected for further analysis.
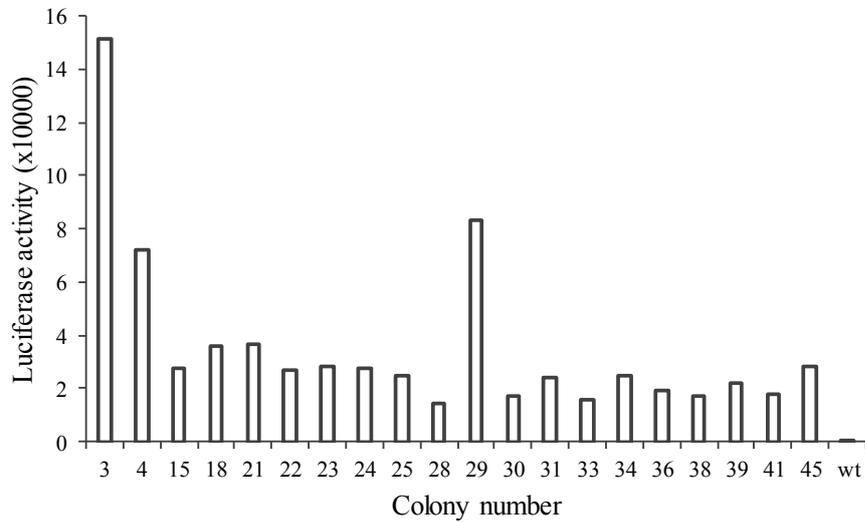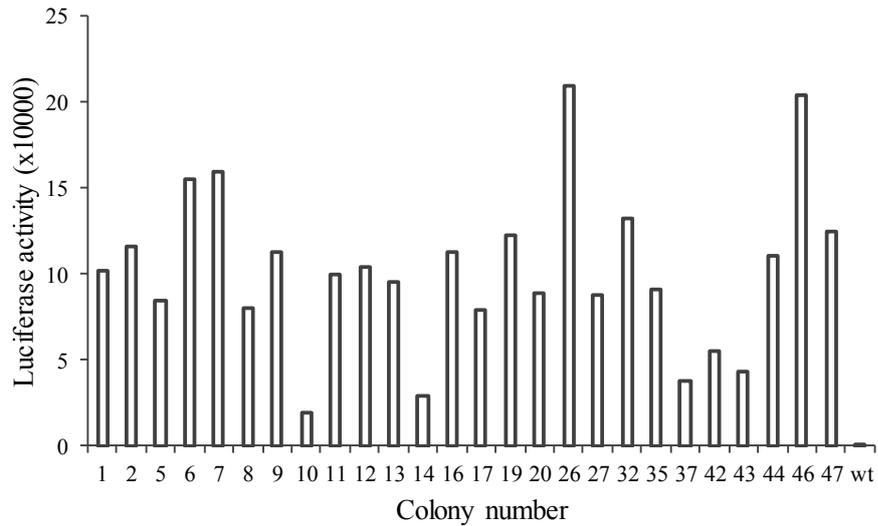

Figure 4.4. Validation of cell-based reporter system by luciferase assay. Puromycin resistance 47 colonies were expanded and their p53 dependent luciferase activities were analyzed under 1 μM doxorubicin treatment for 24 hours. Luciferase activities of the colonies were calculated by subtracting their background luciferase activities from their total luciferase activities.

Further, to make a more specific analysis about p53-dependent activation of luciferase expression, the selected colonies were treated with 10 μM Nutlin-3a for 24 hours which activates p53 by blocking the interaction between p53 and MDM2[65]. In the meantime, selected colonies were separately treated with 1 μM doxorubicin for 24 hours to elucidate the consistency of these reporter cell lines and to compare the doxorubicin response with Nutlin-3a (Figure 4.5). As expected, Nutlin-3a responses of the colonies were lower than their doxorubicin response except colony 29. Nutlin-3a only blocks the p53-MDM2 interaction without changing the p53 mRNA level and without initiating damage signaling.
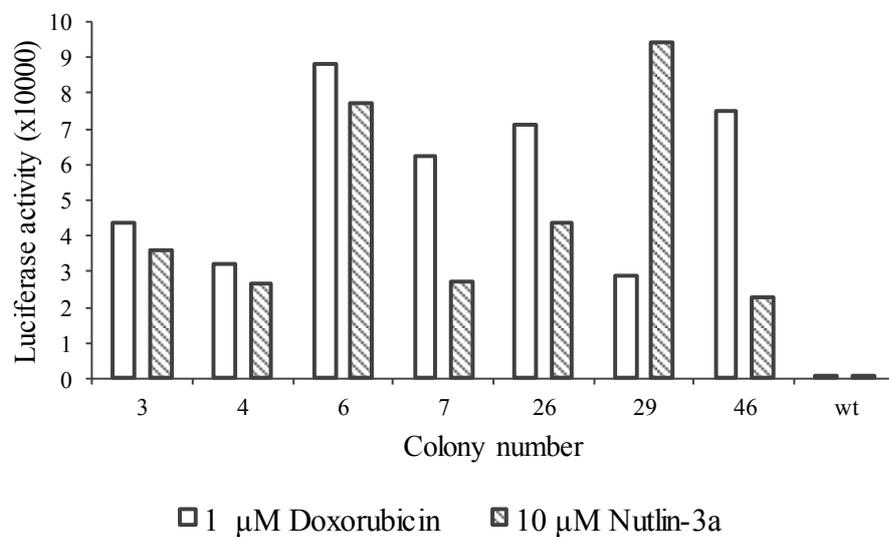

Figure 4.5. Comparison of luciferase responses of doxorubicin and Nutlin-3a. The selected colonies were treated with 1 μM doxorubicin and 10 μM Nutlin-3a for 24 hours separately. Luciferase activities of the colonies were measured by luciferase assay. Luciferase activities of the colonies were calculated by subtracting their background luciferase activities from their total luciferase activities.

Moreover, time-dependent luciferase activities of the selected seven colonies were measured with a time-course experiment. Selected colonies were treated with 1 μM doxorubicin for 0, 2, 6, 12, 18, 24 hours respectively and luciferase activities of these colonies were measured by luciferase assay (Figure 4.6).
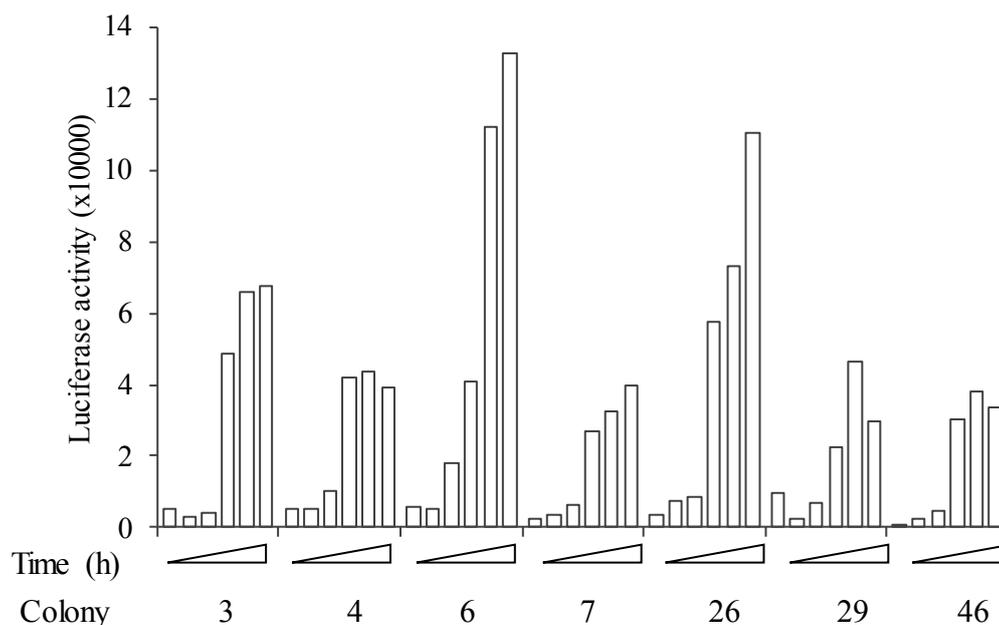
Figure 4.6. Analysis of time-dependent luciferase activity. Selected colonies were treated with 1 μM doxorubicin at increasing times (0,2,6,12,18,24 hours) and their luciferase activities were measured. Luciferase activities of the colonies were calculated by subtracting their background luciferase activities from their total luciferase activities.

Due to fact that colony 6 responded to doxorubicin and to Nutlin-3a treatment with very high luciferase activity and the expected difference between doxorubicin and Nutlin-3a response was observed and a time-dependent response was observed, colony 6 was selected to evaluate the effect of a variety of compounds on the transcriptional activity of p53.

4.1.3.   Cell-Based Reporter Assay Generation by Random Integration

HCT 116 WT cells were also cotransfected with a luciferase cassette containing pG13-luc plasmid and a neomycin cassette containing pSV2-Neo plasmid for selection. Because this luciferase cassette plasmid does not contain any selection marker, a second plasmid was required for selection. After transfection, these cells were subjected to G418 treatment at 800 ng/ml final concentration for 10-14 days to select the cells which have neomycin gene integration. We assumed that if the neomycin gene was integrated into the genome, luciferase cassette could also be integrated into the genome. Therefore, we picked up 26 neomycin resistant colonies and grew them individually to analyze the luciferase cassette integration by luciferase assay (Figure 4.7).
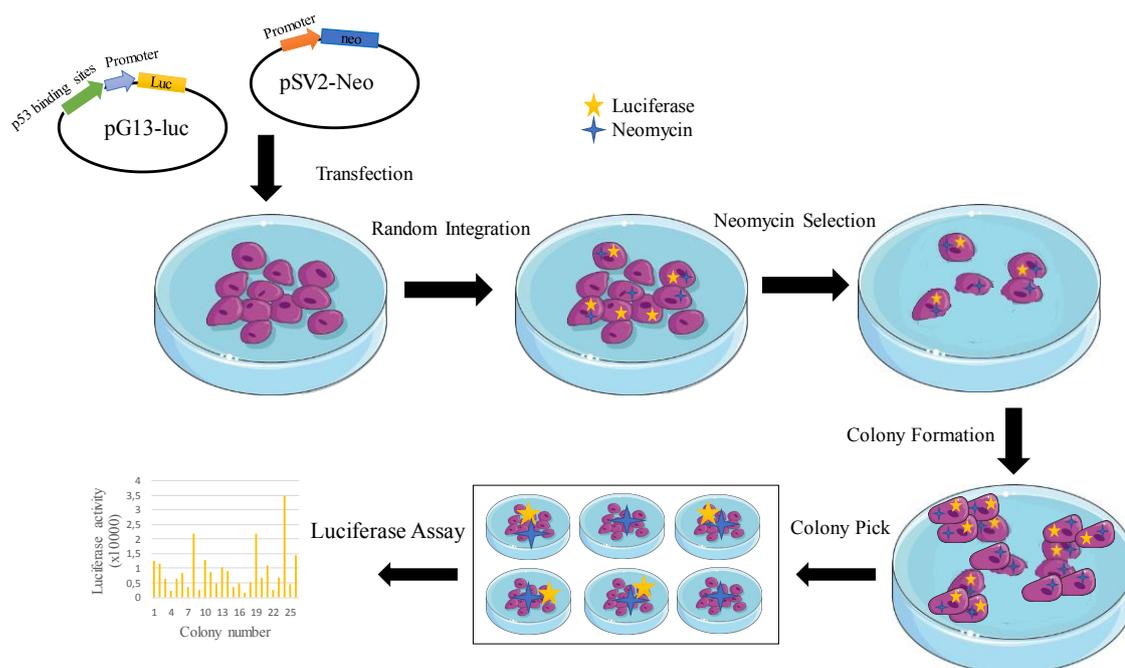
Figure 4.7. Cell-based reporter assay generation through random integration. HCT 116 WT cells were transfected with pG13-luc and pSV2-Neo. Neomycin selection, colony pick, and luciferase assay were performed respectively. Luciferase activity of the colonies was evaluated with luciferase assay.

4.1.3.1.   Evaluation of the random integration by luciferase assay

Neomycin resistant colonies were treated with 1 µM doxorubicin for 24 hours and subsequently, their luciferase activities were measured by spectrophotometry. 3 out of 26 colonies showed higher luciferase activity than the baseline determined by using extract from untreated (Figure 4.8). Nutlin-3a responses of these three colonies (8- 19 and 24) were also examined under 10 µM Nutlin-3a treatment for 24 hours (Figure 4.9). Additionally, these colonies (8- 19 and 24) were treated with 1 µM doxorubicin for 0, 2, 6, 12, 18, and 24 hours respectively and their luciferase activities were measured. As a result, colony 8, 19, and 24 showed lower luciferase activity after treatment with Nutlin-3a compared to treatment with doxorubicin as expected. Moreover, the time-course responses of these colonies showed that the highest luciferase activity was detected after 18 hours for colony 8 and 24 was detected after 18 hours treatment, while it was detected after 12 hours treatment for colony 19 (Figure 4.10).
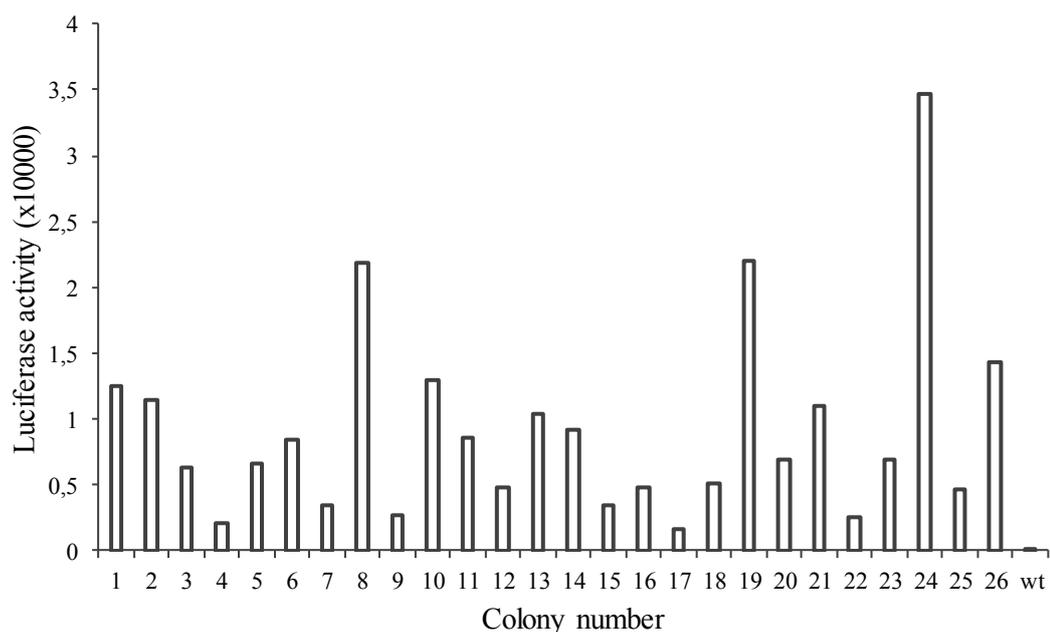
Figure 4.8. Validation of cell-based reporter system generated by random integration. Neomycin positive colonies were expanded, and their p53-dependent luciferase activities were analyzed under 1 μM doxorubicin treatment for 24 hours. Luciferase activities of the colonies were calculated by subtracting their background luciferase activities from their total luciferase activities.
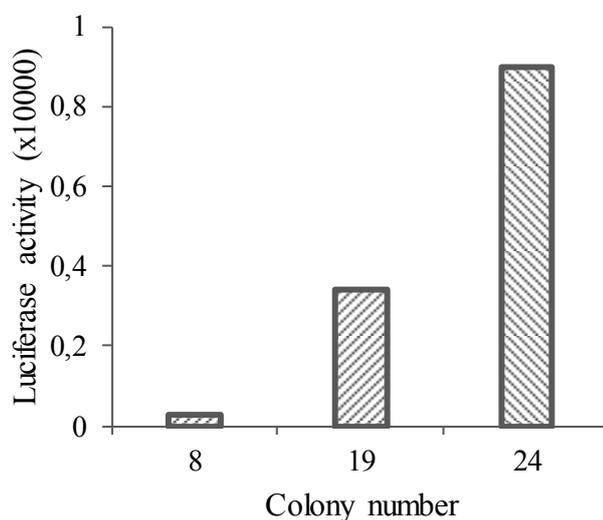
Figure 4.9. Nutlin-3a-dependent luciferase activity of the colonies. The selected colonies were treated with 10 μM Nutlin-3a for 24 hours. Luciferase activities of the colonies were detected with luciferase assay. Luciferase activities of the colonies were calculated as subtracting their background luciferase activities from their total luciferase activities.

Figure 4.10. Time-dependent luciferase activity of the colonies. Selected colonies were treated with 1 µM doxorubicin at increasing times (0,2,6,12,18,24 hours) and their luciferase activities were measured. Luciferase activities of the colonies were calculated by subtracting their background luciferase activities from their total luciferase activities.
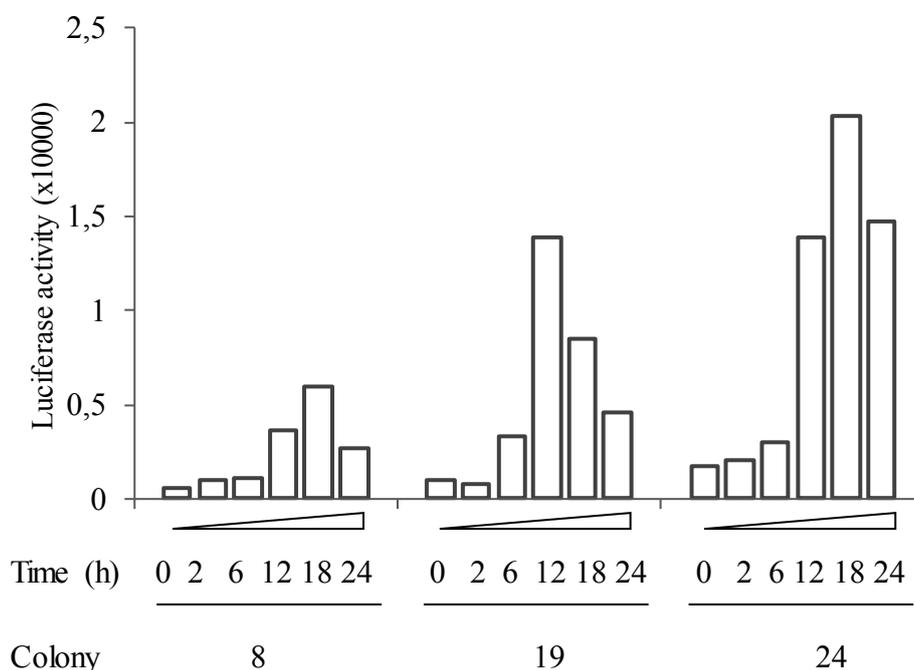
4.2. The Screening of Novel Compounds

We wanted to screen a novel small molecule compound library generated in collaboration with Prof. Burak Erman from Koc University and Prof. Nilgün Karali from Istanbul University, which contains nearly one hundred small molecules. All compounds were screened to identify a small molecule that can activate p53 without causing DNA damage in wild-type p53 carrying cells. For this purpose, we conducted a variety of experiments. The effects of the compounds on p53 accumulation, activation, and phosphorylation were investigated by using different methods. The p53 protein has a very short half-life in the absence of any kind of stimulus that can stabilize p53[7]. The p53 protein can be activated by either specifically blocking its interaction with MDM2[65] or by DNA damage[112]. To check compound-dependent p53 accumulation and phosphorylation in HCT 116 WT cells, we performed several western blotting experiments. We used our cell-based

51

luciferase reporter assay to evaluate if accumulated p53 is transcriptionally active in these cells. Moreover, we analyzed the effect of the compounds on the induction of double-strand breaks through western blotting and we also checked the viability of HCT 116 WT and HCT 116 p53-/- cells by an MTT assay to determine the impact of p53 on cell death.

4.2.1. Effects of The Compounds on Cell Viability

One of the roles of p53 is to regulate apoptosis by activating the expression of pro-apoptotic genes[10]. Thus, p53 activation can cause cell death in some circumstances, such as severe DNA damage. To explore the effects of the compounds on cell viability, we performed an MTT assay. We used two cell lines which were HCT 116 WT and HCT 116 p53-/- to determine whether these effect of compounds on cell viability is p53-dependent. We used HCT 116 p53-/- cells as a negative control to possibly show that the effect of the compounds on cell viability is p53-dependent. In such a case, the viability of these cells should not be affected. To compare the MTT assay results of the compounds, Nulin-3a was chosen as positive control, because of its specificity towards p53-sufficient cells. In the presence of wild-type p53, Nutlin-3a decreased cell viability as correlated with increasing doses, whilst Nutlin-3a did not decrease cell viability in the absence of p53 (Figure 4.11).
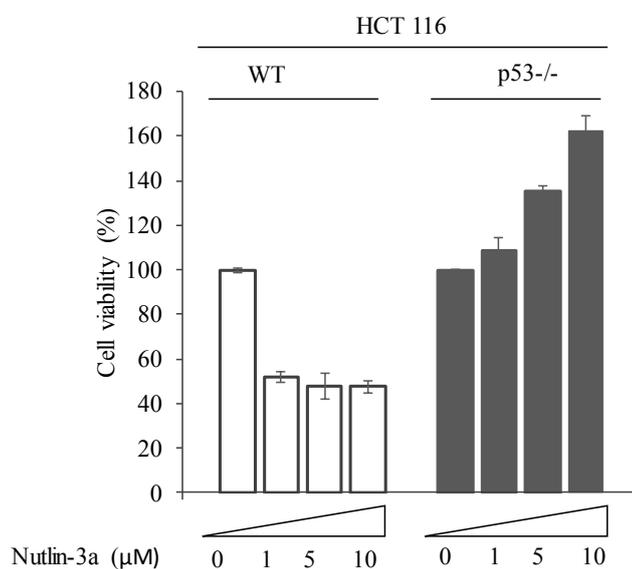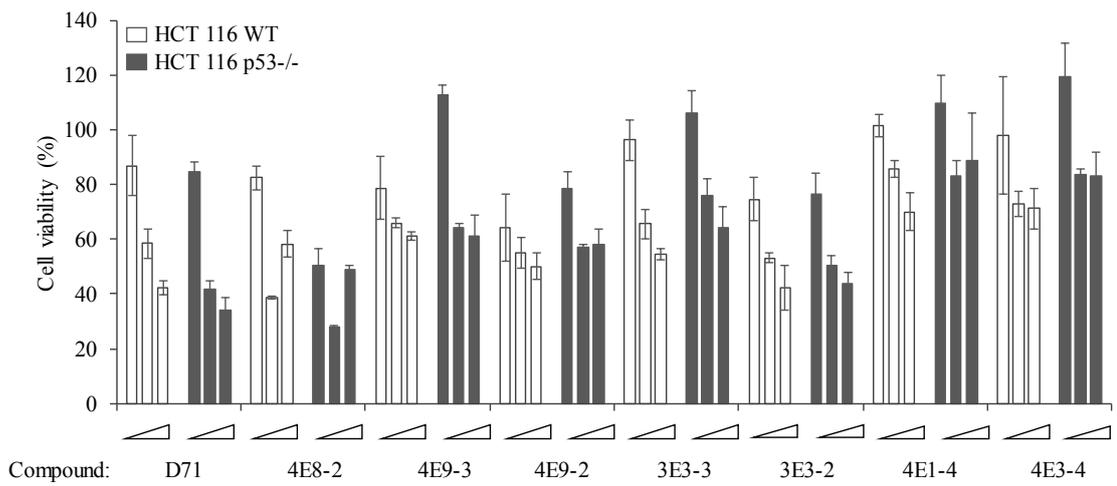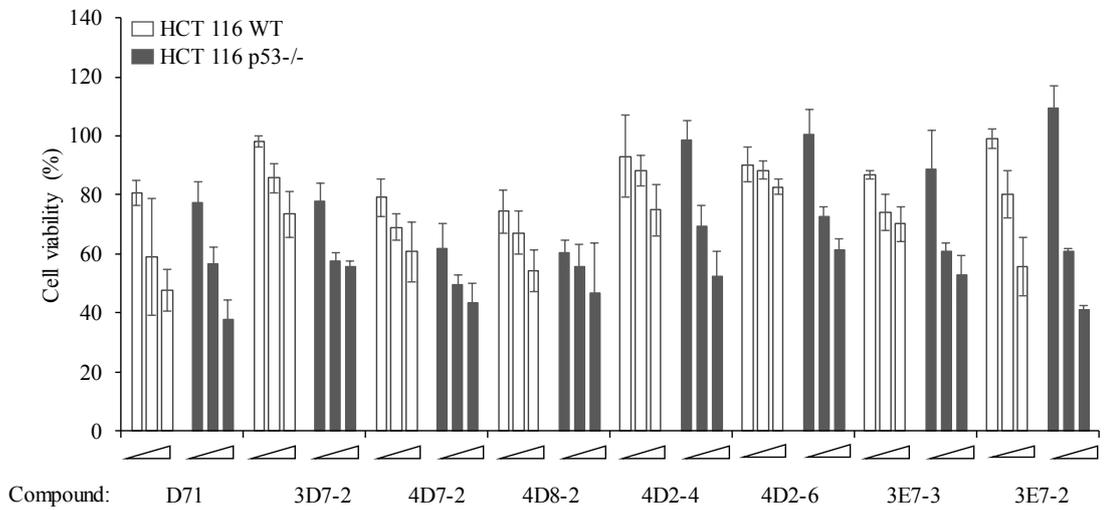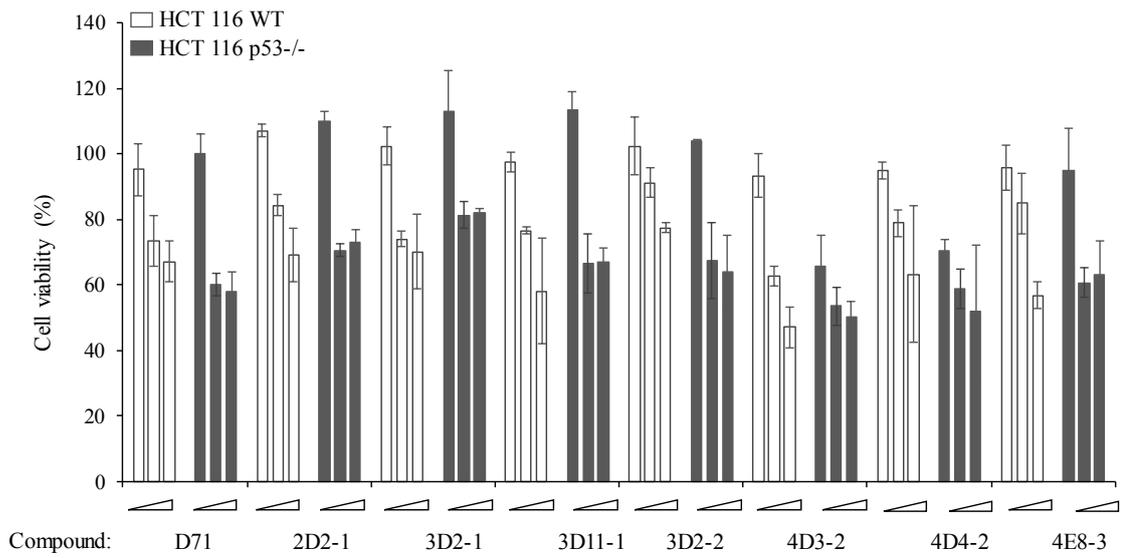

Figure 4.11. Cell viability assay with Nutlin-3a. HCT 116 WT and HCT 116 p53-/- cells were treated with Nutlin-3a at increasing doses (0-1-5-10 μM) respectively for 72 hours and then MTT assay was performed. Result was presented by normalizing to the viability of DMSO treated cells.

52
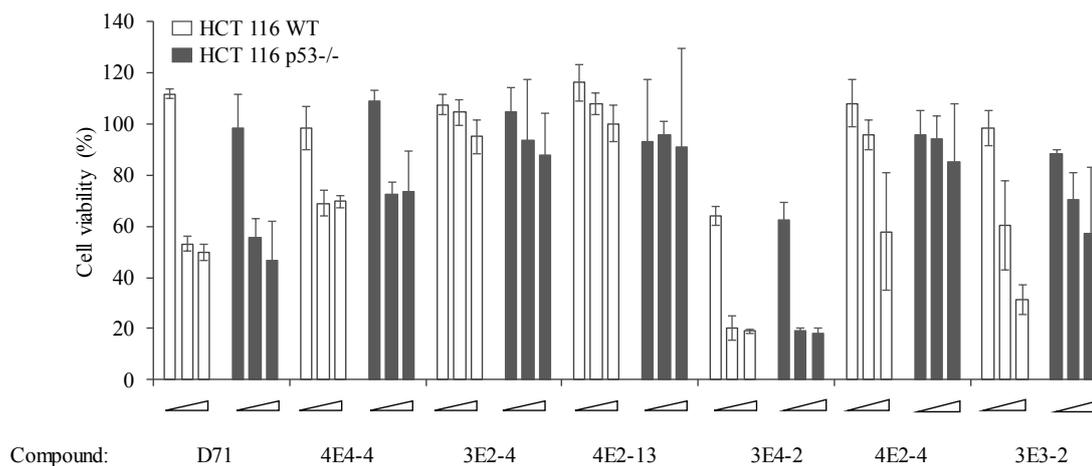
Figure 4.12. The effect of the compounds on cell viability. HCT 116 WT and HCT 116 p53-/- cells were treated with several compounds at increasing doses (1-5-10 μM) respectively for 48 hours and then MTT assay was performed. The results were presented by normalizing to the viability of DMSO treated cells.

We observed that compared to Nutlin-3a, all tested compounds caused a decrease in cell viability in both p53-deficient and sufficient cell lines (Figure 4.12). This result indicates that these compounds at these doses do not show any specificity in inhibiting the interaction between p53 and MDM2.

4.2.2. Detection of Compound-Dependent p53 Accumulation / Phosphorylation and DNA Damage

In the absence of stress or any p53 inducing agents, p53 protein level cannot be detected by western blotting due to its short half-life. If the cells are exposed to any DNA damaging agents or specific inhibitors, that prevent the interaction between p53 and MDM2, the p53 protein level can be detected with western blotting. To investigate the impact of the compounds on the p53 protein and DNA damage formation, we conducted three different western blotting experiments. First, we evaluated the p53 protein level after the treatment with various compounds by western blotting (Figure 4.13). For this purpose, HCT 116 WT cells were treated with a variety of compounds at a concentration of 10 μM for 48 hours and p53 protein levels were detected in whole cell lysates by western blotting. The effect of each of the compounds on p53 protein levels was compared with the effect of compound D71, which was used as positive control. The compound D71 was previously identified as a candidate molecule that interferes with the interaction between p53 and MDM2. Every compound induced the accumulation of the p53 protein in HCT 116 WT

cells at different levels. As a result, many compounds which increased the p53 protein level more than D71 were selected as candidate compound and they were then subjected to DNA damage analysis.
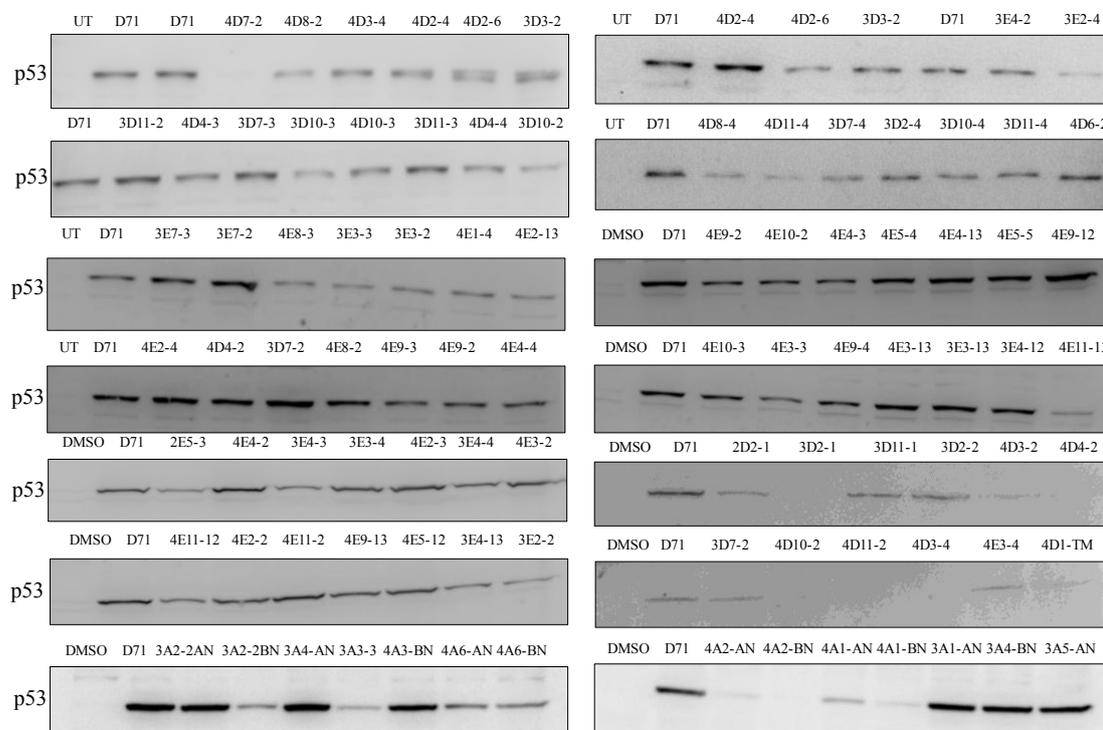
Figure 4.13. The accumulation of the p53 protein. HCT 116 WT cells were treated with a variety of compounds at 10 μM concentration for 48 hours and then the accumulation of the p53 protein (53 kDa) was analyzed in the whole cell lysates. UT/DMSO: negative control, D71: positive control.

In the second part of western blotting, selected compounds were evaluated in terms of their influence on DNA damage by phospho-H2A.X western blotting. H2A.X is a histone variant protein and is phosphorylated in the presence of DNA damage and binds to double-strand breaks on DNA[113]. The increase in the phosphorylated-H2A.X level indicates the occurrence of double-strand breaks. The phosphorylated-H2A.X level is also increased by apoptosis-dependent DNA fragmentation[114]. Like in p53 western blotting, whole cell lysates were prepared after the treatment of HCT 116 WT cells with selected compounds and phospho-H2A.X levels of the selected compounds were determined with a specific antibody. For phospho-H2A.X western blotting, doxorubicin and D71 were used as positive control, Nutlin-3a and DMSO were used as negative control. Phospho-H2A.X western blotting results indicated that all compounds led to significant double-strand break formation at different levels (Figure 4.14).
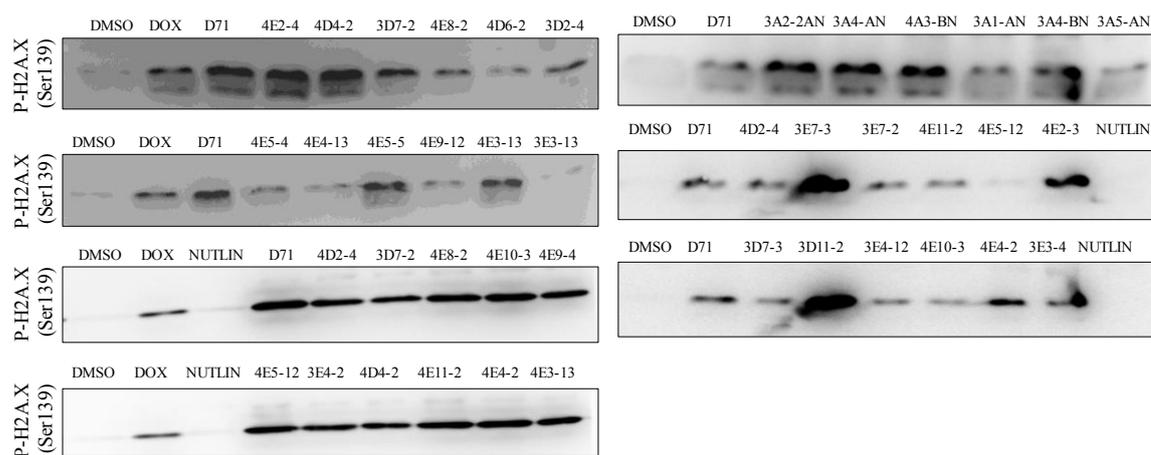
Figure 4.14. Analysis of the double-strand break formation by phospho-H2A.X. HCT 116 WT cells were treated with various compounds at 10 μM concentration for 48 hours and then phosphorylated-H2A.X (15 kDa) level was evaluated in the whole cell lysate. DMSO: negative control, D71 and Doxorubicin (was used at 1 μM concentration): positive control.

To evaluate if the compounds were activating p53 through DNA damage signaling, HCT 116 WT cells again treated with selected compounds and then harvested to check phospho-p53 protein level. Because phosphorylated-p53 on serine 15 is an indicator of damage-dependent activation of p53[115]. Therefore, western blot results indicated that selected compounds caused p53 phosphorylation at different levels (Figure 4.15). While Nutlin-3a was used as negative control, doxorubicin was used positive control for the phosphorylation of p53 in serine 15 residue.

Our aim in these experiments was to find a compound that increases cellular p53 levels by inhibiting the interaction between MDM2 and p53, without causing significant DNA damage. Unfortunately, all compounds showed at least some kind of DNA damage dependent signaling. These findings indicate that we need to increase the library size of the molecules being screened in future experiments.
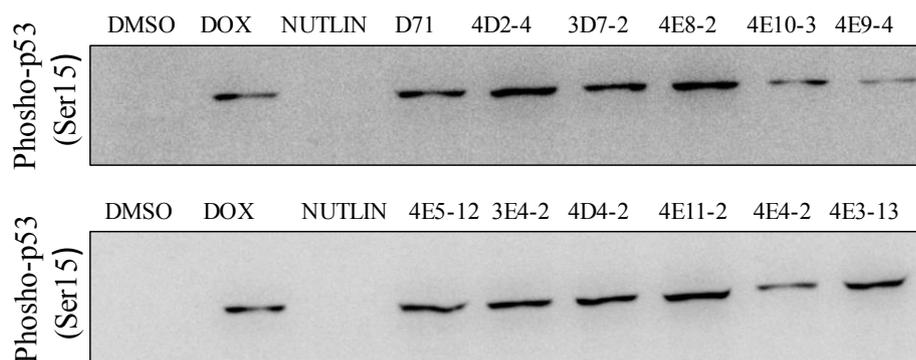
Figure 4.15. Investigation of p53 phosphorylation. HCT 116 WT cells were treated with selected compounds at 10 μM concentration for 48 hours. Afterwards, phosho-p53 level was checked in the whole cell lysate for each compound. DMSO/Nutlin-3a: negative control, D71 and doxorubicin (was used at 1 μM concentration): positive control.

4.2.3. Analysis of Compound-Dependent Changes in p53 Activity

The effect of the compounds on p53 activity was probed through cell-based reporter assay. The small molecule compound library was tested to identify those that cause p53 nuclear translocation and transcriptional activation. The reporter cell line which was generated in the first part of the study was treated with various compounds at 1 μM final concentration for 72 hours and then the changes in the luciferase activity were measured for each compound (Figure 4.16). Total protein amounts in lysates were used to normalize luciferase activity. Cell-based reporter assay results indicated that many compounds showed the same luciferase activity with untreated cells or less luciferase activity than the untreated cells and a few compounds increased the luciferase activity. In order to show that the cell-based reporter assay was working, Nutlin-3a was used as positive control. For this purpose, the reporter cell line was treated with Nutlin-3a at 10 μM concentration for 24 hours. As a result of the initial screen of all compounds, 22 compounds that yield high luciferase values were selected to reproduce these results. As a result, we found that 11 compounds reproducibly increased luciferase expression compared to untreated cells (Figure 4.17).

Figure 4.16. Screening of the compounds by cell-based reporter assay. Reporter cell line was treated with a variety of compounds at 1 µM final concentration for 72 hours. Compound-dependent luciferase activity was normalized to protein amount. The changes in luciferase activity were shown by normalizing to untreated cells' luciferase activity.

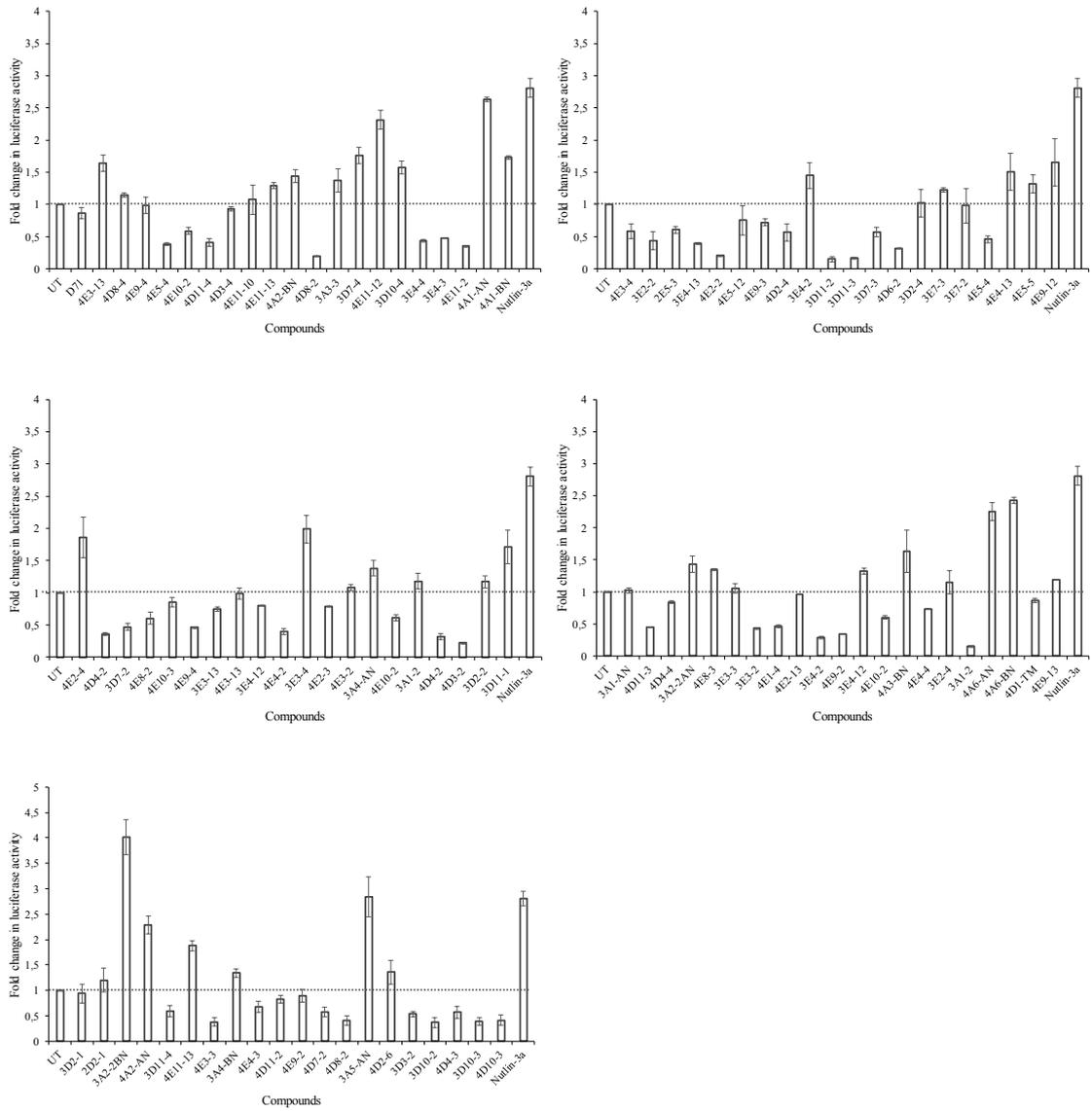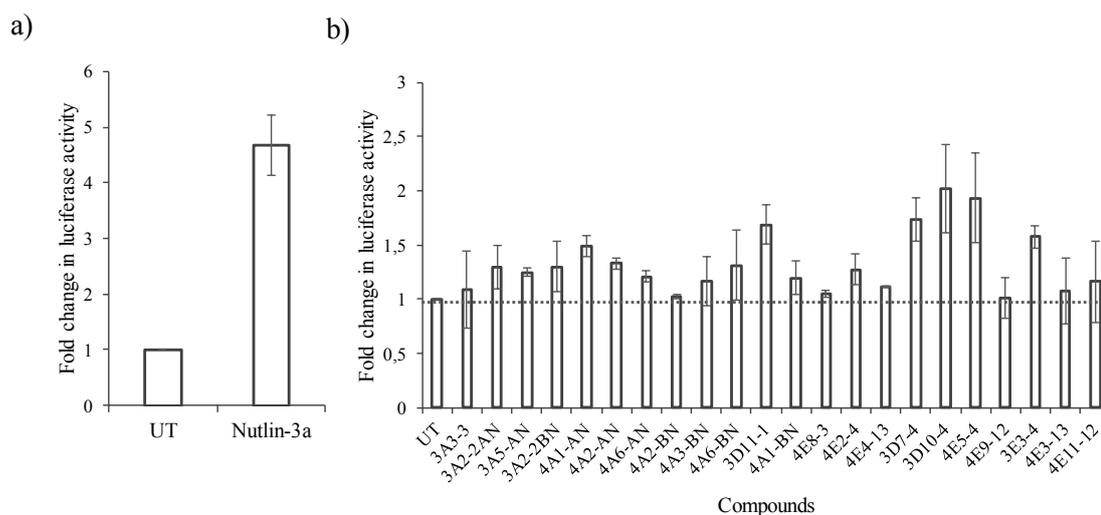**Figure 4.17. Cell-based reporter assay with selected compounds.** (a) Reporter cell line was treated with Nutlin-3a at 10 μM final concentration for 24 hours as a positive control. (b) Reporter cell line was treated with the selected compounds at 1 μM final concentration for 72 hours as triplicate. This experiment was repeated twice, and results were presented as taking the average of two experiments. Luciferase activity was calculated by normalizing to the total protein amount and then the changes in luciferase activity were shown by normalizing to untreated cells' luciferase activity.

4.2.4. Effect of The Compounds on MDM2- p53 Interaction

11 compounds which activated p53 in reporter assays were tested by the F2H assay combined with the live cell imaging technique to explore if this activation is related with the blocking of the interaction between MDM2 and p53. The BHK cell line containing tandem repeats of lac operator sequences inserted into its genome, was transfected with F2H assay's plasmids encoding LacI-GBP, GFP-p53, and RFP-MDM2 fusion proteins. 24 hours after transfection, the cells were treated with the compounds at 10 μM concentration and live cell imaging was performed immediately for 3 hours by In Cell Analyzer 2500 HS microscope. Nutlin-3a, which block the MDM2-p53 interaction, was used to check if all steps of the F2H assay and live cell imaging were working correctly. We clearly observed that Nutlin-3a rapidly reduced both the number of red (MDM2) and yellow foci (MDM2-p53 interaction) without affecting the number of green foci (p53) (Figure 4.18a). The decrease in yellow foci indicates the inhibition of the MDM2-p53 interaction. The green foci do not significantly change because the interaction between p53 and lac operator site is stabilized using a GFP binding nanobody protein fused to the lacI transcription factor. This nanobody is specific for GFP and does not bind to RFP

59

which fused to the MDM2 protein. As a result, we showed that F2H assay coupled with live cell imaging method can be used to analyze the effect of the compounds on MDM2-p53 interaction.

Selected compounds were analyzed with the same approach to identify those that could disrupt the interaction between p53 and MDM2 (Figure 4.18b). We used this assay to specifically identify compounds that inhibit the interaction between p53 and MDM2 without causing DNA damage. D71 was used as negative control because even though it elevated p53 protein levels by western blotting, it also caused DNA damage as indicated by phospho-H2AX western blotting. Moreover, it did not increase the transcriptional activity of p53 in the luciferase assay. Consequently, whilst Nutlin-3a caused a significant decrease in the interaction between MDM2 and p53 in the F2H assay, all tested compounds failed to cause any significant changes in the interaction. Foci counting and data analysis was performed using the IN Cell Developer Software by General Electric.

a)

60

b)

61
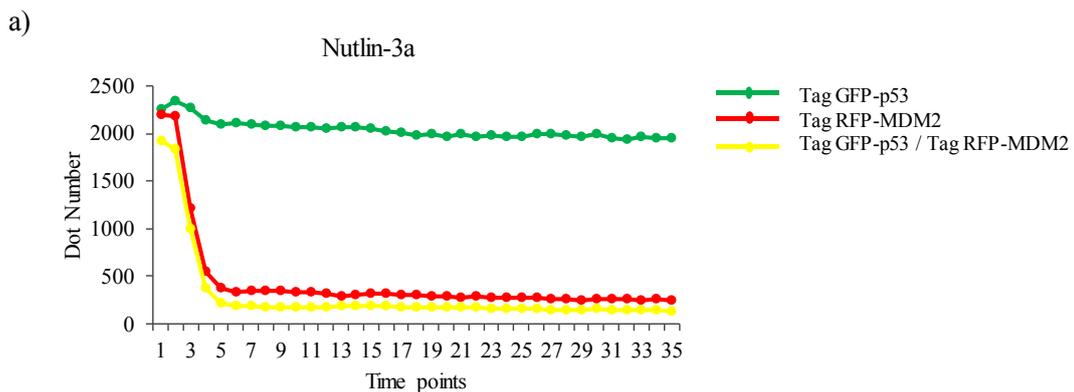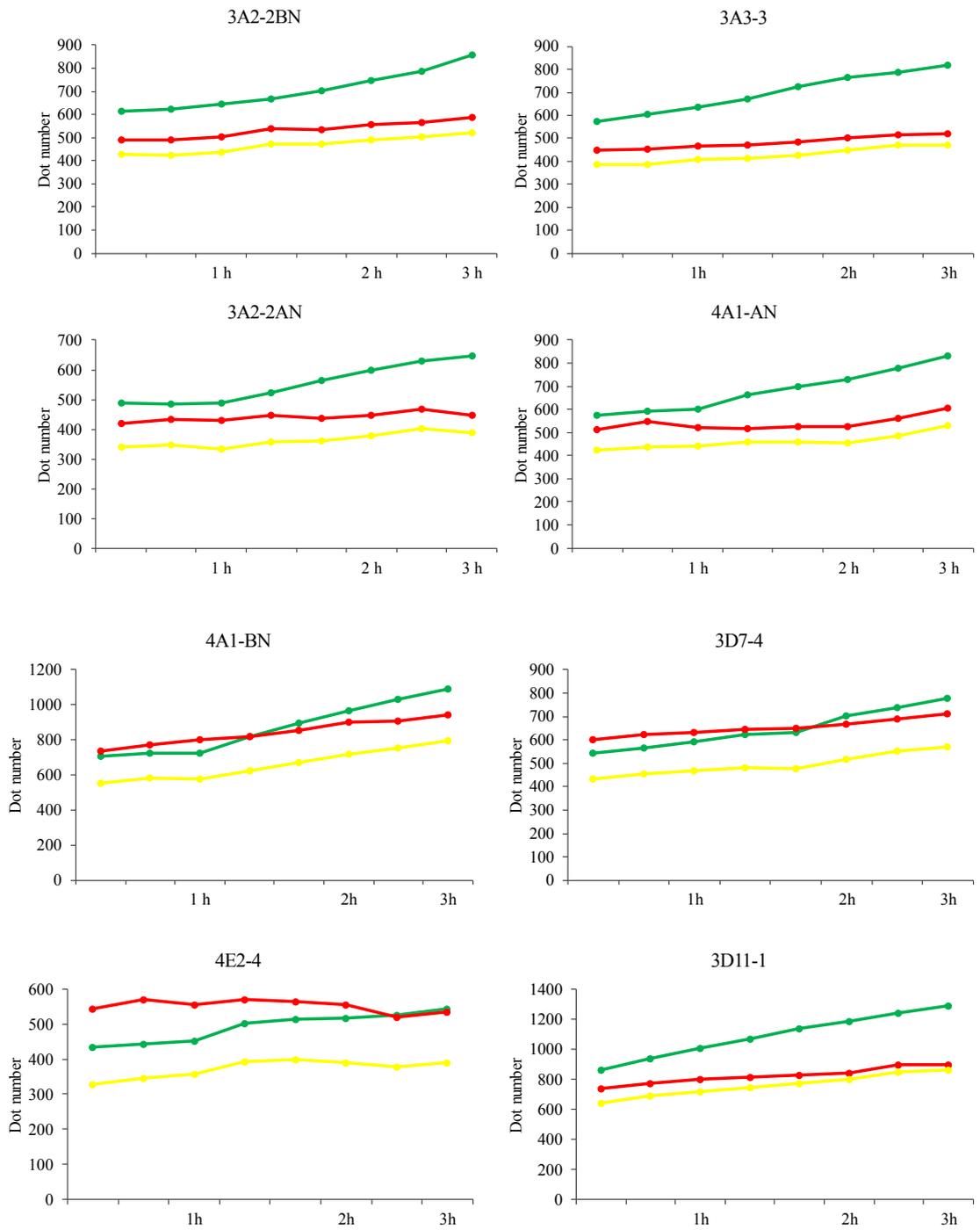
Figure 4.18. Analysis of the blocking of MDM2-p53 interaction. The combination of F2H assay and live cell imaging method was used to analyze compound-dependent disruption of MDM2-p53 interaction. a) Nutlin-3a was used as positive c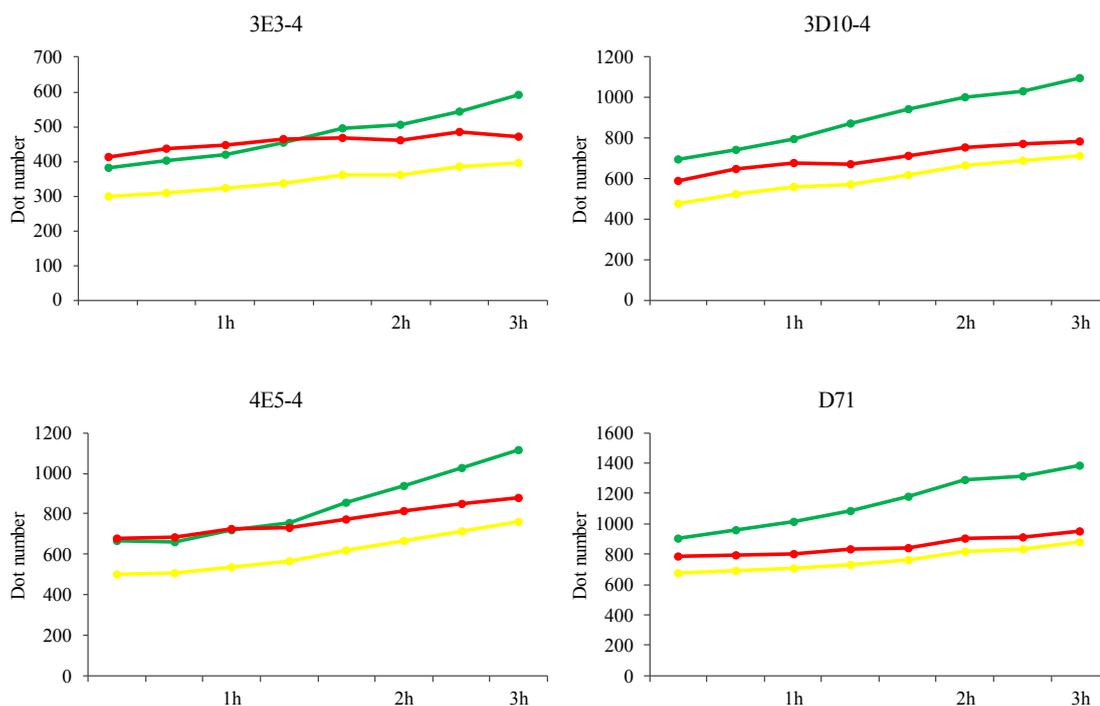ontrol for F2H assay. b) 11 compounds were tested by F2H assay to check their effect on the interaction. Green line: p53, red line: MDM2, yellow line: merge of p53 and MDM2.

5.   DISCUSSION

The sequence-specific transcription factor p53 activates the expression of various genes and regulates important cellular processes, such as apoptosis and cell cycle arrest[1]. Because of its diverse functions, the perturbations in the regulation of p53 and the mutations in the *TP53* gene are mostly associated with tumor development and progression[22,56]. p53 is strictly regulated by MDM2 through a negative feedback loop[27]. Normally, p53 is bound to the N-terminal domain of MDM2 from its transactivation domain and it is rapidly degraded by the 26S proteasome in a ubiquitination-dependent fashion. In the case of genotoxic stress, the p53 protein is activated by posttranslational modifications and translocate into the nucleus[33,35].

We generated reporter cell lines to probe the changes in the transcriptional activity of p53. We utilized genome editing tools to create reporter cell lines. First, we constructed a donor DNA which includes suitable homology arms matching with the AAVS1 target site for homologous integration, a puromycin gene for selection, and a luciferase cassette. The reason for the selection of luciferase as a reporter gene is its sensitivity, high dynamic range and ease of quantification. As noted in the result section, we designed the donor DNA construct to insert the luciferase cassette in a reverse orientation with respect to the *PPPR1C12* gene into which we inserted this cassette by homologous recombination. This design was important as transcription in the same orientation as the *PPPR1C12* gene could potentially interfere with its expression. On the other hand, transcription in the reverse orientation creates a situation where complementary double strand may form, but we did not detect any such inhibitory effect. In this system, the endogenous promoter only controlled the expression of the puromycin selection gene which did not have any promoter in the donor DNA. The endogenous promoter-induced puromycin gene expression was also used as an indicator for the site-specific insertion. We confirmed the luciferase cassette integration into the targeted site by using polymerase chain reaction and checked that if the reporter system was working efficiently by luciferase assay. p53-induced changes in the luciferase activity of the reporter cell lines were confirmed under doxorubicin and Nutlin-3a treatments. We found that most of the integrations occurred in only one allele. This might result because of the inefficiency of TALENs and the homology-directed repair mechanism. We also demonstrated that several colonies

63

contained insertion in two alleles. There are significant differences of the luciferase activity of hemizygous and homozygous colonies. This diversity might be created by the differences in the transcriptional activity of p53 in the different clones. Another reason for this variability may be the epigenetic modification of the promoter of the luciferase gene, such as methylation. Nevertheless, we obtained several colonies which can produce a significant luciferase response against doxorubicin and Nutlin-3a treatment in a stable and reproducible manner.

This study allowed us to compare reporter genes generated by insertion into a targeted safe harbor site as well as the traditional stable transfection approach. Using the second approach, we only obtained three colonies which showed significant luciferase activity depending on the activation of p53. Despite having a high integration copy number, these colonies expressed less luciferase compared to the safe harbor site integrated clones. This difference in transcriptional activity may be integration site dependent. Random integration can occur in almost everywhere the genome. However, every region in the genome does not equally activate gene expression. Additionally, there was a minor difference in the sequence of these two luciferase genes. This discrepancy might affect the luciferase enzyme's affinity towards its substrate and its speed of catalysis.

We screened numerous compounds to identify their effect on cell viability, the cellular levels of p53 protein, and DNA damage formation. We found that almost every compound causes a decrease in cell viability at different levels regardless of p53. Cell viability assay results showed that the compounds might have some side effects, thus causing cell death independent from p53. We obtained important results with respect to the impact of the compounds on p53. In the first instance, we found that each compound can induce the accumulation of p53 at varying degrees in HCT 116 WT cells. We can explain the cause of p53 accumulation with two different approaches: (1) the compounds might increase the stability of p53 by posttranslational modifications. (2) the compounds might block the interaction between MDM2 and p53 by binding to either MDM2 or p53. As a second result related with the p53 protein, we found that all tested compounds induce phosphorylation of p53 on serine 15 residue. This phosphorylation is mostly governed by ATM signaling and results in the stabilization of the p53 protein[33]. Compound-induced specific phosphorylation of the p53 protein showed that the compounds might activate stress signaling which causes the stabilization of p53. Unfortunately, all compounds

tested cause DNA damage and induce double-strand breaks. The compounds likely cause DNA damage by using several mechanisms, such as intercalating into DNA double helices, inhibiting topoisomerase II and cross-linking with DNA strands.

We also answered the following question: Is stabilized p53 transcriptionally active? To answer this question, we created a cell-based reporter assay. Reporter cell line was treated with the compounds and then the changes in luciferase activity were measured. We found that while some compounds could bring p53 to transcriptionally active state, some of them did not change luciferase activity or caused a decrease in luciferase activity. The reason for the decrease might the binding of the compounds to p53 irreversibly or the inhibition of some posttranslational modifications of p53 which might be required for passing p53 from transcriptionally inactive state to active state. These differences may be identified by performing RNAseq to differentiate between pathways that are activated by different compounds.

In this study, we also investigated whether the compounds inhibit the MDM2-p53 interaction. Considering the live-cell imaging results, we showed that the compounds cannot dissociate p53 from MDM2, although they can increase p53-dependent luciferase activity in the cell-based reporter assay. We can explain this situation by postulating that the compounds have a lower affinity against MDM2 than p53 has. This may result in the failed dissociation of p53 and MDM2 in this experimental condition. As a second explanation of the inability of the compounds to dissociate p53-MDM2 while activating p53 reporters, may be the use of alternative pathways or an issue with sensitivity.

In conclusion, we showed that homology-directed repair mechanism can be used to integrate a gene of interest into the targeted site with the help of programmable nucleases. We also confirmed that cell-based reporter assay is an efficient method to probe p53 activity. Additionally, we evaluated several compounds in respect of their influence on the cell viability, the p53 protein, DNA damage, and protein-protein interaction.

The compound screening was performed by using six different methods and all screening results were summarized in Table 5.1.

	Luc Assay	p53	p-H2AX	p-p53	F2H	MTT
D71	−	+	+	+	−	+
4D2-4	−	+	+	+	ND	+
3D7-2	−	+	+	+	−	+
4E8-2	−	+	+	+	−	+
3E7-3	−	+	+	ND	ND	+
3E7-2	−	+	+	ND	−	+
4E2-4	+	+	+	ND	−	+
4E11-2	−	+	+	+	−	ND
4E5-12	−	+	+	+	−	ND
3E4-2	+	+	+	+	ND	ND
4D4-2	−	+	+	+	ND	ND
4E10-3	−	+	+	+	ND	ND
4E9-4	−	+	+	+	ND	ND
4E3-13	−	+	+	+	ND	ND
4E4-2	−	+	+	+	ND	ND
3E3-4	+	+	+	ND	−	ND
3A2-2AN	+	+	+	ND	−	ND
3D11-1	+	+	ND	ND	−	+
3D11-2	−	+	+	ND	−	ND
3D7-3	−	+	+	ND	ND	ND
4D6-2	−	+	+	ND	ND	ND
3D2-4	−	+	+	ND	ND	ND
4E5-4	−	+	+	ND	ND	ND
4E4-13	+	+	+	ND	−	ND
4E5-5	+	+	+	ND	−	ND

	Luc Assay	p53	p-H2AX	p-p53	F2H	MTT
4E9-12	+	+	+	ND	−	ND
3E3-13	−	+	−	ND	ND	ND
3A4-AN	+	+	+	ND	ND	ND
4E2-3	−	+	+	ND	ND	ND
3E4-12	−	+	+	ND	−	ND
4A3-BN	+	+	+	ND	−	ND
3A1-AN	−	+	+	ND	−	ND
3A4-BN	−	+	+	ND	ND	ND
3A5-AN	+	+	+	ND	−	ND
4E8-3	+	+	ND	ND	ND	+
3E3-3	−	+	ND	ND	ND	+
3E3-2	−	+	ND	ND	−	+
4E1-4	−	+	ND	ND	ND	+
4E2-13	−	+	ND	ND	ND	+
3E4-2	−	+	ND	ND	ND	+
4E4-4	−	+	ND	ND	ND	+
3E2-4	−	+	ND	ND	ND	+
4E3-4	−	+	ND	ND	ND	+
4E9-3	−	+	ND	ND	ND	+
4E9-2	−	+	ND	ND	−	+
4D7-2	−	−	ND	ND	ND	+
4D8-2	−	+	ND	ND	ND	+
4D4-2	−	−	ND	ND	ND	+
4D3-2	−	+	ND	ND	−	+
3D2-2	−	+	ND	ND	−	+
3D2-1	−	+	ND	ND	ND	+

	Luc Assay	p53	p-H2AX	p-p53	F2H	MTT
2D2-1	–	+	ND	ND	–	+
4D2-6	–	+	ND	ND	–	+
3A3-3	+	+	ND	ND	–	ND
3D7-4	+	+	ND	ND	–	ND
3D10-4	+	+	ND	ND	–	ND
4A1-AN	+	+	ND	ND	–	ND
4A1-BN	+	+	ND	ND	–	ND
3A2-2BN	+	+	ND	ND	–	ND
4E5-4	–	+	ND	ND	–	ND
4A2-AN	+	+	ND	ND	–	ND
3D11-4	–	+	ND	ND	ND	ND
4E11-13	+	+	ND	ND	ND	ND
4E3-3	–	+	ND	ND	ND	ND
4E4-3	–	+	ND	ND	–	ND
4D11-2	–	–	ND	ND	ND	ND
3D3-2	–	+	ND	ND	ND	ND
3D10-2	–	+	ND	ND	–	ND
4D4-3	–	+	ND	ND	ND	ND
3D10-3	–	+	ND	ND	ND	ND
4D10-3	–	+	ND	ND	ND	ND
4D4-4	–	+	ND	ND	ND	ND
4E11-12	+	+	ND	ND	–	ND
3E4-4	–	+	ND	ND	–	ND
3E4-3	–	+	ND	ND	ND	ND
3E2-2	–	+	ND	ND	ND	ND
2E5-3	–	+	ND	ND	–	ND

	Luc Assay	p53	p-H2AX	p-p53	F2H	MTT
3E4-13	–	+	ND	ND	ND	ND
4E2-2	–	+	ND	ND	ND	ND
3D11-3	–	+	ND	ND	ND	ND
4E3-2	–	+	ND	ND	ND	ND
4E9-2	–	+	ND	ND	–	ND
3E4-12	–	+	ND	ND	ND	ND
4E10-2	–	+	ND	ND	ND	ND
4A6-AN	+	+	ND	ND	–	ND
4A6-BN	+	+	ND	ND	–	ND
4D1-TM	–	+	ND	ND	–	ND
4E9-13	–	+	ND	ND	ND	ND
4E3-13	+	+	ND	ND	–	ND
4D8-4	+	+	ND	ND	ND	ND
4E9-4	–	+	ND	ND	ND	ND
4E10-2	–	+	ND	ND	ND	ND
4D11-4	–	+	ND	ND	–	ND
4D3-4	–	–	ND	ND	ND	ND
4E11-13	–	+	ND	ND	ND	ND
4A2-BN	+	–	ND	ND	–	ND
4D8-2	+	ND	ND	ND	–	ND
4E11-10	–	ND	ND	ND	ND	ND
4E10-2	–	ND	ND	ND	ND	ND
3A1-2	–	ND	ND	ND	–	ND
4D11-3	–	ND	ND	ND	ND	ND
3A1-2	–	ND	ND	ND	ND	ND
4D10-2	ND	–	ND	ND	ND	ND

Table 5.1.**Summary of the results of screened compounds.** Luc assay: p53 activation analysis, p53: p53 accumulation analysis, p-H2AX: DNA damage analysis, p-p53: analysis of p53 phosphorylation, and F2H: MDM2-p53 interaction analysis, MTT: cell viability analysis. In the MTT, positive result means that cell viability was decreased in both p53-sufficient and deficient cells. +: positive result, -: negative result, and ND: not determined.

6.   REFERENCES

1.   Levine AJ. P53, the Cellular Gatekeeper for Growth and Division. *Cell*. 1997;88(3):323-331. doi:10.1016/S0092-8674(00)81871-1.

2.   Lane DP, Crawford L V. T antigen is bound to a host protein in SV40-transformed cells. *Nature*. 1979;278:261-263. doi:10.1038/278261a0.

3.   Oren M, Levine a J. Molecular cloning of a cDNA specific for the murine p53 cellular tumor antigen. *Proc Natl Acad Sci U S A*. 1983;80(1):56-59. doi:10.1073/pnas.80.1.56.

4.   Jenkins JR, Rudge K, Currie GA. Cellular immortalization by a cDNA clone encoding the transformation-associated phosphoprotein p53. *Nature*. 1984;312(5995):651-654. doi:10.1038/312651a0.

5.   Finlay CA, Hinds PW, Levine AJ. The p53 proto-oncogene can act as a suppressor of transformation. *Cell*. 1989;57(7):1083-1093. doi:10.1016/0092-8674(89)90045-7.

6.   Funk WD, Pak DT, Karas RH, Wright WE, Shay JW. A transcriptionally active DNA-binding site for human p53 protein complexes. *Mol Cell Biol*. 1992;12(6):2866-2871. doi:10.1128/MCB.12.6.2866.Updated.

7.   Marine J-C, Francoz S, Maetens M, Wahl G, Toledo F, Lozano G. Keeping p53 in check: essential and synergistic functions of Mdm2 and Mdm4. *Cell Death Differ*. 2006;13(6):927-934. doi:10.1038/sj.cdd.4401912.

8.   Shen H, Maki CG. Pharmacologic activation of p53 by small-molecule MDM2 antagonists. *Curr Pharm Des*. 2011;17(6):560-568. doi:10.2174/138161211795222603.

9.   Shaw P, Bovey R, Tardy S, Sahlit R, Sordat B, Costa J. Induction of apoptosis by wild-type p53 in a human colon tumor-derived cell line. *Biochemistry*. 1992;89(May):4495-4499. doi:10.1073/pnas.89.10.4495.

10.   Bai L, Zhu W. p53 : Structure , Function and Therapeutic Applications. *Cancer Mol*. 2006;2:141-153. doi:10.1007/978-94-017-9211-0_16.

11.   Zilfou JT, Lowe SW. Tumor suppressive functions of p53. *Cold Spring Harb Perspect Biol*. 2009;1(5):1-12. doi:10.1101/cshperspect.a001883.

12.   Michalovitz D, Halevy O, Oren M. Conditional inhibition of transformation and of cell proliferation by a temperature-sensitive mutant of p53. *Cell*. 1990;62(4):671-680. doi:10.1016/0092-8674(90)90113-S.

13.   Wang MO, Vorwald CE, Dreher ML, et al. HHS Public Access. 2016;27(1):138-144. doi:10.1002/adma.201403943.Evaluating.

14.   Rufini A, Tucci P, Celardo I, Melino G. Senescence and aging: the critical roles of p53. *Oncogene*. 2013;32(43):5129-5143. doi:10.1038/onc.2012.640.

15. Qian Y, Chen X. Tumor suppression by p53: Making cells senescent. *Histol Histopathol*. 2010;25(4):515-526. doi:10.14670/HH-25.515.

16. Duan L, Perez RE, Davaadelger B, Dedkova EN, Lothar A, Maki CG. P53-Regulated Autophagy Is Controlled By Glycolysis and Determines Cell Fate. *Oncotarget*. 2015;6(27):23135-23156. doi:10.18632/oncotarget.5218.

17. Brady CA, Attardi LD. P53 At a Glance. *J Cell Sci*. 2010;123(15):2527-2532. doi:10.1242/jcs.064501.

18. Joerger AC, Fersht AR. The tumor suppressor p53: from structures to drug discovery. *Cold Spring Harb Perspect Biol*. 2010;2(6):1-20. doi:10.1101/cshperspect.a000919.

19. Harms KL, Chen X. The functional domains in p53 family proteins exhibit both common and distinct properties. *Cell Death Differ*. 2006;13(6):890-897. doi:10.1038/sj.cdd.4401904.

20. Prives C, Manfredi JJ. The p53 tumor suppressor protein : meeting review. *Genes Dev*. 1993;7:529-534. doi:10.1101/gad.7.4.529.

21. Armstrong SR, Wu H, Wang B, Abuetabh Y, Sergi C, Leng RP. The regulation of tumor suppressor p63 by the ubiquitin-proteasome system. *Int J Mol Sci*. 2016;17(12). doi:10.3390/ijms17122041.

22. Michael D, Oren M. The p53-Mdm2 module and the ubiquitin system. *Semin Cancer Biol*. 2003;13(1):49-58. doi:10.1016/S1044-579X(02)00099-8.

23. Stavridi ES, Huyen Y, Sheston EA, Halazonetis TD. Structure of p53. 2002:25-53.

24. Laptenko O, Shiff I, Freed-Pastor W, et al. The p53 C Terminus Controls Site-Specific DNA Binding and Promotes Structural Changes within the Central DNA Binding Domain. *Mol Cell*. 2015;57(6):1034-1046. doi:10.1016/j.molcel.2015.02.015.

25. Momand J, Zambetti GP, Olson DC, George D, Levine AJ. The mdm-2 oncogene product forms a complex with the p53 protein and inhibits p53-mediated transactivation. *Cell*. 1992;69(7):1237-1245. doi:10.1016/0092-8674(92)90644-R.

26. Fakharzadeh SS, Trusko SP, George DL. Tumorigenic potential associated with enhanced expression of a gene that is amplified in a mouse tumor cell line. *EMBO J*. 1991;10(6):1565-1569.

27. Wu X, Bayle JH, Olson D, Levine AJ. The p53-mdm-2 autoregulatory feedl ack loop. *Genes Dev*. 1993;53:1126-1132. doi:10.1101/gad.7.7a.1126.

28. Iwakuma T, Lozano G. MDM2 , An Introduction. *Mol Cancer Res*. 2003;1(14):993-1000.

29. Freedman DA, Wu L, Levine AJ. Functions of the MDM2 oncoprotein. *Cell Mol Life Sci*. 1999;55(1):96-107. doi:10.1007/s000180050273.

30. Barak Y, Juven T, Haffner R, Oren M. mdm2 expression is induced by wild type p53 activity. *EMBO J*. 1993;12(2):461-468.

31. Picksley SM, Lane DP. What the papers say: The p53-mdm2 autoregulatory

feedback loop: A paradigm for the regulation of growth control by p53? *BioEssays*. 1993;15(10):689-690. doi:10.1002/bies.950151008.

32. Haupt Y, Maya R, Kazaz A, Oren M. Mdm2 promotes the rapid degradation of p53. *Nature*. 1997;387(6630):296-299. doi:10.1038/387296a0.

33. Moll UM, Petrenko O. The MDM2-p53 Interaction. 2003;1(December):1001-1008. doi:10.1016/s0092-8674(00)81871-1.

34. Kubbutat H. M, Jones SN, H VK. Regulation of p53 stability by Mdm2. *Nature*. 1997;387:299-303. doi:10.1038/387299a0.

35. Kruse JP, Gu W. Modes of p53 Regulation. *Cell*. 2009;137(4):609-622. doi:10.1016/j.cell.2009.04.050.

36. Toledo F, Wahl GM. MDM2 and MDM4: p53 regulators as targets in anticancer therapy. *Int J Biochem Cell Biol*. 2007;39(7-8):1476-1482. doi:10.1016/j.biocel.2007.03.022.

37. Shvarts A, Steegenga WT, Riteco N, et al. MDMX: a novel p53-binding protein with some functional properties of MDM2. *EMBO J*. 1996;15(19):5349-5357. doi:10.1002/J.1460-2075.1996.TB00919.X.

38. Tanimura S, Ohtsuka S, Mitsui K, Shirouzu K, Yoshimura A, Ohtsubo M. MDM2 interacts with MDMX through their RING finger domains. *FEBS Lett*. 1999;447(1):5-9. doi:10.1016/S0014-5793(99)00254-9.

39. Gu J, Kawai H, Nie L, et al. Mutual dependence of MDM2 and MDMX in their functional inactivation of p53. *J Biol Chem*. 2002;277(22):19251-19254. doi:10.1074/jbc.C200150200.

40. Kamijo T, Weber JD, Zambetti G, Zindy F, Roussel MF, Sherr CJ. Functional and physical interactions of the ARF tumor suppressor with p53 and Mdm2. *Med Sci*. 1998;95(July):8292-8297. doi:10.1073/pnas.95.14.8292.

41. Brooks CL, Gu W. Ubiquitination, phosphorylation and acetylation: The molecular basis for p53 regulation. *Curr Opin Cell Biol*. 2003;15(2):164-171. doi:10.1016/S0955-0674(03)00003-6.

42. Kruse JP, Gu W. SnapShot: p53 Posttranslational Modifications. *Cell*. 2008;133(5):5-6. doi:10.1016/j.cell.2008.05.020.

43. Reed SM, Quelle DE. P53 acetylation: Regulation and consequences. *Cancers (Basel)*. 2014;7(1):30-69. doi:10.3390/cancers7010030.

44. Gu W, Roeder RG. Activation of p53 sequence-specific DNA binding by acetylation of the p53 C-terminal domain. *Cell*. 1997;90(4):595-606. doi:10.1016/S0092-8674(00)80521-8.

45. Mellert H, Sykes SM, Murphy ME, McMahon SB. The ARF/oncogene pathway activates p53 acetylation within the DNA binding domain. *Cell Cycle*. 2007;6(11):1304-1306. doi:10.4161/cc.6.11.4343.

46. Tang Y, Luo J, Zhang W, Gu W. Tip60-Dependent Acetylation of p53 Modulates the Decision between Cell-Cycle Arrest and Apoptosis. *Mol Cell*. 2006;24(6):827-

839. doi:10.1016/j.molcel.2006.11.021.

47. Chène P. Inhibiting the p53–MDM2 interaction: an important target for cancer therapy. *Nat Rev Cancer*. 2003;3(2):102-109. doi:10.1038/nrc991.

48. Chen J, Marechal V, Levine a J. Mapping of the p53 and mdm-2 interaction domains. *Mol Cell Biol*. 1993;13(7):4107-4114. doi:10.1128/MCB.13.7.4107.Updated.

49. Kussie PH, Gorina S, Marechal V, et al. Structure of the MDM2 Oncoprotein Bound to the p53 Tumor Suppressor Transactivation Domain. *Science (80-)*. 1996;274(5289):948-953. doi:10.1126/science.274.5289.948.

50. Bernstein PR, Buschauer A, Georg GJ, Kiso Y, Lowe J, Stilz HU. Preface to the series. *Top Med Chem*. 2012;8:57-80. doi:10.1007/978-3-642-28965-1.

51. Vogelstein B, Lane D, Levine AJ. Surfing the p53 network. *Nature*. 2000;408(6810):307-310. doi:10.1038/35042675.

52. Vijayakumaran R, Tan KH, Miranda PJ, Haupt S, Haupt Y. Regulation of Mutant p53 Protein Expression. *Front Oncol*. 2015;5(December):3-10. doi:10.3389/fonc.2015.00284.

53. Srivastava S, Zou Z, Pirollo K, Blattner W, Chang EH. Germ-line transmission of a mutated p53 gene in a cancer-prone family with Li–Fraumeni syndrome. *Nature*. 1990;348(6303):747-749. doi:10.1038/348747a0.

54. Donehower LA, Harvey M, Slagle BL, et al. Mice deficient for p53 are developmentally normal but susceptible to spontaneous tumours. *Nature*. 1992;356(6366):215-221. doi:10.1038/356215a0.

55. Muller PAJ, Vousden KH. P53 Mutations in Cancer. *Nat Cell Biol*. 2013;15(1):2-8. doi:10.1038/ncb2641.

56. Yue X, Zhao Y, Xu Y, Zheng M, Feng Z, Hu W. Mutant p53 in Cancer: Accumulation, Gain-of-Function, and Therapy. *J Mol Biol*. 2017;429(11):1595-1606. doi:10.1016/j.jmb.2017.03.030.

57. Olive KP, Tuveson DA, Ruhe ZC, et al. Mutant p53 gain of function in two mouse models of Li-Fraumeni syndrome. *Cell*. 2004;119(6):847-860. doi:10.1016/j.cell.2004.11.004.

58. Ribeiro CJA, Rodrigues CMP, Moreira R, Santos MMM. Chemical variations on the p53 reactivation theme. *Pharmaceuticals*. 2016;9(2). doi:10.3390/ph9020025.

59. Shi D, Gu W. Dual Roles of MDM2 in the Regulation of p53: Ubiquitination Dependent and Ubiquitination Independent Mechanisms of MDM2 Repression of p53 Activity. *Genes Cancer*. 2012;3(3-4):240-248. doi:10.1177/1947601912455199.

60. Brown CJ, Lain S, Verma CS, Fersht AR, Lane DP. Awakening guardian angels: drugging the p53 pathway. *Nat Rev Cancer*. 2009;9(12):862-873. doi:10.1038/nrc2763.

61. Pei D, Zhang Y, Zheng J. Regulation of p53: a collaboration between Mdm2 and

MdmX. *Oncotarget*. 2012;3(3):228-235. doi:10.18632/oncotarget.443.

62. Kastan MB. Wild-Type p53: Tumors Can't Stand It. *Cell*. 2007;128(5):837-840. doi:10.1016/j.cell.2007.02.022.

63. Manuscript A, Therapy C. NIH Public Access. *Annu Rev Pharmacol Toxicol*. 2010:223-241.doi:10.1146/annurev.pharmtox.48.113006.094723.Small-Molecule.

64. Yang Y, Ludwig RL, Jensen JP, et al. Small molecule inhibitors of HDM2 ubiquitin ligase activity stabilize and activate p53 in cells. *Cancer Cell*. 2005;7(6):547-559. doi:10.1016/j.ccr.2005.04.029.

65. Vassilev LT. In Vivo Activation of the p53 Pathway by Small-Molecule Antagonists of MDM2. *Science (80-)*. 2004;303(5659):844-848. doi:10.1126/science.1092472.

66. Grasberger BL, Lu T, Schubert C, et al. Discovery and cocrystal structure of benzodiazepinedione HDM2 antagonists that activate p53 in cells. *J Med Chem*. 2005;48(4):909-912. doi:10.1021/jm049137g.

67. Ding K, Lu Y, Nikolovska-Coleska Z, et al. Structure-based design of spiro-oxindoles as potent, specific small-molecule inhibitors of the MDM2-p53 interaction. *J Med Chem*. 2006;49(12):3432-3435. doi:10.1021/jm051122a.

68. Issaeva N, Bozko P, Enge M, et al. Small molecule RITA binds to p53, blocks p53–HDM-2 interaction and activates p53 function in tumors. *Nat Med*. 2004;10(12):1321-1328. doi:10.1038/nm1146.

69. Reed D, Shen Y, Shelat AA, et al. Identification and characterization of the first small molecule inhibitor of MDMX. *J Biol Chem*. 2010;285(14):10786-10796. doi:10.1074/jbc.M109.056747.

70. Suzuki K, Matsubara H. Recent advances in p53 research and cancer treatment. *J Biomed Biotechnol*. 2011;2011. doi:10.1155/2011/978312.

71. Michelini E, Cevenini L, Mezzanotte L, Coppa A, Roda A. Cell-based assays: Fuelling drug discovery. *Anal Bioanal Chem*. 2010;398(1):227-238. doi:10.1007/s00216-010-3933-z.

72. Allard STM, Kopish K. Luciferase Reporter Assays : Powerful , Adaptable Tools for Cell Biology Research. *Cell Notes*. 2008;(21):23-26.

73. Dube A, Gupta R, Singh N. Reporter genes facilitating discovery of drugs targeting protozoan parasites. *Trends Parasitol*. 2009;25(9):432-439. doi:10.1016/j.pt.2009.06.006.

74. Zhang Z, Guan N, Li T, Mais DE, Wang M. Quality control of cell-based high-throughput drug screening. *Acta Pharm Sin B*. 2012;2(5):429-438. doi:10.1016/j.apsb.2012.03.006.

75. Jiang T, Xing B, Rao J. Recent developments of biological reporter technology for detecting gene expression. *Biotechnol Genet Eng Rev*. 2008;25(1):41-76. doi:10.5661/bger-25-41.

76. New DC, Miller-Martini DM, Wong YH. Reporter gene assays and their applications to bioassays of natural products. *Phyther Res*. 2003;17(5):439-448. doi:10.1002/ptr.1312.

77. Soboleski MR, Oaks J, Halford WP. Green fluorescent protein is a quantitative reporter of gene expression in individual eukaryotic cells. *Fed Am Soc Exp Biol*. 2005;19(3):440-442. doi:10.1096/fj.04-3180fje.

78. Auld DS, Southall NT, Jadhav A, et al. Characterization of chemical libraries for luciferase inhibitory activity. *J Med Chem*. 2008;51(8):2372-2386. doi:10.1021/jm701302v.

79. Badr CE, Wurdinger T, Tannous BA. Functional Drug Screening Assay Reveals Potential Glioma Therapeutics. *Assay Drug Dev Technol*. 2011;9(3):281-289. doi:10.1089/adt.2010.0324.

80. Kim H, Kim JS. A guide to genome engineering with programmable nucleases. *Nat Rev Genet*. 2014;15(5):321-334. doi:10.1038/nrg3686.

81. Oceguera-Yanez F, Kim S Il, Matsumoto T, et al. Engineering the AAVS1 locus for consistent and scalable transgene expression in human iPSCs and their differentiated derivatives. *Methods*. 2016;101:43-55. doi:10.1016/j.ymeth.2015.12.012.

82. He X, Tan C, Wang F, et al. Knock-in of large reporter genes in human cells via CRISPR/Cas9-induced homology-dependent and independent DNA repair. *Nucleic Acids Res*. 2016;44(9). doi:10.1093/nar/gkw064.

83. Chen F, Pruett-miller SM, Huang Y, Gjoka M, Biotechnology S, Louis S. NIH Public Access. 2013;8(9):753-755. doi:10.1038/nmeth.1653.High-frequency.

84. Gaj T, Sirk SJ, Shui S, Liu J. Genome-Editing Technologies : Principles and Applications. *Cold Spring Harb Perspect Biol*. 2016;8(10):1-20. doi:10.1101/cshperspect.a023754.

85. Kim YG, Cha J, Chandrasegaran S. Hybrid restriction enzymes: zinc finger fusions to Fok I cleavage domain. *Proc Natl Acad Sci*. 1996;93(3):1156-1160. doi:10.1073/pnas.93.3.1156.

86. Gaj T, Gersbach C, Barbas III C. ZFN, TALEN and CRISPR/Cas based methods for genome engineering. *Trends Biotechnol*. 2014;31(7):397-405. doi:10.1016/j.tibtech.2013.04.004.ZFN.

87. Pavletich NP, Pabo C. Zinc Structure of a Recognition : Complex Zif268-DNA. *Adv Sci*. 1991;252(5007):809-817. doi:10.1126/science.2028256.

88. Christian M, Cermak T, Doyle EL, et al. Targeting DNA double-strand breaks with TAL effector nucleases. *Genetics*. 2010;186(2):756-761. doi:10.1534/genetics.110.120717.

89. Schornack S, Meyer A, Römer P, Jordan T, Lahaye T. Gene-for-gene-mediated recognition of nuclear-targeted AvrBs3-like bacterial effector proteins. *J Plant Physiol*. 2006;163(3):256-272. doi:10.1016/j.jplph.2005.12.001.

90. Chandrasegaran S, Carroll D, Street NW, City SL. Origins of Programmable

Nucleases for Genome Engineering. *J Mol Biol*. 2017;428(5 Pt B):963-989. doi:10.1016/j.jmb.2015.10.014.Origins.

91. Nemudryi AA, Valetdinova KR, Medvedev SP, Zakian SM. TALEN and CRISPR / Cas Genome Editing Systems : Tools of Discovery. *Acta Naturae*. 2014;6(22):19-40. doi:10.1007/s11103-014-0188-7.

92. Sanjana NE, Cong L, Zhou Y, Cunniff MM, Feng G, Zhang F. A transcription activator-like effector toolbox for genome engineering. *Nat Protoc*. 2012;7(1):171-192. doi:10.1038/nprot.2011.431.

93. Schmid-burgk JL, Schmidt T, Kaiser V, Höning K. Europe PMC Funders Group Europe PMC Funders Author Manuscripts A ligation-independent cloning technique for high-throughput assembly of transcription activator − like effector genes. *Nat Biotechnol*. 2014;31(1):76-81. doi:10.1038/nbt.2460.A.

94. Rouet P, Smih F, Jasin M. Introduction of double-strand breaks into the genome of mouse cells by expression of a rare-cutting endonuclease. *Mol Cell Biol*. 1994;14(12):8096-8106. doi:10.1128/MCB.14.12.8096.

95. Porteus M. Genome Editing: A New Approach to Human Therapeutics. *Annu Rev Pharmacol Toxicol*. 2016;56(1):163-190. doi:10.1146/annurev-pharmtox-010814-124454.

96. Davis A, Chen D. DNA double strand break repair via non-homologous end-joining. *Transl Cancer Res*. 2013;2(3):130-143. doi:10.3978/j.issn.2218-676X.2013.04.02.DNA.

97. Jasin M, Rothstein R. Repair of strand breaks by homologous recombination. *Cold Spring Harb Perspect Biol*. 2013;5(11):1-18. doi:10.1101/cshperspect.a012740.

98. Capecchi MR. Gene targeting in mice: Functional analysis of the mammalian genome for the twenty-first century. *Nat Rev Genet*. 2005;6(6):507-512. doi:10.1038/nrg1619.

99. Sadelain M, Papapetrou EP, Bushman FD. Safe harbours for the integration of new DNA in the human genome. *Nat Rev Cancer*. 2012;12(1):51-58. doi:10.1038/nrc3179.

100. Papapetrou EP, Schambach A. Gene insertion into genomic safe harbors for human gene therapy. *Mol Ther*. 2016;24(4):678-684. doi:10.1038/mt.2016.38.

101. Kim R, Trubetskoy A, Suzuki T, et al. Genome-Based Identification of Cancer Genes by Proviral Tagging in Mouse Retrovirus-Induced T-Cell Lymphomas Genome-Based Identification of Cancer Genes by Proviral Tagging in Mouse Retrovirus-Induced T-Cell Lymphomas. *J Virol*. 2003;77(3):2056-2062. doi:10.1128/JVI.77.3.2056.

102. Irion S, Luche H, Gadue P, Fehling HJ, Kennedy M, Keller G. Identification and targeting of the ROSA26 locus in human embryonic stem cells. *Nat Biotechnol*. 2007;25(12):1477-1482. doi:10.1038/nbt1362.

103. Kasparek P, Krausova M, Haneckova R, et al. Efficient gene targeting of the Rosa26 locus in mouse zygotes using TALE nucleases. *FEBS Lett*.

2014;588(21):3982-3988. doi:10.1016/j.febslet.2014.09.014.

104. Perez EE, Wang J, Miller JC, et al. Editing Using Zinc-Finger Nucleases. *Nat Biotechnol*. 2012;26(7):808-816. doi:10.1038/nbt1410.Establishment.

105. Kotin RM, Linden RM, Berns KI. Characterization of a preferred site on human chromosome 19q for integration of adeno-associated virus DNA by non-homologous recombination. *EMBO J.* 1992;11(13):5071-5078. doi:10.1182/blood-2008-10-181479.

106. Smith JR, Maguire S, Davis LA, et al. Robust, Persistent Transgene Expression in Human Embryonic Stem Cells Is Achieved with AAVS1-Targeted Integration. *Stem Cells*. 2008;26(2):496-504. doi:10.1634/stemcells.2007-0039.

107. Hockemeyer D, Wang H, Kiani S, et al. Genetic engineering of human ES and iPS cells using TALE nucleases. *Nat Biotechnol*. 2012;29(8):731-734. doi:10.1038/nbt.1927.Genetic.

108. Yurlova L, Derks M, Buchfellner A, et al. The fluorescent two-hybrid assay to screen for protein-protein interaction inhibitors in live cells: Targeting the interaction of p53 with Mdm2 and Mdm4. *J Biomol Screen*. 2014;19(4):516-525. doi:10.1177/1087057113518067.

109. Zolghadr K, Mortusewicz O, Rothbauer U, et al. A Fluorescent Two-hybrid Assay for Direct Visualization of Protein Interactions in Living Cells. *Mol Cell Proteomics*. 2008;7(11):2279-2287. doi:10.1074/mcp.M700548-MCP200.

110. Hockemeyer D, Soldner F, Beard C, et al. Highly efficient gene targeting of expressed and silent genes in human ESCs and iPSCs using zinc finger nucleases. *Nat Biotechnol*. 2014;27(9):851-857. doi:10.1038/nbt.1562.Highly.

111. El-Deiry WS, Tokino T, Velculescu VE, et al. WAR, a Potential Mediator of p53 Tumor Suppression. *Cell*. 1993;75:817-825.

112. Lüpertz R, Wätjen W, Kahl R, Chovolou Y. Dose- and time-dependent effects of doxorubicin on cytotoxicity, cell cycle and apoptotic cell death in human colon cancer cells. *Toxicology*. 2010;271(3):115-121. doi:10.1016/j.tox.2010.03.012.

113. Fernandez-Capetillo O, Lee A, Nussenzweig M, Nussenzweig A. H2AX: The histone guardian of the genome. *DNA Repair (Amst)*. 2004;3(8-9):959-967. doi:10.1016/j.dnarep.2004.03.024.

114. Rogakou EP, Nieves-Neira W, Boon C, Pommier Y, Bonner WM. Initiation of DNA fragmentation during apoptosis induces phosphorylation of H2AX histone at serine 139. *J Biol Chem*. 2000;275(13):9390-9395. doi:10.1074/jbc.275.13.9390.

115. Wade M, Wang Y V., Wahl GM. The p53 orchestra: Mdm2 and Mdmx set the tone. *Trends Cell Biol*. 2010;20(5):299-309. doi:10.1016/j.tcb.2010.01.009.

7. APPENDICES

APPENDIX A – Chemicals

Chemicals and Media Components	Supplier Company
2-Mercaptoethanol	Sigma, Germany
Acetic acid (glacial)	Merck Millipore, USA
Acrylamide/ Bis-acrylamide	Sigma, Germany
Agarose	Sigma, Germany
Ammonium Persulfate	Sigma, Germany
Ampicillin Sodium Salt	Cellgro, USA
Betaine	Sigma, Germany
Boric Acid	Molekula France
Bromophenol Blue	Sigma, Germany
Calcium Chloride	Sigma, Germany
D-Glucose	Sigma, Germany
Distilled Water	Merck Millipore, USA
DMEM	Thermo Fisher Scientific, USA
DMEM Phenol Red Free	Thermo Fisher Scientific, USA
DMSO	Sigma, Germany
DNA Gel Loading Dye, 6X	NEB, USA
Doxorubicin Hydrochloride	Sigma, Germany
EDTA	Sigma, Germany
Ethanol	Sigma, Germany
Ethidium Bromide	Sigma, Germany
Fetal Bovine Serum	Thermo Fisher Scientific, USA
Glycerol	Sigma, Germany
Glycine	Sigma, Germany
Hydrochloric Acid	Sigma, Germany
Hydrogen Peroxide	Sigma, Germany
Isopropanol	Sigma, Germany
Kanamycin Sulphate	Thermo Fisher Scientific, USA
LB Agar	Sigma, Germany
LB Broth	Invitrogen, USA

Liquid Nitrogen	Karbogaz, Turkey
Luminol	Sigma, Germany
Methanol	Sigma, Germany
Nutlin-3a	Sigma, Germany / MCE, USA
PBS	Thermo Fisher Scientific, USA
p-Coumaric Acid	Sigma, Germany
Penicillin/Streptomycin	Thermo Fisher Scientific, USA
pH4.0 Buffer Solution	Merck Millipore, USA
pH7.0 Buffer Solution	Merck Millipore, USA
PIPES	Sigma, Germany
Polyethyleneimine	Polysciences, USA
Potassium Acetate	Merck Millipore, USA
Potassium Chloride	Sigma, Germany
Puromycin Dihydrochloride	Sigma, Germany
RNase A	Roche, Germany
SDS	Sigma, Germany
Skim Milk Powder	Sigma, Germany
Sodium Azide	Amresco, USA
Sodium Chloride	Amresco, USA
Sodium Hydroxide	Sigma, Germany
TEMED	Applichem, Germany
Tris Base	Sigma, Germany
Tris Hydrochloride	Amresco, USA
Trypan Blue Solution	Thermo Fisher Scientific
Tween-20	Sigma, Germany

APPENDIX B – Equipment

Equipment	Supplier Company
Autoclave	HiClave HV-110, Hirayama, Japan
Balance	Isolab, Germany Sartorius, Germany
Biomolecular Imager	ImageQuant LAS 4000 mini – GE Healthcare, USA
Centrifuge	5418R, Eppendorf, Germany 5702, Eppendorf, Germany 5415R Eppendorf, Germany Allegra X-15R, Beckman Coulter, USA
CO_2 Incubator	Binder, Germany
Countless II Automated Cell Counter	Thermo Fisher Scientific, USA
Deepfreeze	-80, Forma 88000 Series, Thermo Fisher Scientific, USA -20, Bosch, Germany
Distilled Water	Millipore, Elix – S, France
Electrophoresis Apparatus	VWR, USA
Filters (0.22 μm and 0.45 μm)	Merck Millipore, USA
Freezing Container	Mr. Frosty, Thermo Fisher Scientific, USA
Gel Documentation	Gel Doc EZ, Biorad, USA
Heater	Thermomixer Comfort, Eppendorf, Germany
Hemocytometer	Neubauer Improved, Isolab, Germany
Ice Machine	AF20, Scotsman Inc., USA
Incubator	BE300, Memmert, Germany
Incubator Shaker	Innova 44, New Brunswick Scientific, USA, Heidolph Titramax 1000,Heidolph, Germany
Laminar Flow	HeraSafe HS15, Heraeus, Germany HeraSafe HS12, Heraeus, Germany
Liquid Nitrogen Tank	Taylor-Wharton, 300RS, USA
Magnetic Stirrer	SB162, Stuart, UK
Microliter Pipettes	Thermo Fisher Scientific, USA

Microplate Reader	iMark Reader, Bio-Rad, USA
	Model 680, Bio-Rad, USA
Microscope	Primovert, Zeiss, Germany
	CK40, Olympus, Japan
	IN Cell Analyzer, General Electric, USA
Microwave Oven	Bosch, Germany
pH Meter	SevenCompact, Mettler Toledo, USA
Power Supply	Biorad, PowerPac 300, USA
Refrigerator	Bosch, Germany
	Arcelik, Turkey
	Panasonic, Japan
Spectrophotometer	Fluoroskan Ascent FL, Thermo Fisher Scientific, USA
	NanoDrop 2000, Thermo Fisher Scientific, USA
	Ultrospec 2100 pro, Amersham Biosciences, UK
Thermal Cycler	C1000 Touch, Biorad, USA
	PTC-200, MJ Research Inc., Canada
Vortex	VWR, USA
Water Bath	Innova 3100, New Brunswick Scientific, USA

APPENDIX C – Molecular Biology Kits

Commercial Kit	Supplier Company
Cell Proliferation Kit I (MTT)	Roche, Switzerland
Dual Luciferase Reporter Assay System	Promega, USA
F2H®-Kits p53-Mdm2/4	ChromoTek, USA
GenElute Agarose Spin Columns	Sigma-Aldrich, USA
Luciferase Assay System	Promega, USA
Multisource Genomic DNA Miniprep Kit	Axygen, USA
NuceloSpin Gel and PCR Clean-up	Macherey-Nagel, USA
Pierce^{TM} BCA Protein Assay Kit	Thermo Fisher Scientific, USA
PureLink Genomic DNA Mini Kit	Invitrogen, USA
PureLink HiPure Plasmid Midiprep Kit	Invitrogen, USA
PureLink Quick Gel Extraction Kit	Invitrogen, USA
ZymoPure Plasmid Maxiprep Kit	Zymo Research, USA

APPENDIX D – Antibodies

Antibody	Supplier Company	Catalog Number
P53 (1C12) Mouse	Cell Signaling Technology	2524S
p-p53 (S15) (16G8) Mouse	Cell Signaling Technology	9286P
P53 Rabbit Ab	Cell Signaling Technology	9282S
p-Histone H2A.x (S139) (20E) Rabbit	Cell Signaling Technology	9718S
Beta-Actin Rabbit	Cell Signaling Technology	4967L
Anti-rabbit IgG HRP-linked	Cell Signaling Technology	7074S
Anti-mouse IgG Peroxidase	Sigma	A9044

APPENDIX E – DNA Molecular Weight Marker
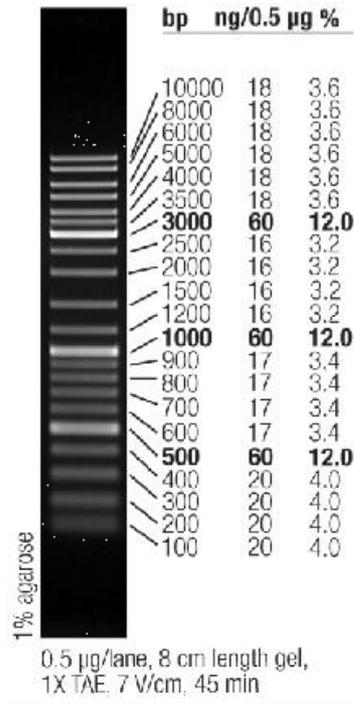
Figure E.1. Thermo Scientific GeneRuler DNA Ladder Mix (SM0331)
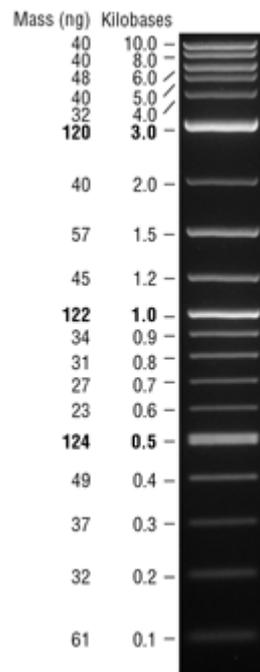
Figure E.2. New England BioLabs 2-Log DNA Ladder (N3200S)
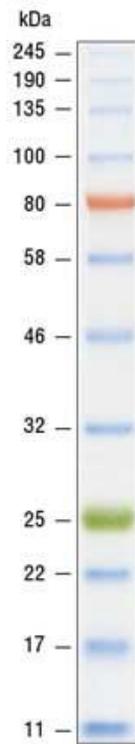
Figure E.3. New England BioLabs Color Prestained Protein Standard, Broad Range (11–245 kDa) (P7712S)
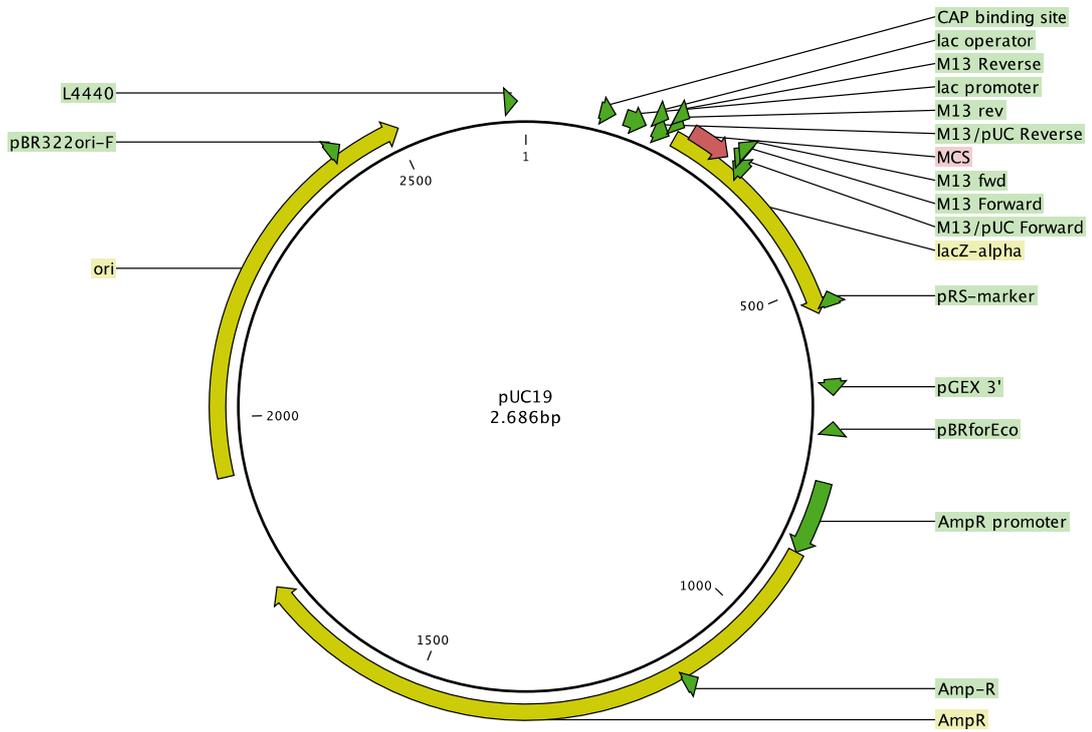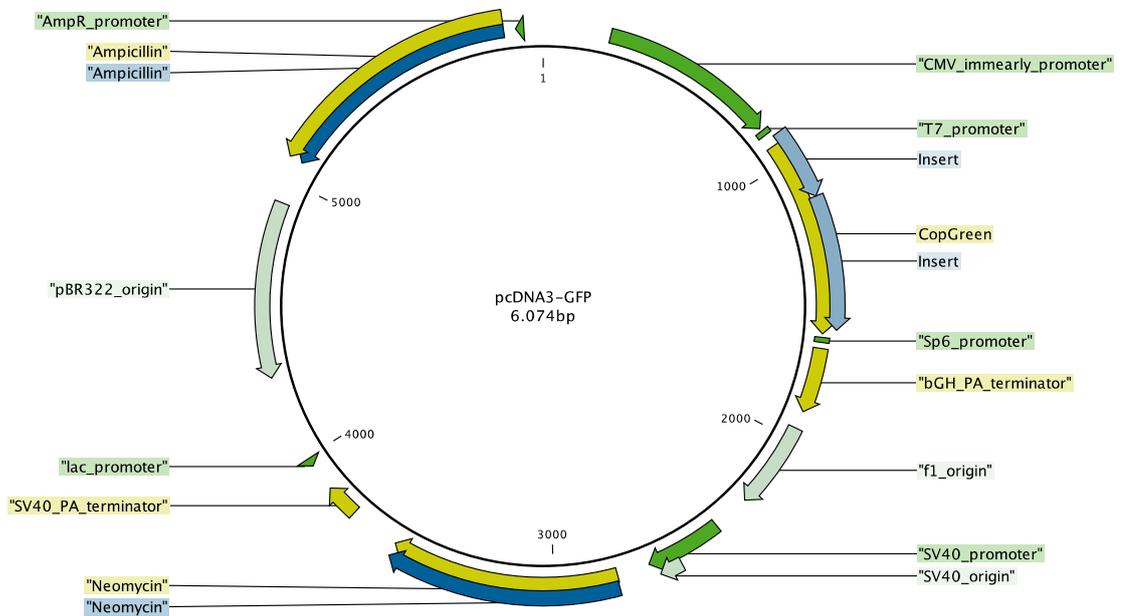
Figure F.4. The plasmid map of pUC19
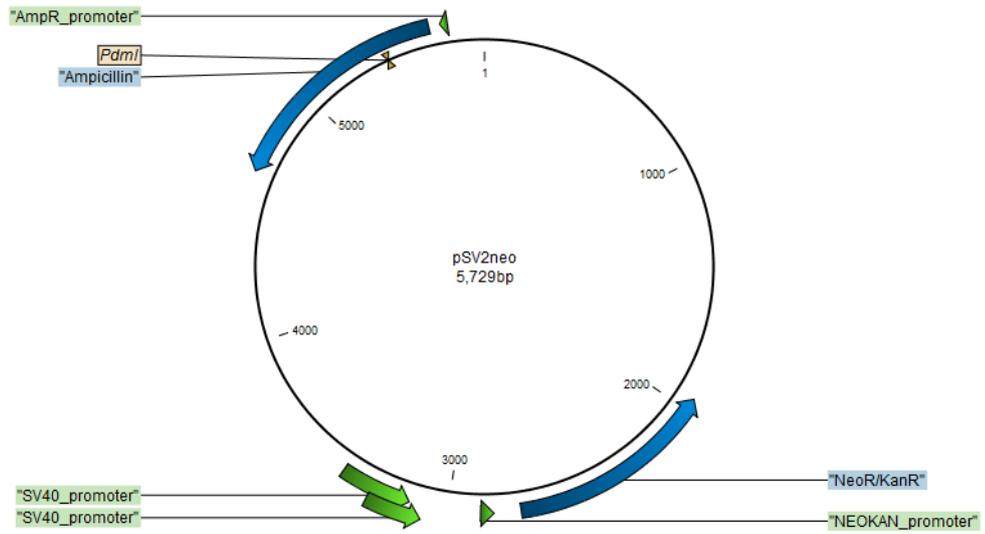

Figure F.5. The plasmid map of pcDNA3-GFP
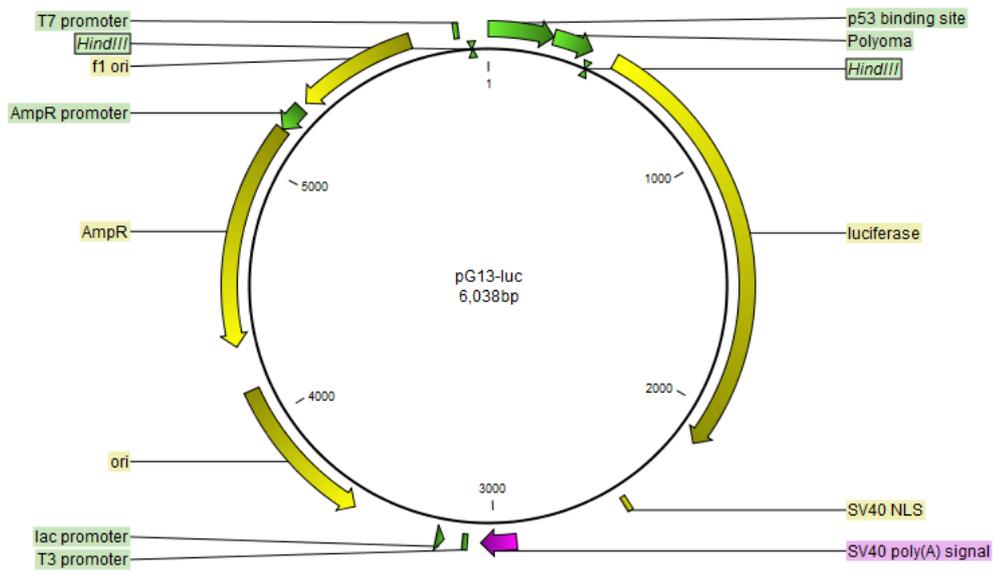
Figure F.6. The plasmid map of pSV2-Neo
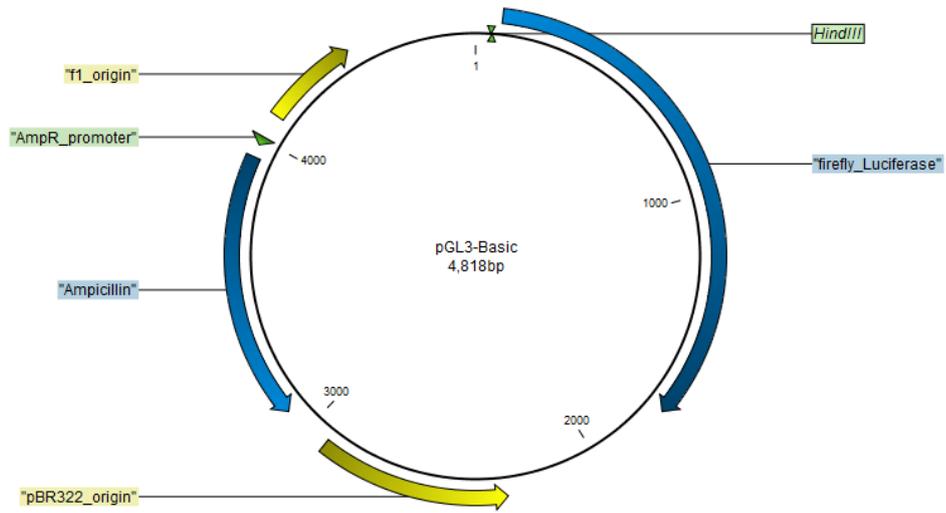

Figure F.7. The plasmid map of pG13-luc

Figure F.8. The plasmid map of pGl3-Basic
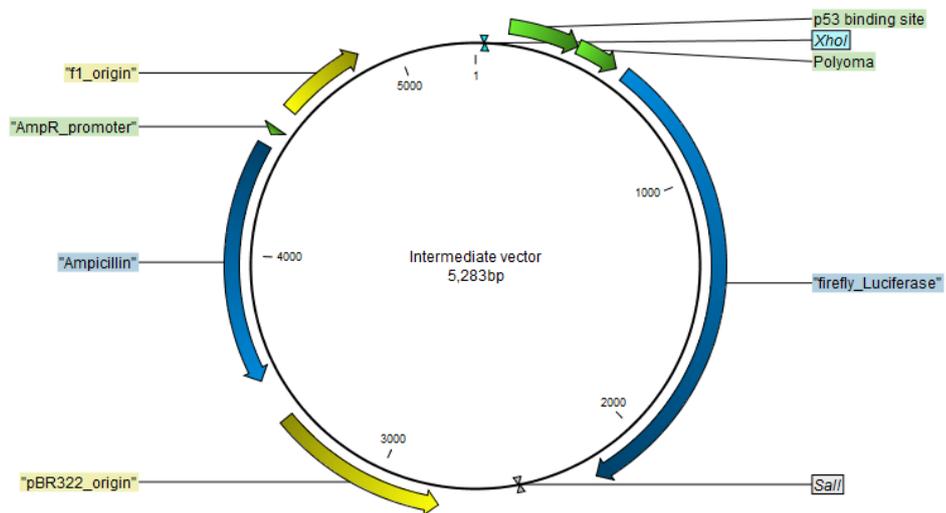
Figure F.9. The plasmid map of intermediate vector
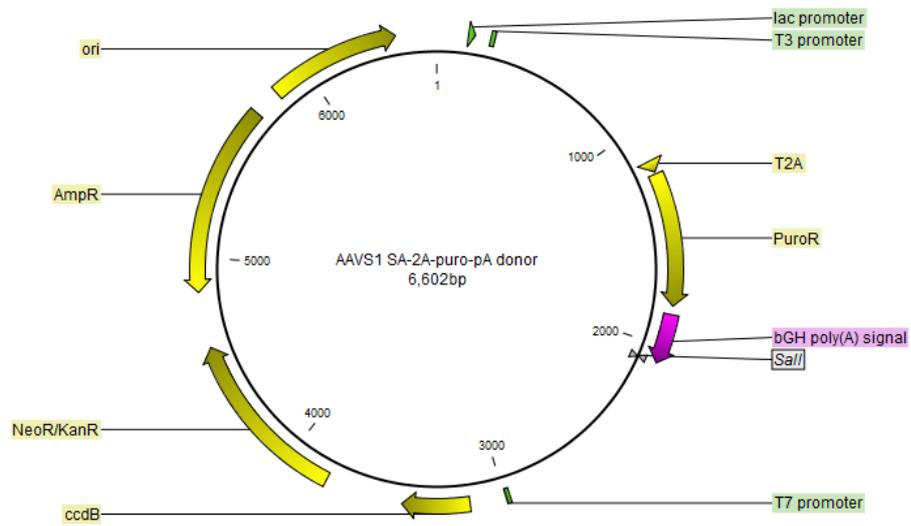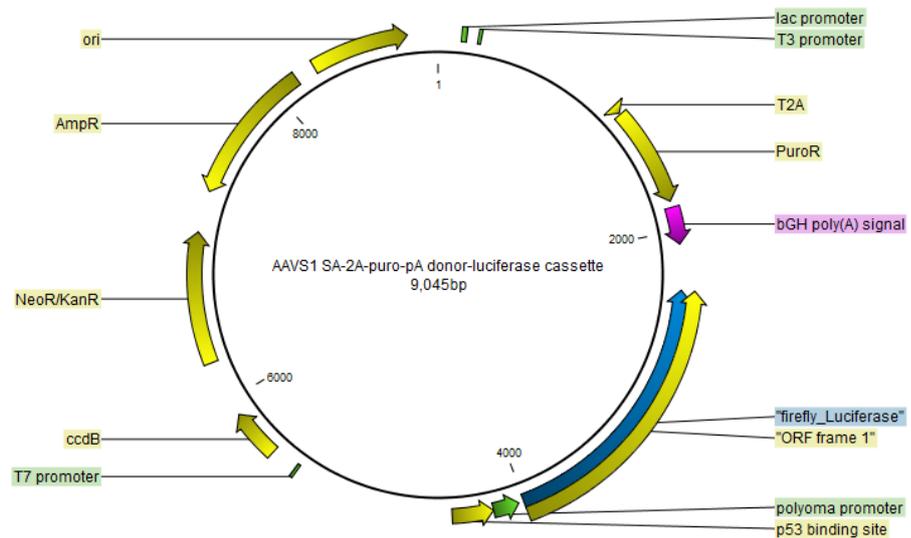
Figure F.10. The plasmid map of AAVS1 SA-2A-puro-pA donor

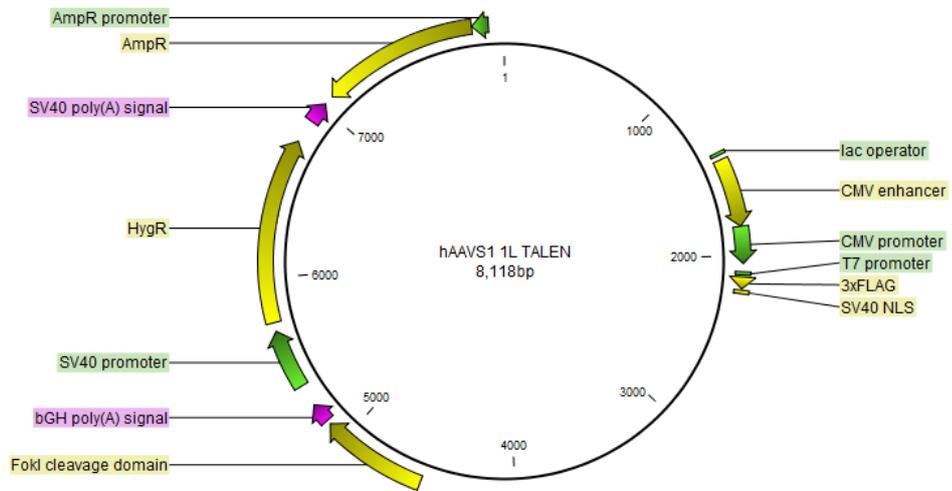**Figure F.11. The plasmid map of AAVS1 SA-2A-puro-pA donor-luciferase cassette**
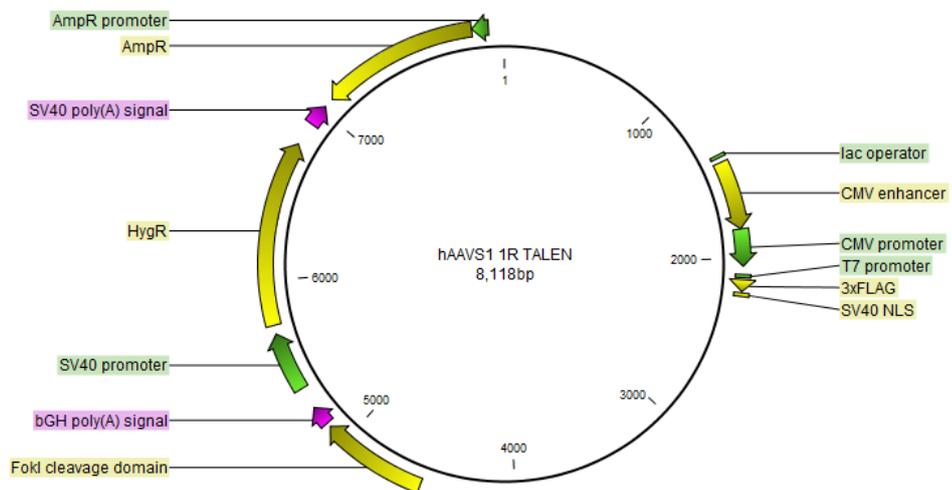
Figure F.12. The plasmid map of hAAVS1 1L TALEN

Figure F.13. The plasmid map of hAAVS1 1R TALEN